Petrogenesis of Two Contrasting, Late Archean Granitoids, Wind River Range, Wyoming

---

U.S. GEOLOGICAL SURVEY PROFESSIONAL PAPER 1491

U.S. DEPARTMENT OF THE INTERIOR

March 3, 1849

AVAILABILITY OF BOOKS AND MAPS OF THE U.S. GEOLOGICAL SURVEY

Instructions on ordering publications of the U.S. Geological Survey, along with prices of the last offerings, are given in the current-year issues of the monthly catalog "New Publications of the U.S. Geological Survey." Prices of available U.S. Geological Survey publications released prior to the current year are listed in the most recent annual "Price and Availability List." Publications that are listed in various U.S. Geological Survey catalogs **(see back inside cover)** but not listed in the most recent annual "Price and Availability List" are no longer available.

Prices of reports released to the open files are given in the listing "U.S. Geological Survey Open-File Reports," updated monthly, which is for sale in microfiche from the U.S. Geological Survey, Books and Open-File Reports Section, Federal Center, Box 25425, Denver, CO 80225. Reports released through the NTIS may be obtained by writing to the National Technical Information Service, U.S. Department of Commerce, Springfield, VA 22161; please include NTIS report number with inquiry.

Order U.S. Geological Survey publications **by mail** or **over the counter** from the offices given below.

BY MAIL

Books

Professional Papers, Bulletins, Water-Supply Papers, Techniques of Water-Resources Investigations, Circulars, publications of general interest (such as leaflets, pamphlets, booklets), single copies of Earthquakes & Volcanoes, Preliminary Determination of Epicenters, and some miscellaneous reports, including some of the foregoing series that have gone out of print at the Superintendent of Documents, are obtainable by mail from

U.S. Geological Survey, Books and Open-File Reports
Federal Center, Box 25425
Denver, CO 80225

Subscriptions to periodicals (Earthquakes & Volcanoes and Preliminary Determination of Epicenters) can be obtained ONLY from the

Superintendent of Documents
Government Printing Office
Washington, D.C. 20402

(Check or money order must be payable to Superintendent of Documents.)

Maps

For maps, address mail orders to

U.S. Geological Survey, Map Distribution
Federal Center, Box 25286
Denver, CO 80225

Residents of Alaska may order maps from

Alaska Distribution Section, U.S. Geological Survey,
New Federal Building - Box 12
101 Twelfth Ave., Fairbanks, AK 99701

OVER THE COUNTER

Books

Books of the U.S. Geological Survey are available over the counter at the following Geological Survey Public Inquiries Offices, all of which are authorized agents of the Superintendent of Documents:

- **WASHINGTON, D.C.**--Main Interior Bldg., 2600 corridor, 18th and C Sts., NW.
- **DENVER, Colorado**--Federal Bldg., Rm. 169, 1961 Stout St.
- **LOS ANGELES, California**--Federal Bldg., Rm. 7638, 300 N. Los Angeles St.
- **MENLO PARK, California**--Bldg. 3 (Stop 533), Rm. 3128, 345 Middlefield Rd.
- **RESTON, Virginia**--503 National Center, Rm. 1C402, 12201 Sunrise Valley Dr.
- **SALT LAKE CITY, Utah**--Federal Bldg., Rm. 8105, 125 South State St.
- **SAN FRANCISCO, California**--Customhouse, Rm. 504, 555 Battery St.
- **SPOKANE, Washington**--U.S. Courthouse, Rm. 678, West 920 Riverside Ave..
- **ANCHORAGE, Alaska**--Rm. 101, 4230 University Dr.
- **ANCHORAGE, Alaska**--Federal Bldg, Rm. E-146, 701 C St.

Maps

Maps may be purchased over the counter at the U.S. Geological Survey offices where books are sold (all addresses in above list) and at the following Geological Survey offices:

- **ROLLA, Missouri**--1400 Independence Rd.
- **DENVER, Colorado**--Map Distribution, Bldg. 810, Federal Center
- **FAIRBANKS, Alaska**--New Federal Bldg., 101 Twelfth Ave.

Petrogenesis of Two Contrasting, Late Archean Granitoids, Wind River Range, Wyoming

By JOHN S. STUCKLESS

U.S. GEOLOGICAL SURVEY PROFESSIONAL PAPER 1491

UNITED STATES GOVERNMENT PRINTING OFFICE, WASHINGTON : 1989

DEPARTMENT OF THE INTERIOR

DONALD PAUL HODEL, *Secretary*

U. S. GEOLOGICAL SURVEY

Dallas L. Peck, *Director*

Library of Congress Cataloging-in-Publication Data

Stuckless, John S.
Petrogenesis of two contrasting, Late Archean granitoids, Wind River Range, Wyoming.

(U.S. Geological Survey professional paper ; 1491)
Bibliography: p.
1. Granite—Wyoming—Wind River Range. 2. Petrogenesis—Wyoming—Wind River Range. 3. Geology, Stratigraphic—Archean. I. Title. II. Series: Geological Survey professional paper ; 1491.
QE462.G7S78 1989 552'.3 88-600459

For sale by the Books and Open-File Reports Section, U.S. Geological Survey,
Federal Center, Box 25425, Denver, CO 80225

CONTENTS

Page

Abstract 1

Introduction 1

Geologic setting 2

Analytical procedures 6

  Chemical methods 6

  Q-mode method 7

Results and discussions 11

  Louis Lake batholith 11

Results and discussions—Continued

  Bears Ears pluton 26

  Comparison of the Louis Lake batholith and Bears Ears pluton 34

  Comparison to other Late Archean granitoids of Wyoming 35

Summary 36

References cited 37

ILLUSTRATIONS

Page

FIGURE 1. Index map of Wyoming showing areas of Precambrian uplift and location of uranium deposits in Tertiary rocks 2

2. Generalized geologic map of Wind River Range 3

3. Photographs of the Bears Ears pluton 4

4. Factor variance diagram for the Louis Lake batholith 17

5. Chondrite-normalized rare-earth-element diagrams for the Louis Lake batholith 18

6. Chondrite-normalized rare-earth-element diagrams for metamorphic rocks and igneous rocks 20

7. Stereographic projection of the three-factor Q-mode vector solution for the Louis Lake batholith 24

8. Q-Ab-Or ternary diagram for the Louis Lake batholith 24

9. Normative-feldspar ternary diagram for the Louis Lake batholith 24

10. Chondrite-normalized rare-earth-element diagrams for model phases fractionally crystallized from the Louis Lake batholith 28

11. Factor variance diagram for the Bears Ears pluton 30

12. Chondrite-normalized rare-earth-element diagrams for the Bears Ears pluton 32

13. Q-Ab-Or ternary diagram for the Bears Ears pluton 34

14. Normative-feldspar ternary diagram for the Bears Ears pluton 34

15. X-Y plots for data from the Louis Lake batholith and Bears Ears pluton 35

TABLES

Page

TABLE 1. Chemical data and CIPW normative mineralogy for samples from the Louis Lake batholith 8

2. Chemical data and CIPW normative mineralogy for samples from the Bears Ears pluton 10

3. Chemical data and CIPW normative mineralogy for miscellaneous samples of crystalline rocks 12

4. Statistical summary of chemical data for samples from the Louis Lake batholith and Bears Ears pluton 15

5. Proportions of total chemical variance in the Louis Lake batholith that could be accounted for by factor models with 2–10 end members 16

6. Proportional differences between original chemical data and data recomputed from the 3-end-member factor model for the Louis Lake batholith 22

7. Chemical compostions and CIPW normative mineralogy for the 3 end members of the factor model for the Louis Lake batholith 25

8. Mixing proportions for the 3-end-member factor model for the Louis Lake batholith 25

9. Possible mineralogy of solids fractionally crystallized from the Louis Lake batholith 26

10. Rare-earth-element contents of minerals in equilibrium with a proposed initial liquid for the Louis Lake batholith and for proposed solidus compositions 27

11. Proportions of total chemical variance in the Bears Ears pluton that could be accounted for by factor models with 2–10 end members 29

12. Proportional differences between original chemical data and data recomputed from the 5-end-member factor model for the Bears Ears pluton 31

CONVERSION FACTORS

For readers who wish to convert measurements from the metric system of units to U.S. customary units, the conversion factors are listed below.

Metric unit	Multiply by	To obtain U.S. customary unit
centimeter (cm)	0.3937	inch
meter (m)	3.281	foot
gram (g)	0.03527	ounce
kilogram (kg)	2.205	pound

PETROGENESIS OF TWO CONTRASTING, LATE ARCHEAN GRANITOIDS, WIND RIVER RANGE, WYOMING

By JOHN S. STUCKLESS

ABSTRACT

Data for two Late Archean granitoids from the Wind River Range, Wyoming, demonstrate contrasting petrogenetic histories. The Louis Lake batholith, the older unit, is an I-type granitoid that formed by partial melting of trondhjemitic to tonalitic protolith of Early Archean age. Melting and at least some crystallization took place at high pressure and water-saturated conditions. The chemistry of the batholith can be well approximated by a three-end-member mixing (unmixing) model in which an initial primitive granodioritic magma is differentiated by fractionation of two different solidus assemblages, possibly at two different pressures.

The Bears Ears pluton, the younger unit, is a coarsely porphyritic, S-type granite that formed by partial melting of a peraluminous and petrologically evolved protolith of Early to Middle Archean age. Some time prior to magma formation, the protolith preferentially lost labile elements, such as uranium and alkali metals, probably in response to granulite-facies metamorphism. Crystallization (and possibly partial melting) took place at much lower pressures than those that existed for the Louis Lake batholith, and at least end-stage crystallization probably occurred at water-saturated conditions.

Q-mode factor analysis of chemical data for the Bears Ears pluton shows that at least five end members are needed in any mixing model in order to approximate the chemical variations observed for the granite. Field relations and isotopic data indicate that contamination with xenolithic material is common, and therefore, much of the chemical variability may be due to incorporation of country rock. In addition, the magma may have been generated from an inhomogeneous metasedimentary section such that initial volumes of liquid were inhomogeneous and never mixed completely.

Unlike some Late Archean granitoids of Wyoming, neither the Louis Lake batholith nor the Bears Ears pluton is associated with uranium deposits, and isotopic studies have shown that neither unit lost large amounts of uranium that could be trapped by adjacent sedimentary formations. The lack of uranium favorability for the Louis Lake batholith is attributed to its I-type affinity. The high-grade metamorphic history and consequent depletion in labile elements for the protolith of the Bears Ears pluton probably prevented formation of a favorable source granite for uranium deposits. In addition, late magmatic loss of volatiles to pegmatites may have removed uranium that in favorable source rocks is loosely bound and easily lost to sedimentary traps.

INTRODUCTION

The Archean rocks of the Wyoming province are exposed as up-faulted blocks that form the cores of Laramide-age mountain ranges (fig. 1). The Wind River Range, which is the largest block of Precambrian rocks exposed in Wyoming, is about 200 km long and 60 km wide. Paleozoic and Mesozoic strata are asymetrically disposed about the Precambrian core; they dip gently off the eastern flank into the Wind River Basin and are folded and faulted against the Precambrian along the northern, western, and southern flanks. The southern and western boundaries of the range are marked by major faults that place Precambrian crystalline rocks over Paleozoic and Mesozoic rocks of the Green River Basin (fig. 2). Along the southern and western flanks of the range, the fault traces and the upturned and folded Paleozoic and Mesozoic strata are covered by younger deposits including Tertiary gravels and Pleistocene glacial materials. Most of the Precambrian rocks of the range are felsic gneisses and felsic igneous rocks, such as typify high-grade regional metamorphic terranes throughout the world. The southernmost part of the Range is made up of metavolcanic and metasedimentary rocks of greenschist facies.

The Archean felsic rocks of Wyoming have been proposed as source rocks for Cenozoic uranium deposits. The Wind River Basin contains large, sediment-hosted uranium deposits that are largely disposed around the flanks of the Granite Mountains (fig. 1). Studies by Rosholt and others (1973) and Stuckless and Nkomo (1978) have utilized uranium-thorium-lead isotopic systematics to demonstrate as much as 80 percent loss of uranium from apparently fresh granite to depths of 400 m. Similar studies of granites in the Owl Creek Mountains suggest that uranium in fracture fillings may have been derived from the enclosing granite (Stuckless, Nkomo, and Butt, 1986). Seeland (1976)

Manuscript approved for publication, June 14, 1988.

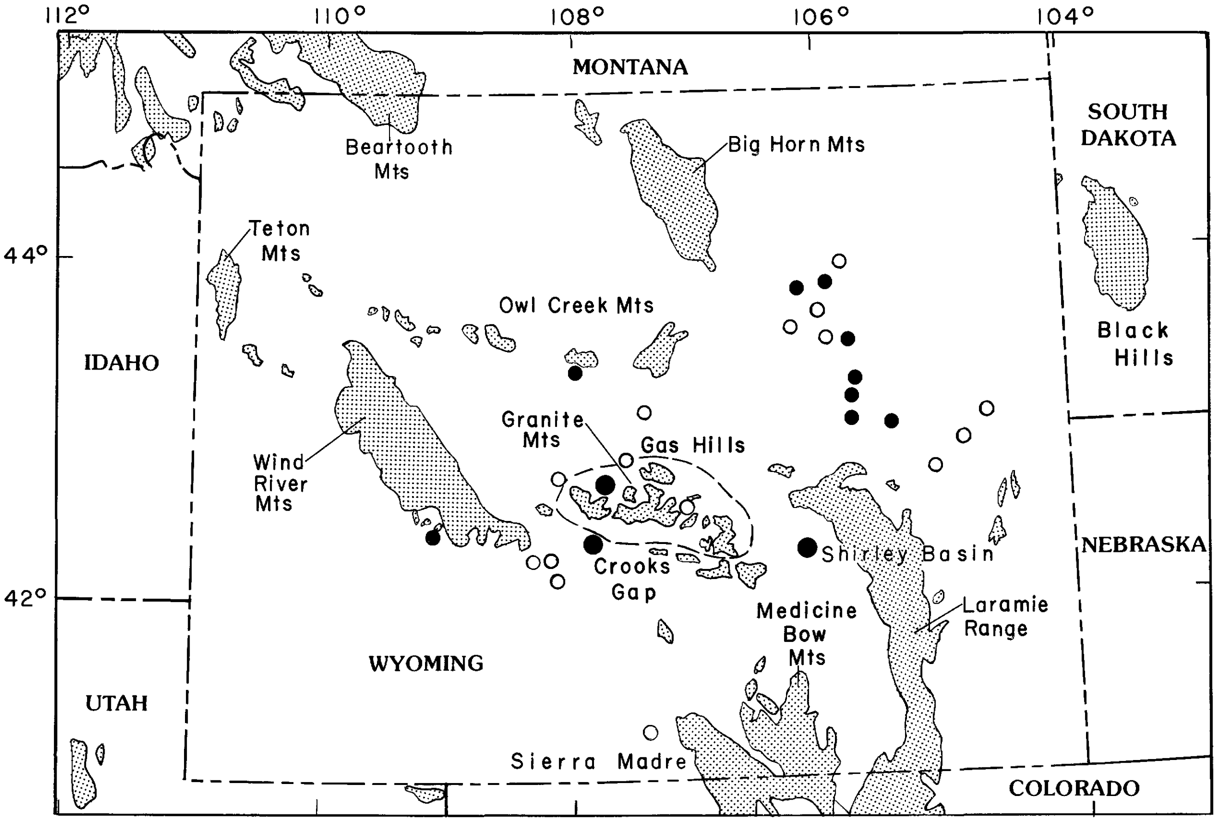

FIGURE 1.—Index map of Wyoming (from Stuckless and Nkomo, 1978) showing areas of Precambrian uplifts (patterned) and location of uranium deposits in Tertiary rocks (circles and dots). The large dots represent the three recently producing districts with reserves plus production of ore (U_3O_8 >0.1 percent) of over 1,000,000 tons. Deposits with ore reserves of 1,000–1,000,000 tons are shown by small dots, and deposits with reserves between 1 and 1,000 tons are shown by circles (uranium data from Butler, 1972).

has suggested that even uranium deposits in the Powder River Basin have Precambrian granite as a source rock.

Uranium deposits are not known to occur within sediments for which the provenance is the Wind River Range (Seeland, 1978), and uranium-thorium-lead isotopic studies indicate only minor losses of uranium from granitic units in this range during the Tertiary (Stuckless and others, 1985). Radioactive anomalies do exist within veins and pegmatites that cut the Precambrian rocks west and southwest of the main part of the range. Stuckless and others (1985) postulated that these may have formed from uranium-rich fluids that escaped from the Bears Ears pluton during end stages of crystallization. This hypothesis also accounts for the origin of a granite that is enriched in thorium but not uranium.

The petrogeneses of granitic rocks from the Granite Mountains and the Owl Creek Mountains have been modeled by extended Q-mode factor analysis (Stuckless and Miesch, 1981; Stuckless, Miesch, and Wenner, 1986). In each case, a complex origin was indicated such that five end members were needed in a mixing model to adequately account for the observed chemical variability. In addition, both studies identified several elements (including uranium) for which the current distribution of concentrations could not be well explained by a magmatic model. The current study was undertaken in part to see how the Late Archean plutonic rocks of the Wind River Range differ geochemically from similar aged granites that apparently supplied uranium to the Wind River Basin.

GEOLOGIC SETTING

Most of the core of the Wind River Range is composed of an igneous and high-grade metamorphic complex. Metamorphic grade ranges from amphibolite to granulite facies. Compositional types range from ultramafitolites to silexites, but felsic orthogneiss and paragneiss are the most common metamorphic types. Quartz diorites to granites are the most common plutonic types. Contacts between rock units are often gradational, and there is field evidence for injection, metasomatic

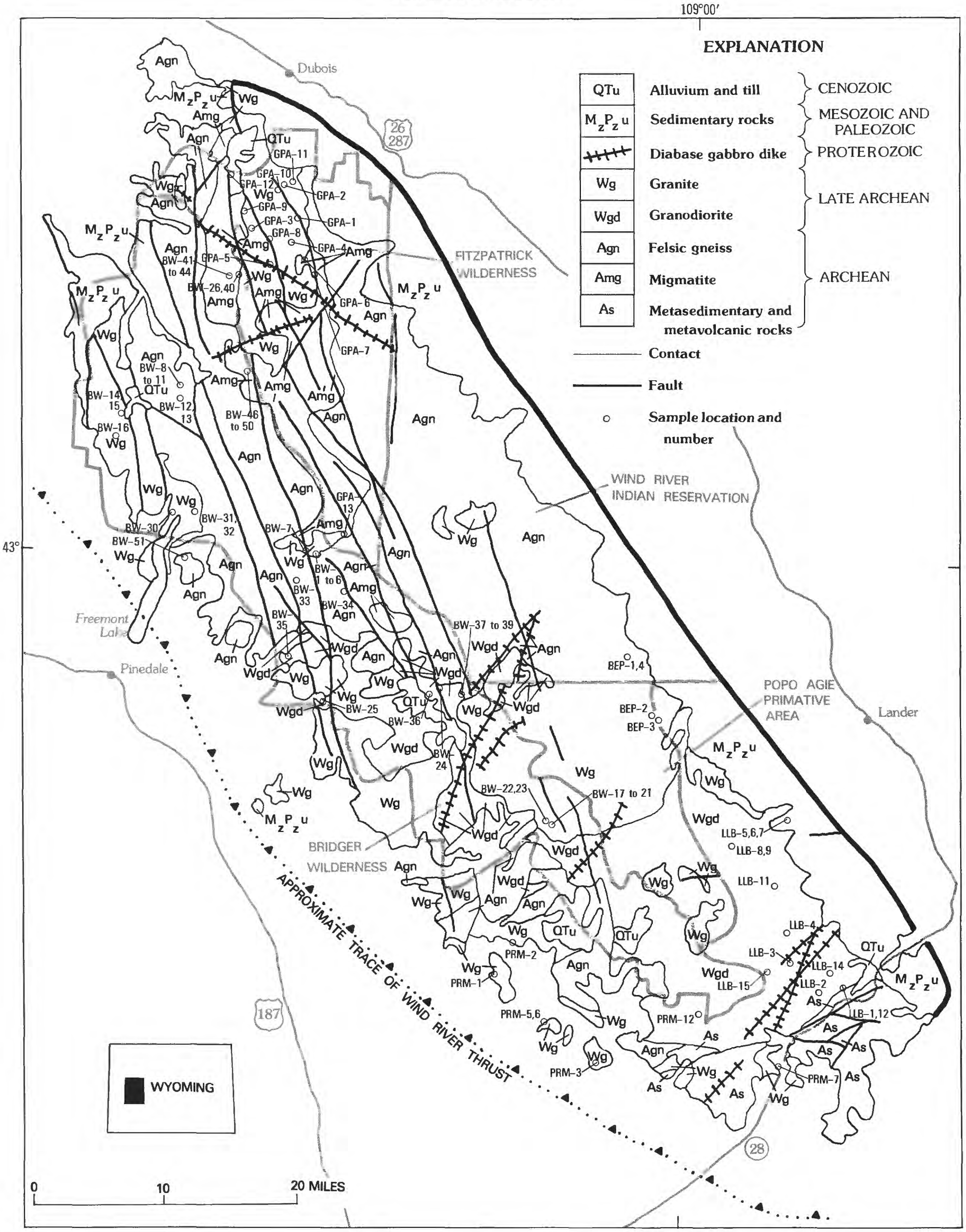

FIGURE 2.—Generalized geologic map of the Wind River Range showing sample locations and wilderness boundaries (from Stuckless and others, 1985).

alteration, and more than one period of penetrative deformation. An older and a younger generation of migmatites have been identified (Worl and others, 1984, 1986): the older one is generally layered, and the younger one is spatially related to the felsic intrusive rocks.

The oldest mappable unit of regional extent in the high-grade metamorphic complex is the layered migmatite (Pearson and others, 1971; Worl and others, 1986). A pyroxene granulite within this unit yields a zircon age of at least 3,300 Ma, and some zircon cores must have formed much earlier (J. N. Aleinikoff, written commun., 1987). The layered migmatite contains a very diverse group of rock types, including amphibolite, hornblende-biotite gneiss, taconite (banded iron-formation), metagabbro, biotite schist, ultramafic rocks, ferruginous-garnet gneiss, sillimanite gneiss, and diopside-hornblende gneiss. The regional migmatites and older felsic gneisses are intruded by metagabbro and ultramafic rocks. The youngest metamorphic rocks yield an age of about 2,670 Ma (J.N. Aleinikoff, written commun., 1985). Both younger and older metamorphic rocks are intruded by and converted to migmatites of the younger generation.

A band of greenschist-facies metasedimentary and metavolcanic rocks is exposed in the southern part of the range, and three mappable formations have been defined (Bayley, 1965a, b, c). The Goldman Meadow Formation is lowermost and contains an economic deposit of iron formation near Atlantic City. The Miners Delight Formation is uppermost and has been dated by the rubidium-strontium whole-rock method as 2,800 ± 100 Ma (Z.E. Peterman, written commun., 1982). The Roundtop Mountain Greenstone separates these two units. Lithologies similar to those of the greenstone formations occur as boudins within biotite gneiss in the northeastern part of the range (Granger and others, 1971), as boudins in migmatite in the north-central part of the range (Worl and others, 1986), and as bands in paragneiss in the southwestern part of the range (Worl and others, 1986). A paragneiss sequence that overlies a regional migmatite unit has been reported as possibly correlative with the greenschist-facies rocks in

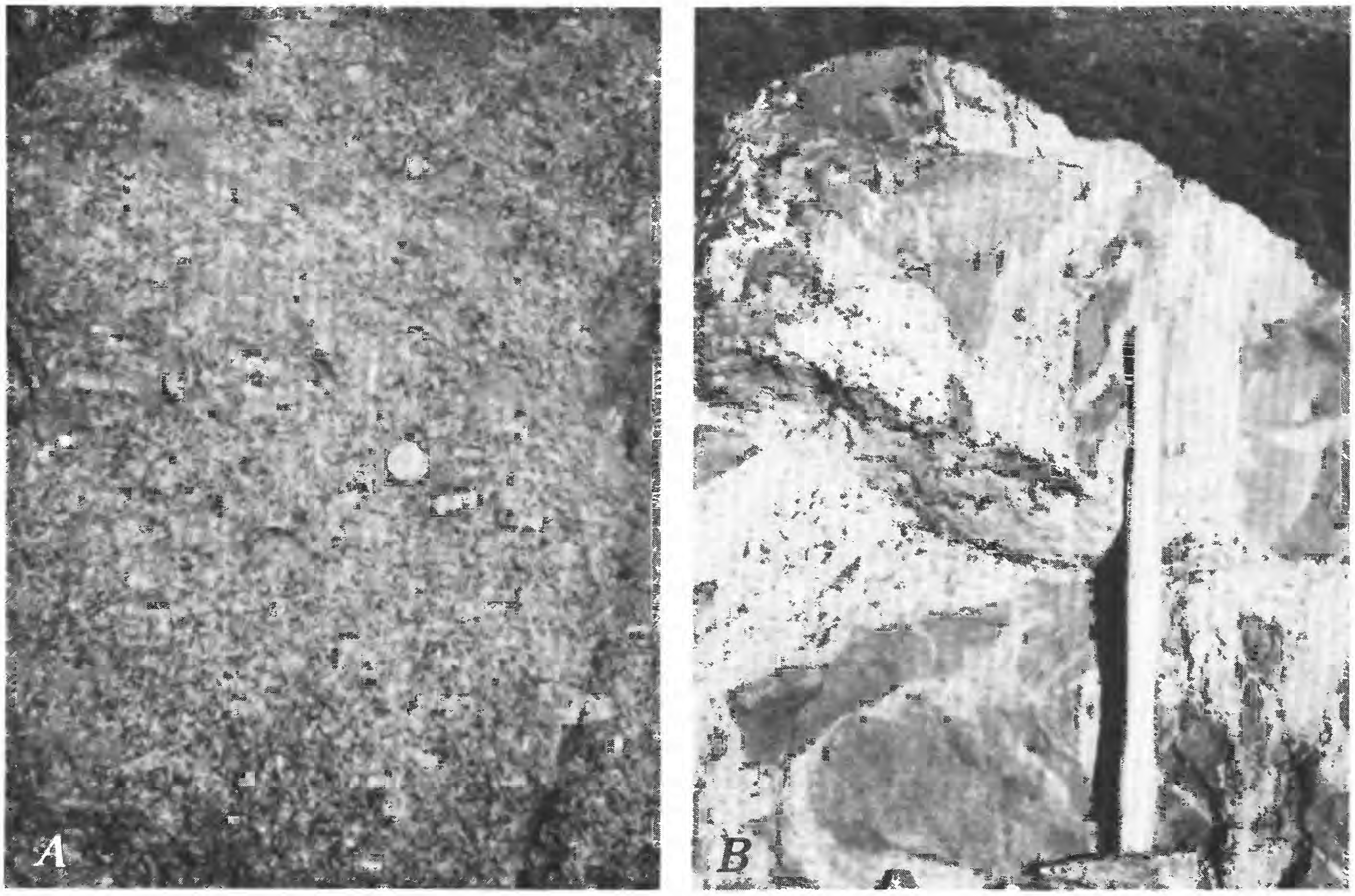

FIGURE 3 (above and facing page).—Photographs of the Bears Ears pluton: *A*, Typical coarsely porphyritic granite; *B*, Contact zone with orthogneiss near sample locality BW-51 (hammerhead is 15 cm long); *C*, Flow-banded section with abundant inclusions near sample locality BW-12; and *D*, Coarsely porphyritic granite near contact with the Louis Lake batholith (sample locality BW-39).

the southern part of the range (Pearson and others, 1971).

Orthogneisses in the northeastern part of the Wind River Range (east of the Fitzpatrick Wilderness in the Wilson Creek area) have yielded an approximate age of 2,800–3,000 Ma by the rubidium-strontium whole-rock method (Barker and others, 1979). These rocks are generally amphibolite grade but attain granulite grade north of Wilson Creek. Gneisses in the northern part of the range are cut by granitic pegmatites that yield rubidium-strontium mineral ages (as recalculated using decay constants of Steiger and Jager, 1977) of 2,000–2,795 Ma (Giletti and Gast, 1961; Bassett and Giletti, 1963). Recalculated potassium-argon ages for these minerals range from 1,485 to 2,420 Ma (Bassett and Giletti, 1963). The older rubidium-strontium ages and younger potassium-argon ages suggest that the granitic pegmatites are as old as 2,800 Ma and that the rocks of this region have been variably affected by secondary events which may be as young as Middle Proterozoic.

All the metamorphic units are cut by rocks of the Louis Lake batholith lithology. The Louis Lake batholith (Bayley, 1965a, b, c) is a fairly uniform granodiorite in the southern part of the range (Bayley and others, 1973), but quartz diorite to quartz monzonite varieties exist within the Popo Agie Wilderness to the north (Pearson and others, 1971) and within the Bridger Wilderness (Worl and others, 1986). Stuckless and others (1985) have summarized uranium-lead zircon ages as well as thorium-lead, uranium-lead, lead-lead, and rubidium-strontium whole-rock ages and have estimated a best age for the Louis Lake batholith as 2,545 ± 30 Ma. This age is concordant with a potassium-argon hornblende age of 2,640 Ma (Bayley and others, 1973), but potassium-argon biotite ages and rubidium-strontium mineral ages are all somewhat lower (Giletti and Gast, 1961; Naylor and others, 1970; Bayley and others, 1973). Initial lead and strontium isotopic compositions are consistent with derivation of the Louis Lake batholith from a trondhjemitic to tonalitic protolith of Early Archean age.

The youngest felsic unit is a coarsely porphyritic granite (fig. 3*A*) which has been variously called the Bears Ears pluton (Naylor and others, 1970), the Popo Agie batholith (Pearson and others, 1971), and the Middle Mountain batholith (Granger and others, 1971). All these authors noted that the contact of this plutonic unit with the country rock is invariably gradational over a distance of at least several meters (fig. 3*B*). In some

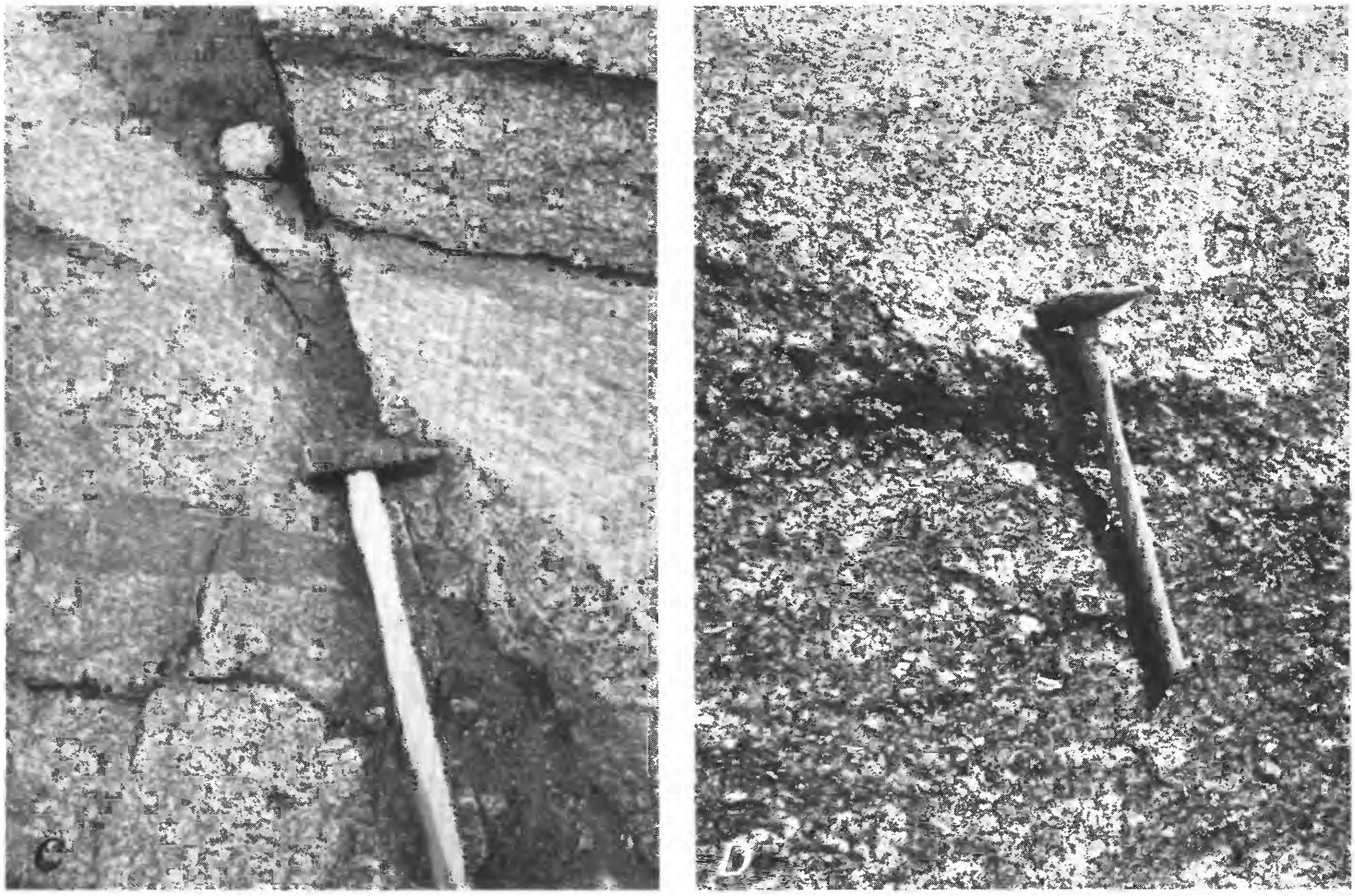

areas there is petrologic evidence that the granite has assimilated large amounts of preexisting rocks (fig. 3*C*) at a considerable distance from any apparent contact (Pearson and others, 1971). The rock is typically coarsely porphyritic with potassium feldspars which attain 5 cm in length (fig. 3*A*), but medium grained, equigranular granites are common in the Wind River Range and are genetically related to the porphyritic granite (Stuckless and others, 1985). In this report, all the late granitic intrusions are referred to by the earliest published name, the Bears Ears pluton (Naylor and others, 1970), even though few of the occurrences can be traced back to the Bears Ears locality.

Stuckless and others (1985) have reported a range in ages for the Bears Ears pluton of 2,504 ± 40 Ma to 2,575 ± 50 Ma as determined by uranium-lead in zircon and whole-rock thorium-lead, uranium-lead, lead-lead, and rubidium-strontium methods. The best estimated age is 2,545 ± 30 Ma. The scatter in apparent ages has been attributed to an isotopically inhomogeneous magma at the time of intrusion. The protolith for the Bears Ears pluton has been postulated to be younger and more evolved than that of the Louis Lake batholith, and the protolith may have been subjected to high-grade metamorphism prior to derivation of the granitic magma (Stuckless and others, 1985).

Diabase dikes were intruded as the last identifiable Precambrian event in the Wind River Range. Potassium-argon ages for whole-rock samples (recalculated with decay constants of Steiger and Jager, 1977) yield a range of 1,270–2,010 Ma (Condie and others, 1969). These authors interpreted the results for the entire Wyoming province as representing four periods of diabase emplacement; however, field studies throughout the Wind River Range indicate that all the dikes are either of one generation (Pearson and others, 1971; Bayley and others, 1973) or of no more than two generations (Worl and others, 1984). Potassium-argon ages for pyroxenes separated from the diabases of the southern part of the range yield ages of 1,660–1,880 Ma and are older than corresponding whole-rock ages (Spall, 1971). These ages, together with petrographic and paleomagnetic data, indicate only one period of diabase intrusion (Spall, 1971) and suggest that the spread in whole-rock ages is due to one or more younger thermal disturbances.

Peterman (1979) has postulated that a Proterozoic uplift reset potassium-argon and rubidium-strontium mineral ages south of a line which passes through the southern end of the Wind River Range. As a result, Archean rocks to the south of the line yield apparent ages that are generally less than 1,500 Ma, whereas those to the north yield apparent ages that are generally greater than 2,000 Ma. Potassium feldspars in granite from the Granite Mountains acquired radiogenic lead about 1,700 Ma (Stuckless and Nkomo, 1978), and hydrothermally altered samples lost lead at about the same time (Stuckless and others, 1982). These isotopic changes may be related to a non-rock-forming regional event that was possibly related to the plate collision along the Nash Fork-Mullen Creek shear zone to the south (Hills and Armstrong, 1974). Zircons and some whole-rock samples of granite from the Owl Creek Mountains (fig. 1) also record a nonrock forming event between 1,700 and 2,300 Ma (Hedge and others, 1986). Non-rock-forming events may have affected element distribution in rocks of at least the southern part of the Wind River Range after the last plutonic episode, and there may have been events of local extent as well.

Except for periods of uplift and erosion, post-Precambrian events have not been identified within the Wind River Range. Tertiary intrusive rocks do crop out several kilometers to the north in the Yellowstone region and a few kilometers south of the Precambrian exposures (Love and others, 1955).

ANALYTICAL PROCEDURES

CHEMICAL METHODS

Samples of granitic rock were collected from natural outcrops except in the southern part of the study area where several samples were collected from blasted road-cuts or quarries. Each sample was judged to be representative of the freshest material available at the sample locality. Large samples were taken to insure representativeness, especially for the very coarse grained rocks. Between 2 and 5 kg were ground to about -32 mesh and split. Analyses were made on aliquots from a 30-g split that had been ground to -200 mesh except as noted below.

Major-element concentrations (reported in weight percent, tables 1–3) were determined by high-precision XRF (X-ray fluorescence) on 0.8-g splits of fused sample powder according to the methods described by Taggart and others (1982). Abundances greater than 1 percent absolute are precise and accurate within ± 2 percent of the amount reported (2σ). The fourth digit reported for SiO_2 and Al_2O_3 is not significant for any single sample, but may be significant in a statistical treatment of the entire data set (A.T. Miesch, oral commun., 1980). Nine samples had reported values for P_2O_5 below the limit of detection (0.05) and were arbitrarily assigned a value of 0.02 for purposes of statistical and normative calculations. Iron concentrations were determined as total ferric iron, but for purposes of normative calculations, a ferric-ferrous ratio of 1:2 has been assumed (tables 1–3 and 8). Normative mineralogy was calculated according to the methods described by Stuckless and VanTrump (1979).

Nearly half of the samples used in the current study were analyzed for uranium and thorium by isotope dilution (Stuckless and others, 1985). Concentrations of uranium for the remaining samples were determined on 8- to 10-g splits of sample powder by the delayed-neutron technique (Millard, 1976). The precision and accuracy for individual determinations are dependent on counting statistics. These in turn are dependent on total weight of the sample aliquot, absolute concentrations, and relative proportions of uranium and thorium. Uranium contents obtained for this study are generally accurate to within ± 5 percent of the amount reported (2σ) for concentrations >1 ppm. Detection limit for a 10-g aliquot is 0.1 ppm U. Thorium contents for the samples not analyzed by isotope dilution were determined on approximately 600-g samples of coarsely crushed material (-32 mesh) by sealed-can gamma-ray spectrometry (Bunker and Bush, 1966). Although this method does not determine thorium directly, disequilibrium within the thorium decay chain is unlikely. Precision for thorium is better than plus or minus the quantity (2 percent of the amount reported plus 0.1 ppm absolute). Accuracies for the gamma-ray technique are generally equal to precision except where relative proportions of uranium, thorium, and potassium deviate markedly from normal (approximately by more than a factor of 10), in which case accuracy for the element with relatively low abundance is decreased. Because of the large sample, this technique provides measurements that are less susceptible to splitting errors that can produce anomalous results for trace-element contents in coarse-grained rocks.

Concentrations for rubidium and strontium for about a third of the samples were determined by isotope dilution (Stuckless and others, 1985). The remaining rubidium and strontium concentrations, as well as yttrium, zirconium, niobium, copper, and zinc contents, were determined by energy-dispersive XRF on loosely packed, finely ground (-200 mesh) sample powders (tables 1-3). Precision, as determined from replicate analyses, and presumably accuracy, as determined from a limited number of standards, is ±10.5 percent for zirconium, ±25.8 percent for yttrium, and ±42.9 percent for niobium at the concentration levels found for most of the samples used in the current study. Precisions and accuracy for copper and zinc determinations are presumed to be similar to those of niobium. Comparison of XRF and isotope-dilution results for rubidium and strontium shows that precision and accuracy for the XRF data are equal and that for concentrations >50 ppm results are precise to within ±3.2 and ±3.4 percent (2σ) of the amount reported, respectively. Errors for both elements increase to 100 percent at a concentration of about 5 ppm.

Concentrations of REE (rare-earth elements) and concentrations for a selected suite of trace elements (those listed in parts per million in tables 1-3, except as described above) were determined by instrumental activation analysis (INAA) by use of methods similar to those described by Gordon and others (1968). Samples were irradiated twice: once with a flux of 2.5×10^{13} neutrons per cm^2 followed by immediate counting, and once with a flux of 6.88×10^{16} neutrons per cm^2 followed by counting at about 7, 14, and 60 days. Data for any REE that were masked by interference in a given sample were obtained by interpolation of chondrite-normalized values of adjacent REE.

Accuracies for the values determined by INAA are estimated (on the basis of analyses of standards) to be ± 1 percent for tantalum, ± 2 percent for lanthanum, cerium, and neodymium, ± 3 percent for samarium, europium, ytterbium, scandium, and cobalt, ± 4 percent for terbium, hafnium, and antimony, ± 5 percent for dysprosium, lutetium, and cesium, ± 7 percent for thulium, and ± 14 percent for gadolinium. REE data reported in tables 1-3 have been adjusted within counting statistics to yield smooth chondrite-normalized REE patterns (Stuckless and Miesch, 1981). The chondrite values of Evensen and others (1978) have been used for normalization throughout this report.

Europium anomalies are reported as Eu/Eu* which is the ratio of the measured europium (Eu) to that calculated from the values of samarium and gadolinium so as to yield a smooth pattern through the middle REEs (Eu*). Thus Eu/Eu* of 1 is no europium anomaly; values less than 1 are referred to as negative anomalies, and values greater than 1 are referred to as positive anomalies.

Q-MODE METHOD

The mathematical modeling of the data was accomplished by use of the extended form of Q-mode factor analysis (Miesch, 1976a, b, 1981). This method has proved to be useful in examining the petrogenesis of Archean granitoids elsewhere in Wyoming (Stuckless and Miesch, 1981; Stuckless, Miesch, and Wenner, 1986) because it can be used to identify the number of end members (total number of liquidus and solidus assemblages) needed to describe the petrogenesis. The method can also be used in conjunction with petrographic data and other petrologic constraints to search for possible end-member compositions. The extended form of Q-mode analysis is particularly advantageous because it allows conversion of the scaled data (dimensionless numbers) back to its original form (weight percent) such that the results of modeling can be evaluated by standard petrologic techniques.

Prior to modeling, data for water content were eliminated and total iron was computed as ferrous iron because these variables do not usually retain a magmatic

TABLE 1.—*Chemical data and CIPW normative mineralogy for samples from the Louis Lake batholith*

[Norm calculated assuming one-third of the iron is oxidized. D index is differentiation index of Thornton and Tuttle (1960). PERAL is the molar ratio Al/(Na+K+Ca). PERALK is the molar ratio Al/(Na+K). Leaders (---) indicate no value]

Sample	BW-3	BW-4	BW-5	BW-7	BW-9	BW-11	BW-19
Weight percent							
SiO_2	68.67	69.70	70.76	60.66	72.67	63.71	68.81
Al_2O_3	15.24	15.66	14.95	17.00	14.53	15.51	15.96
FeO	3.60	2.43	2.54	3.48	1.76	5.87	3.59
MgO	.92	.86	.81	1.65	.44	1.88	.89
CaO	2.23	2.80	2.70	5.66	1.31	4.67	3.63
Na_2O	3.77	3.96	4.14	4.24	3.01	3.02	4.40
K_2O	4.38	3.85	3.40	5.82	5.58	3.42	1.70
TiO_2	.61	.23	.24	.57	.31	1.09	.66
P_2O_5	.15	.16	.13	.34	.12	.39	.17
Parts per million							
ThO_2	41.9	21.5	58.6	10.3	57.1	26.6	8.5
UO_2	3.5	2.3	1.7	2.9	3.2	3.2	2.1
CuO	62.4	62.2	62.2	62.0	10.1	63.6	62.0
ZnO	110.2	69.4	65.7	96.8	68.1	101.3	93.1
Rb_2O	130.2	86.5	85.4	97.2	226.0	93.4	50.8
SrO	583.4	779.6	645.5	1804.3	170.1	577.2	357.4
Y_2O_3	47.8	20.6	12.9	32.1	16.7	60.7	7.7
ZrO_2	623.8	195.9	211.0	120.1	296.9	612.6	284.0
Nb_2O_5	21.8	7.3	4.4	26.0	5.8	24.7	7.2
La_2O_3	168.2	99.1	133.5	101.9	106.1	114.3	43.8
Ce_2O_3	328.0	176.3	234.7	242.6	205.7	206.7	91.2
Nd_2O_3	132.5	60.0	76.4	116.3	76.0	85.8	32.3
Sm_2O_3	19.8	8.7	8.9	18.8	10.7	15.4	5.3
Eu_2O_3	2.8	1.9	1.8	4.5	1.4	3.6	1.8
Gd_2O_3	15.0	7.3	4.8	12.8	6.5	14.0	4.0
Tb_2O_3	1.8	.9	.6	1.4	.9	2.2	.5
Dy_2O_3	9.8	4.4	2.8	6.9	4.1	11.4	2.4
Tm_2O_3	.6	.3	.2	.4	.2	.9	.2
Yb_2O_3	3.5	1.8	1.0	2.0	1.4	5.8	1.1
Lu_2O_3	.5	.3	.1	.3	.2	.8	.2
Cs_2O	.5	.2	.3	.1	1.2	.6	.6
BaO	1590.0	1452.7	1138.4	1918.9	1305.1	1816.6	557.4
Ta_2O_5	1.3	.4	.2	2.3	.4	1.5	.6
HfO_2	13.6	5.2	5.6	3.3	8.8	15.2	8.0
Sc_2O_3	3.2	5.4	4.7	7.7	5.7	18.2	3.7
Cr_2O_3	6.1	14.0	13.7	25.7	1.0	29.1	16.2
CoO	8.6	6.0	6.0	11.4	3.0	17.5	8.0
MnO	356.0	369.3	417.9	978.5	179.2	640.8	364.1
CIPW norms (weight percent)							
Q	22.16	23.50	25.56	1.52	29.56	18.74	26.30
C	.49	.18	---	---	1.36	---	.66
Z	.09	.03	.03	.02	.05	.09	.04
Or	26.36	23.23	20.43	34.95	33.38	20.66	10.18
Ab	31.77	33.36	34.90	35.76	25.40	25.30	36.97
An	10.00	12.78	11.93	9.77	5.67	18.15	16.77
Wo	---	---	.23	6.66	---	.95	---
En	2.27	2.14	2.01	4.08	1.08	4.64	2.20
Fs	3.38	2.60	2.72	3.43	1.64	5.34	3.30
Mt	1.92	1.30	1.36	1.87	.94	3.12	1.92
Cm	0	0	0	0	---	0	0
Il	1.15	.44	.46	1.07	.59	2.05	1.24
Ap	.36	.38	.31	.81	.29	.91	.40
Cc	---	---	---	---	---	---	---
Total ..	99.95	99.95	99.96	99.94	99.96	99.95	99.99
salic	90.87	93.08	92.86	82.01	95.42	82.94	90.92
femic	9.08	6.87	7.10	17.93	4.54	17.01	9.07
D index ..	80.28	80.09	80.89	72.23	88.34	64.7	73.44
PERAL	1.01	.99	.97	.72	1.08	.90	1.02
PERALK ...	1.38	1.45	1.42	1.27	1.31	1.76	1.75

TABLE 1.—*Chemical data and CIPW normative mineralogy for samples from the Louis Lake batholith*—Continued

[Norm calculated assuming one-third of the iron is oxidized. D index is differentiation index of Thornton and Tuttle (1960). PERAL is the molar ratio Al/(Na+K+Ca). PERALK is the molar ratio Al/(Na+K). Leaders (---) indicate no value]

Sample	BW-22	BW-24	GPA-1	GPA-6	LLB-2	LLB-3	LLB-4
Weight Percent							
SiO_2	67.82	63.72	75.23	70.42	66.59	65.96	64.70
Al_2O_3	15.41	16.59	13.51	16.19	16.29	16.29	16.29
FeO	3.71	5.02	1.84	2.34	3.82	3.96	4.98
MgO	.97	1.87	.20	.67	1.52	1.72	1.94
CaO	2.96	5.25	1.65	2.49	3.34	3.84	4.30
Na_2O	4.05	4.35	3.13	4.13	4.35	4.45	3.91
K_2O	3.66	1.63	4.10	3.14	2.83	2.43	2.45
TiO_2	.73	.78	.09	.28	.61	.67	.72
P_2O_5	.28	.43	.05	.05	.26	.31	.31
Parts per million							
ThO_2	38.4	15.2	32.4	22.0	18.0	10.1	17.0
UO_2	1.8	.7	4.0	3.8	4.0	3.0	3.2
CuO	62.1	62.3	181.2	67.5	62.1	62.1	62.5
ZnO	85.7	122.6	54.2	81.0	85.7	103.3	43.1
Rb_2O	85.2	56.6	119.5	122.3	71.9	65.3	63.5
SrO	563.8	1051.8	100.5	589.2	935.9	999.0	1024.1
Y_2O_3	29.6	41.3	6.4	12.9	23.1	28.3	18.1
ZrO_2	474.4	300.4	140.8	217.0	267.9	282.9	316.5
Nb_2O_5	14.5	10.2	4.3	8.7	10.1	11.6	7.3
La_2O_3	165.8	75.2	45.2	39.9	75.5	48.0	82.0
Ce_2O_3	326.8	164.2	77.8	77.1	140.6	112.0	148.0
Nd_2O_3	138.8	83.9	28.2	30.8	57.7	57.5	58.9
Sm_2O_3	20.8	17.2	4.0	5.3	9.1	11.8	9.5
Eu_2O_3	2.8	3.3	1.1	1.2	2.3	2.7	2.5
Gd_2O_3	15.7	13.5	2.6	4.2	5.7	8.6	7.0
Tb_2O_3	1.7	1.8	.3	.5	.8	1.2	1.0
Dy_2O_3	7.4	8.6	1.6	2.8	4.1	6.8	5.1
Tm_2O_3	.5	.5	.1	.2	.3	.4	.3
Yb_2O_3	2.9	2.6	.4	1.1	1.8	2.1	1.8
Lu_2O_3	.4	.4	.1	.2	.3	.3	.2
Cs_2O	.4	.2	.4	2.0	1.7	1.1	1.7
BaO	1446.4	979.4	991.1	1282.9	1536.6	1355.5	1450.2
Ta_2O_5	1.1	1.0	.2	.3	.9	1.0	.7
HfO_2	14.2	8.2	3.0	5.4	6.3	6.2	6.9
Sr_2O_3	14.0	16.0	1.9	4.4	9.5	10.8	12.2
Cr_2O_3	26.9	17.8	18.8	21.3	20.3	19.4	37.1
CoO	8.4	14.5	2.9	4.4	12.4	12.1	14.8
MnO	479.6	607.0	172.5	249.5	552.8	452.0	702.5
CIPW norms (weight percent)							
Q	21.25	17.29	36.25	26.47	20.94	19.92	18.96
C	---	---	1.02	1.41	.55	.08	.22
Z	.07	.04	.02	.03	.04	.04	.05
Or	22.06	9.94	24.51	18.96	17.39	14.83	14.86
Ab	34.06	36.48	26.46	35.13	36.99	37.63	32.49
An	12.73	20.59	7.83	11.98	14.85	16.82	18.86
Wo	0	1.04	---	---	---	---	---
En	2.41	4.62	.50	1.66	3.80	4.28	4.78
Fs	3.34	4.84	2.10	2.40	1.24	1.46	4.89
Mt	1.98	2.67	.98	1.25	3.39	2.78	2.65
Cm	0	0	0	0	0	.04	.01
Il	1.38	1.47	.17	.54	.12	1.27	1.36
Ap	.67	1.00	.12	.12	.63	.74	.72
Cc	---	---	---	---	.02	.07	.11
Total ..	99.96	99.98	99.96	99.95	99.95	99.96	99.96
salic	90.17	84.35	96.09	93.98	90.75	89.33	85.43
femic	9.78	15.64	3.88	5.97	9.20	10.64	14.53
D index ..	77.38	63.71	87.22	80.56	75.31	72.39	66.31
PERAL	.96	.90	1.07	1.09	.99	.96	.96
PERALK ...	1.44	1.85	1.40	1.56	1.58	1.62	1.79

distribution in plutonic rocks. The remaining oxides were summed to 100 percent. At the start of mathematical analysis, the original data were scaled on the basis of mean and standard deviation (table 4) such that each variable had the same mean and variance. This ensures that major-oxide data, especially SiO_2 and Al_2O_3, and widely varying oxide data, such as Cr_2O_3, would have no greater influence on the final model than data for minor constituents or constituents with only limited variability.

Q-mode factor analysis differs from standard petrologic approaches in that all variables can be

TABLE 1.—*Chemical data and CIPW normative mineralogy for samples from the Louis Lake batholith*—Continued

[Norm calculated assuming one-third of the iron is oxidized. D index is differentiation index of Thornton and Tuttle (1960). PERAL is the molar ratio Al/(Na+K+Ca). PERALK is the molar ratio Al/(Na+K). Leaders (---) indicate no value]

Sample	LLB-5	LLB-7	LLB-8	LLB-9	LLB-11	LLB-12	LLB-15
Weight percent							
SiO_2	65.68	59.45	66.05	73.00	65.06	72.17	64.93
Al_2O_3	15.97	16.88	15.02	14.28	16.22	14.72	16.23
FeO	5.05	6.44	5.38	2.09	4.88	2.05	5.01
MgO	1.61	3.54	1.12	.05	1.81	.78	1.80
CaO	3.94	5.62	2.94	1.84	4.25	2.28	4.36
Na_2O	4.32	4.15	3.25	3.02	4.23	3.63	4.31
K_2O	2.00	2.11	4.59	5.03	2.26	3.77	1.96
TiO_2	.65	1.02	.92	.29	.60	.22	.71
P_2O_5	.40	.40	.30	.10	.30	.10	.30
Parts per million							
ThO_2	14.4	24.5	73.5	51.4	16.2	17.4	11.1
UO_2	5.9	4.0	8.3	4.9	6.9	2.5	3.6
CuO	61.6	62.0	88.9	96.9	61.8	64.3	61.5
ZnO	112.5	68.0	40.4	55.1	107.8	60.2	132.2
Rb_2O	113.1	124.9	180.8	149.5	71.6	131.2	55.9
SrO	905.0	697.0	349.1	322.2	962.4	641.3	1029.7
Y_2O_3	33.2	29.5	64.4	19.2	32.0	15.4	20.4
ZrO_2	245.6	353.7	766.1	268.9	292.5	157.9	320.8
Nb_2O_5	12.9	14.5	42.1	18.7	13.0	7.2	10.0
La_2O_3	50.0	106.6	213.0	75.2	66.9	37.4	57.9
Ce_2O_3	118.8	207.2	410.0	139.0	140.4	74.1	122.1
Nd_2O_3	63.6	80.8	155.0	52.3	69.0	31.2	56.2
Sm_2O_3	13.3	12.3	28.0	8.2	12.6	4.8	10.4
Eu_2O_3	2.7	2.8	3.3	1.3	2.8	1.1	2.6
Gd_2O_3	8.8	7.1	18.3	4.8	8.6	3.3	7.3
Tb_2O_3	1.2	.9	2.8	.7	1.1	.5	.9
Dy_2O_3	6.5	5.2	15.0	4.2	6.2	2.7	4.8
Tm_2O_3	.4	.4	.9	.3	.4	.2	.3
Yb_2O_3	2.3	2.4	5.1	1.9	2.6	1.5	1.8
Lu_2O_3	.3	.4	.7	.3	.4	.2	.2
Cs_2O	4.3	4.1	2.2	1.3	2.8	3.6	2.2
BaO	1244.7	572.3	1370.6	1526.8	1270.7	1215.3	1129.9
Ta_2O_5	1.3	1.1	3.4	1.7	1.4	1.4	.7
HfO_2	7.7	8.0	18.9	7.1	6.6	3.6	7.4
Sc_2O_3	11.0	16.9	10.6	5.4	12.6	4.3	11.9
Cr_2O_3	36.8	137.6	24.0	16.5	38.4	17.5	37.3
CoO	12.0	25.5	9.9	3.9	13.3	4.7	14.1
MnO	689.9	1274.1	524.0	225.9	690.2	437.3	692.2
CIPW norms (weight percent)							
Q	20.40	8.84	19.67	31.06	18.29	29.51	18.62
C	.42	---	---	.67	---	.68	---
Z	.04	.05	.12	.04	.04	.02	.05
Or	12.16	12.56	27.37	30.18	13.69	22.66	11.92
Ab	36.25	34.69	27.24	25.45	35.52	30.62	36.17
An	16.77	20.89	12.49	8.45	18.22	10.61	18.79
Wo	---	1.70	0	---	.31	---	.30
En	3.97	8.72	2.76	.12	4.48	1.93	4.46
Fs	5.10	6.25	5.01	2.07	4.98	2.17	4.96
Mt	2.69	3.42	2.86	1.12	2.59	1.09	2.67
Cm	.01	.02	0	0	.01	0	.01
Il	1.23	1.92	1.74	.55	1.14	.42	1.34
Ap	.94	.95	.71	.24	.71	.24	.71
Cc	---	---	---	---	---	---	---
Total	99.97	100.00	99.96	99.95	99.97	99.96	99.97
salic	86.04	77.02	86.88	95.84	85.75	94.10	85.54
femic	13.93	22.98	13.08	4.11	14.22	5.86	14.43
D index	68.81	56.09	74.27	86.69	67.49	82.78	66.70
PERAL	.97	.87	.95	1.03	.94	1.03	.94
PERALK	1.71	1.85	1.44	1.36	1.71	1.45	1.75

TABLE 1.—*Chemical data and CIPW normative mineralogy for samples from the Louis Lake batholith*—Continued

[Norm calculated assuming one-third of the iron is oxidized. D index is differentiation index of Thornton and Tuttle (1960). PERAL is the molar ratio Al/(Na+K+Ca). PERALK is the molar ratio Al/(Na+K). Leaders (---) indicate no value]

Sample	PRM-1	PRM-2	PRM-3	PRM-5	PRM-6
Weight percent					
SiO_2	69.80	70.51	73.59	72.41	62.57
Al_2O_3	15.03	15.49	14.02	14.38	14.90
FeO	2.87	1.98	1.73	2.34	5.76
MgO	.85	.78	.41	.51	2.25
CaO	1.92	2.11	1.16	1.84	4.01
Na_2O	3.23	3.72	3.20	3.02	2.96
K_2O	5.14	4.32	5.37	4.88	4.99
TiO_2	.48	.47	.15	.21	1.10
P_2O_5	.22	.22	.10	.05	.81
Parts per million					
ThO_2	74.3	29.3	57.2	21.2	60.9
UO_2	4.9	1.4	7.5	2.1	6.1
CuO	107.3	61.7	63.2	61.7	62.6
ZnO	52.7	85.1	39.8	51.3	108.0
Rb_2O	132.4	93.5	152.2	101.2	131.7
SrO	675.2	735.1	541.2	903.9	1051.4
Y_2O_3	26.9	6.4	13.1	7.7	45.4
ZrO_2	429.2	417.1	207.4	254.0	557.1
Nb_2O_5	15.9	8.6	4.4	4.3	26.3
La_2O_3	171.3	107.8	61.9	61.6	241.8
Ce_2O_3	314.6	191.0	101.9	104.4	472.3
Nd_2O_3	116.9	64.2	39.6	35.8	194.1
Sm_2O_3	15.8	8.6	6.7	4.5	28.6
Eu_2O_3	2.0	2.0	.9	1.0	4.9
Gd_2O_3	9.0	4.2	3.6	2.3	16.7
Tb_2O_3	1.1	.5	.5	.3	1.8
Dy_2O_3	5.5	2.1	2.7	1.5	8.6
Tm_2O_3	.3	.1	.2	.1	.5
Yb_2O_3	1.6	.4	1.1	.6	3.0
Lu_2O_3	.2	.1	.2	.1	.4
Cs_2O	.8	1.5	1.8	.9	1.4
BaO	2049.7	1830.4	1058.7	1740.5	2655.5
Ta_2O_3	1.1	.4	.8	.3	1.9
HfO_2	9.8	7.9	5.7	6.8	13.1
Sc_2O_3	2.5	5.5	1.9	2.2	18.8
Cr_2O_3	14.1	9.6	11.8	17.6	56.7
CoO	7.4	5.2	2.9	4.1	17.0
MnO	255.3	205.2	177.0	214.3	659.1
CIPW norms (weight percent)					
Q	25.77	26.11	30.44	29.97	13.94
C	1.08	1.28	1.00	.79	---
Z	.06	.06	.03	.04	.08
Or	31.15	26.25	32.05	29.37	30.22
Ab	27.32	31.51	26.97	25.45	24.83
An	8.00	8.98	5.09	8.77	12.04
Wo	---	---	---	---	1.03
En	2.11	1.96	1.02	1.27	5.54
Fs	.78	1.60	1.88	2.49	5.21
Mt	2.19	.76	.92	1.25	3.07
Cm	0	0	0	0	.01
Il	.92	.90	.29	.40	2.08
Ap	.53	.52	.24	.12	1.89
Cc	.02	.02	---	---	---
Total	99.93	99.94	99.96	99.94	99.94
salic	93.38	94.18	95.60	94.40	81.11
femic	6.55	5.76	4.36	5.54	18.83
D index	84.24	83.87	89.47	84.79	68.99
PERAL	1.04	1.05	1.06	1.05	.84
PERALK	1.36	1.42	1.26	1.39	1.43

considered simultaneously without preassigning interdependence as is done, for example, when several oxides are recast as a single mineral or when three variables are summed to 100 and plotted on a ternary diagram. The method is fully described in the references listed above. The following paragraph provides a brief geometric description of the mathematical process.

TABLE 2.—*Chemical data and CIPW normative mineralogy for samples from the Bears Ears pluton*

[Norm calculated assuming one-third of the iron is oxidized. D index is differentiation index of Thornton and Tuttle (1960). PERAL is the molar ratio Al/(Na+K+Ca). PERALK is the molar ratio Al/(Na+K). Leaders (---) indicate no value]

Sample	BEP-1	BEP-2	BEP-3	BEP-4	BW-15	BW-16	BW-18
Weight percent							
SiO_2	68.46	75.47	70.08	71.49	70.17	71.01	73.01
Al_2O_3	15.08	13.48	14.80	14.92	14.75	13.92	13.86
FeO	3.94	1.09	3.21	2.12	2.88	3.33	2.11
MgO	1.43	.23	1.11	.43	.80	.93	.60
CaO	2.65	1.41	3.02	1.81	2.38	2.45	2.16
Na_2O	3.67	3.12	3.73	3.73	3.11	3.09	3.14
K_2O	3.57	4.73	3.12	4.74	4.74	4.12	4.23
TiO_2	.59	.15	.48	.33	.56	.60	.43
P_2O_5	.26	.07	.19	.11	.20	.20	.14
Parts per million							
ThO_2	42.4	7.9	18.6	112.7	61.4	82.4	49.4
UO_2	4.7	1.1	1.8	6.7	3.7	3.7	2.4
CuO	62.5	61.7	61.8	61.8	62.2	63.4	66.9
ZnO	46.9	35.1	80.2	41.4	59.3	59.3	36.4
Rb_2O	95.8	117.8	106.8	180.8	128.7	93.1	102.5
SrO	549.4	246.3	264.4	267.1	416.3	343.8	371.9
Y_2O_3	34.9	5.1	16.6	7.7	37.4	36.0	15.4
ZrO_2	286.3	115.5	223.1	303.7	472.8	406.4	299.6
Nb_2O_5	18.9	4.3	10.1	10.1	11.6	11.6	7.2
La_2O_3	108.7	20.9	56.8	147.0	157.6	141.0	165.2
Ce_2O_3	221.6	35.2	108.1	284.3	296.3	249.0	292.8
Nd_2O_3	81.3	13.1	40.1	94.7	120.6	96.8	102.1
Sm_2O_3	13.7	1.9	6.8	12.0	17.8	14.4	12.4
Eu_2O_3	2.2	1.0	1.3	1.6	3.2	2.5	2.2
Gd_2O_3	9.9	1.4	5.2	5.2	13.6	10.5	8.7
Tb_2O_3	1.3	.2	.8	.6	1.5	1.3	.9
Dy_2O_3	6.3	1.2	4.2	2.9	7.6	6.4	4.1
Tm_2O_3	.4	.1	.1	.1	.5	.4	.2
Yb_2O_3	2.5	.4	1.4	.7	2.7	2.5	1.2
Lu_2O_3	.4	.1	.2	.1	.4	.4	.2
Cs_2O	.5	.5	1.1	1.0	1.3	.2	.6
BaO	1433.2	1584.2	948.9	1238.3	1806.3	1422.8	1238.0
Ta_2O_5	1.6	.3	.6	.4	.9	.5	.4
HfO_2	7.3	2.8	5.8	7.7	12.2	11.4	8.7
Sc_2O_3	9.5	.8	10.7	3.9	7.6	10.9	6.0
Cr_2O_3	25.3	4.9	23.1	2.4	14.1	12.1	11.8
CoO	10.7	2.5	9.5	4.3	6.7	8.6	4.9
MnO	413.1	150.7	491.5	296.9	353.7	385.9	247.3
CIPW norms (weight percent)							
Q	26.00	35.58	27.55	27.41	27.14	30.10	32.74
C	1.09	.87	.22	1.19	.53	.31	.45
Z	.04	.02	.03	.04	.07	.06	.05
Or	21.56	28.51	18.79	28.38	28.76	24.97	25.54
Ab	30.98	26.38	31.51	31.49	26.44	26.33	26.60
An	10.88	6.14	13.67	6.48	10.54	10.87	9.81
En	3.55	.58	2.76	1.08	2.00	2.33	1.51
Fs	.53	.55	2.44	.89	1.52	1.84	1.08
Mt	3.39	.71	1.61	1.46	1.40	1.62	1.03
Cm	0	0	0	0	0	0	0
Il	1.12	.29	.92	.63	1.06	1.14	.83
Ap	.63	.17	.45	.26	.48	.48	.34
Cc	.19	.14	.02	.64	---	---	---
Total	99.96	99.94	99.97	99.96	99.94	99.96	99.96
salic	90.56	97.51	91.77	95.00	93.47	92.55	95.18
femic	9.40	2.44	8.20	4.96	6.47	7.41	4.78
D index	78.54	90.47	77.85	87.28	82.33	81.30	84.87
PERAL	1.02	1.04	.98	1.02	1.00	.99	1.01
PERALK	1.51	1.30	1.55	1.31	1.42	1.44	1.41

TABLE 2.—*Chemical data and CIPW normative mineralogy for samples from the Bears Ears pluton*—Continued

[Norm calculated assuming one-third of the iron is oxidized. D index is differentiation index of Thornton and Tuttle (1960). PERAL is the molar ratio Al/(Na+K+Ca). PERALK is the molar ratio Al/(Na+K). Leaders (---) indicate no value]

Sample	GPA-2	GPA-3	GPA-4	GPA-5	GPA-8	GPA-9	GPA-10
Weight percent							
SiO_2	73.53	73.25	71.74	75.29	67.71	73.19	74.33
Al_2O_3	13.87	14.22	14.45	13.21	16.96	14.01	14.03
FeO	2.39	2.31	2.76	.81	3.36	2.47	1.76
MgO	.30	.41	.69	.31	1.12	.41	.57
CaO	1.41	1.57	.70	.42	2.86	1.02	.55
Na_2O	2.72	3.05	3.44	1.94	4.04	2.66	3.05
K_2O	5.26	4.71	5.52	7.69	3.02	5.67	5.17
TiO_2	.22	.18	.30	.08	.49	.27	.26
P_2O_5	.05	.05	.10	.05	.20	.05	.05
Parts per million							
ThO_2	38.3	47.7	85.8	12.2	31.7	91.6	62.3
UO_2	7.2	3.0	6.7	2.0	2.8	3.1	9.9
CuO	79.5	137.1	81.7	62.5	62.7	62.7	62.7
ZnO	42.7	56.8	39.3	40.6	42.0	47.1	57.2
Rb_2O	172.0	159.7	163.8	252.8	172.1	175.6	174.4
SrO	228.9	214.7	178.4	120.4	155.9	114.9	158.3
Y_2O_3	9.0	15.5	20.7	3.9	10.4	22.1	11.7
ZrO_2	204.2	315.1	380.0	59.1	263.7	230.7	254.0
Nb_2O_5	4.3	8.7	4.4	8.7	5.8	5.9	5.8
La_2O_3	11.2	61.3	91.7	9.8	46.3	136.9	25.0
Ce_2O_3	21.9	112.7	159.4	14.4	93.5	241.1	46.6
Nd_2O_3	9.7	39.0	50.7	5.8	33.8	78.3	16.5
Sm_2O_3	1.8	6.3	7.6	1.4	6.1	12.9	2.8
Eu_2O_3	1.3	1.1	1.3	.7	1.4	1.2	.9
Gd_2O_3	1.7	4.4	5.2	1.5	5.0	8.1	2.2
Tb_2O_3	.3	.6	.7	.2	.8	1.1	.4
Dy_2O_3	1.7	3.2	4.1	1.5	4.4	5.7	2.2
Tm_2O_3	.1	.1	.3	.1	.3	.3	.2
Yb_2O_3	1.0	.7	1.9	.8	1.9	1.6	1.1
Lu_2O_3	.1	.1	.3	.1	.3	.2	.2
Cs_2O	1.1	.9	.8	.6	.9	1.1	.5
BaO	1373.0	1039.6	1206.2	1318.8	967.6	1091.6	1221.0
Ta_2O_5	.3	.4	.5	.6	.5	.8	.5
HfO_2	6.7	5.7	9.5	2.4	9.0	8.8	6.5
Sc_2O_3	3.4	4.4	5.3	3.7	7.6	5.5	3.9
Cr_2O_3	18.1	19.0	96.4	17.4	23.6	43.2	15.2
CoO	4.0	4.3	4.6	1.6	7.1	3.7	3.8
MnO	248.6	197.8	218.5	111.8	258.6	212.6	139.9
CIPW norms (weight percent)							
Q	33.17	32.77	27.07	32.84	24.06	32.47	34.08
C	1.20	1.30	1.68	1.01	2.19	1.70	2.40
Z	.03	.05	.06	.01	.04	.04	.04
Or	31.67	28.27	33.14	45.98	18.27	33.96	31.08
Ab	23.08	25.82	29.37	16.39	34.66	22.55	26.00
An	6.69	7.49	2.83	1.74	12.89	4.75	2.41
En	.75	1.01	1.73	.76	2.81	1.02	1.43
Fs	1.65	1.65	1.89	.56	2.01	1.65	1.06
Mt	1.16	1.12	1.38	.38	1.63	1.19	.85
Cm	0	0	.02	0	0	.01	0
Il	.42	.35	.56	.15	.93	.51	.49
Ap	.12	.12	.24	.12	.49	.12	.12
Cc	---	---	---	---	---	---	---
Total	99.95	99.96	99.96	99.95	99.97	99.96	99.95
salic	95.84	95.70	94.14	97.96	92.10	95.47	96.01
femic	4.11	4.26	5.81	1.99	7.87	4.49	3.94
D index	87.92	86.87	89.58	95.20	76.99	88.99	91.16
PERAL	1.08	1.09	1.11	1.07	1.11	1.13	1.19
PERALK	1.36	1.40	1.23	1.14	1.69	1.32	1.31

In Q-mode factor analysis, the data for each sample define a vector in *M*-dimensional space, where *M* is the number of oxide variables. All sample vectors have a common origin, and the vector cluster always occupies the full *M*-dimensional space. However, if the petrogenesis involved mixing (or unmixing) of only two end members, the *M* vectors would cluster tightly about a plane, and as such, the vector cluster could be projected onto that plane with little or no loss of information. Similarly, if the mixing process involved three end members, vectors would cluster tightly in three-dimensional space, and they could be projected

TABLE 2.—*Chemical data and CIPW normative mineralogy for samples from the Bears Ears pluton*—Continued

[Norm calculated assuming one-third of the iron is oxidized. D index is differentiation index of Thornton and Tuttle (1960). PERAL is the molar ratio Al/(Na+K+Ca). PERALK is the molar ratio Al/(Na+K). Leaders (---) indicate no value]

Sample	GPA-11	GPA-12	GPA-13	PRM-7
		Weight percent		
SiO_2	74.97	72.73	73.24	76.21
Al_2O_3	13.55	14.09	14.51	13.00
FeO	1.87	2.88	2.46	.92
MgO	.54	.31	.80	.10
CaO	.22	1.07	2.71	.36
Na_2O	3.02	2.67	3.69	2.60
K_2O	5.41	5.84	2.05	6.65
TiO_2	.17	.18	.30	.02
P_2O_3	.05	.05	.05	.05
		Parts per million		
ThO_2	54.5	84.8	22.8	17.2
UO_2	4.8	2.8	1.4	2.5
CuO	63.6	62.4	85.7	88.9
ZnO	41.8	38.0	67.4	44.8
Rb_2O	190.2	183.6	74.9	212.2
SrO	73.4	111.9	338.3	82.8
Y_2O_3	11.6	14.2	11.7	22.9
ZrO_2	218.4	221.3	219.4	35.1
Nb_2O_5	14.5	4.4	10.2	4.3
La_2O_3	67.6	96.9	45.4	9.9
Ce_2O_3	126.3	184.3	84.8	21.2
Nd_2O_3	46.7	68.2	25.5	10.6
Sm_2O_3	7.6	11.7	4.2	2.7
Eu_2O_3	.9	1.0	.9	.2
Gd_2O_3	5.0	6.9	2.7	2.9
Tb_2O_3	.7	1.0	.4	.5
Dy_2O_3	3.6	4.8	2.3	3.1
Tm_2O_3	.2	.2	.2	.3
Yb_2O_3	.9	1.2	1.1	1.6
Lu_2O_3	.1	.2	.2	.2
Cs_2O	.3	.6	.9	2.2
BaO	999.1	665.9	624.0	154.1
Ta_2O_5	.6	.2	.7	.5
HfO_2	5.7	6.3	5.7	1.0
Sc_2O_3	4.1	5.0	7.0	2.8
Cr_2O_3	16.5	9.5	15.8	8.0
CoO	3.2	2.8	6.9	.7
MnO	99.8	153.8	319.3	149.8
		CIPW norms (weight percent)		
Q	34.60	31.38	36.35	34.51
C	2.30	1.51	1.40	.98
Z	.03	.03	.03	.01
Or	32.41	34.87	12.39	39.40
Ab	25.87	22.46	31.20	22.03
An	.78	4.98	13.13	1.46
En	1.35	.76	1.99	.25
Fs	1.28	2.12	1.62	.75
Mt	.90	1.39	1.19	.45
Cm	0	0	0	0
Il	.33	.35	.56	.04
Ap	.12	.12	.12	.12
Cc	---	---	---	----
Total	99.96	99.98	99.98	100.00
salic	95.99	95.23	94.49	98.39
femic	3.97	4.74	5.48	1.61
D index	92.87	88.71	79.94	95.94
PERAL	1.19	1.11	1.10	1.07
PERALK	1.24	1.31	1.74	1.13

into that space with little loss of information. After any projection from *M*-dimensional space to a space of fewer dimensions, the data as represented by the projected vectors can be compared with the original data, and the proportion of information retained can be calculated. Table 5 shows results of such projections for the 26 samples of the Louis Lake batholith as represented by 2- through 10-dimensional space.

RESULTS AND DISCUSSIONS

LOUIS LAKE BATHOLITH

The first step in developing a mathematical model for a batholithic unit is to determine which samples and which oxides will be used. Previous studies (for example, Stuckless and Miesch, 1981; Stuckless, Miesch, and Wenner, 1986) have shown that several variables (oxide concentrations) are easily affected by postmagmatic events. Thus, contents of certain labile elements, such as uranium and cesium, and some volatile components, such as water and carbon dioxide, as well as the oxidation state of iron no longer reflect magmatic distributions. The distribution of some elements may be poorly explained because the amount of variation in concentrations is small relative to analytical error. Some samples may not be usable due to contamination by assimilation or postmagmatic alteration.

The factor variance diagram for the Louis Lake batholith (fig. 4) shows that the proportion of variance accounted for is greater than 50 percent for most elements at three end members and that subsequent increases in the number of end members do not improve the variance accounted for substantially. Data for oxides of eight elements (uranium, cessium, copper, chromium, barium, strontium, tantalum, and zinc) are not represented well by three end members. However, uranium and cessium are known to be poorly bound in many igneous rocks (Zielinski and others, 1977; Stuckless and Miesch, 1981; Stuckless, Miesch, and Wenner, 1986), and copper, zinc, chromium, and tantalum all have large analytical errors relative to their average concentrations and standard deviations (table 4). Thus, a three-end-member model seems to provide a good representation for almost all the data that are expected to represent magmatic distribution accurately.

Most samples of the Louis Lake batholith could be identified unambiguously on the basis of mineralogy and field occurrence, but a few samples were of questionable relation to the batholith. For example, sample BW-25, which was collected near the contact with the Bears Ears pluton, was suspected of being metasomatically altered. Sample LLB-14 was collected at an inclusion-rich locality, thus it could have been interpreted as containing cognate, genetically related material or xenolithic contaminant. None of the known samples of the Louis Lake batholith show a positive

TABLE 3.—*Chemical data and CIPW normative mineralogy for miscellaneous samples of crystalline rocks*

[Norm calculated assuming one-third of the iron is oxidized. D index is differentiation index of Thornton and Tuttle (1960). PERAL is the molar ratio Al/(Na+K+Ca). PERALK is the molar ratio Al/(Na+K). Leaders (---) indicate no value]

Sample	BW-1	BW-2	BW-6	BW-8	BW-10	BW-12	BW-13	BW-14
Weight percent								
SiO_2 ..	74.12	65.34	71.31	71.68	73.99	71.19	71.75	65.00
Al_2O_3 .	14.25	16.71	14.98	14.96	14.27	15.21	15.02	18.65
FeO ...	1.50	3.40	1.87	2.13	1.39	2.02	1.87	2.54
MgO ...	.49	1.54	.71	.53	.38	.54	.49	.71
CaO ...	2.35	4.05	2.40	1.43	1.44	1.32	1.58	3.77
Na_2O ..	3.34	3.90	3.82	3.05	3.03	3.24	3.23	4.44
K_2O ...	3.50	4.22	4.21	5.41	5.15	5.72	5.30	3.83
TiO_2 ..	.16	.24	.25	.37	.15	.38	.34	.48
P_2O_5 ..	.05	.23	.11	.12	.02	.13	.10	.18
Parts per million								
ThO_2 ..	21.1	15.4	19.9	79.1	20.2	59.6	53.6	37.9
UO_2 ...	1.3	2.0	1.3	3.3	2.6	2.8	1.6	1.0
CuO ...	64.7	119.4	62.1	62.4	62.2	62.1	62.2	62.5
ZnO ...	56.7	94.7	65.5	55.7	36.6	59.2	41.6	45.7
Rb_2O ..	77.5	73.2	86.3	197.9	104.3	205.8	186.2	64.6
SrO ...	414.4	525.6	826.8	180.4	116.4	152.0	234.9	555.6
Y_2O_3 ..	5.1	47.7	16.7	24.5	7.7	12.8	7.7	29.8
ZrO_2 ..	197.0	233.0	200.9	351.6	152.1	308.9	305.3	323.5
Nb_2O_5 .	4.3	10.2	5.8	14.5	7.3	4.3	4.3	11.7
La_2O_3 .	38.3	52.5	61.5	139.1	31.3	109.6	112.5	173.5
Ce_2O_3 .	43.1	106.4	115.5	266.9	53.8	215.7	203.9	333.0
Nd_2O_3 .	14.9	54.5	45.8	98.6	22.3	76.3	73.2	127.5
Sm_2O_3 .	2.2	11.9	7.1	14.7	4.2	10.5	9.4	18.7
Eu_2O_3 .	1.1	2.0	1.9	1.8	.8	1.4	1.7	4.0
Gd_2O_3 .	1.2	10.5	5.3	9.0	3.4	6.2	5.5	14.5
Tb_2O_3 .	.2	1.4	.7	1.2	.4	.8	.7	1.7
Dy_2O_3 .	1.2	8.2	3.4	5.7	1.9	3.6	3.0	8.1
Tm_2O_3 .	.1	.6	.2	.3	.1	.2	.2	.5
Yb_2O_3 .	.5	3.3	1.5	1.9	.5	1.2	1.1	2.9
Lu_2O_3 .	.1	.5	.2	.3	.1	.2	.2	.4
Cs_2O ..	.2	.2	.3	.8	.4	.8	1.3	.1
BaO ...	1225.6	1533.9	1473.0	1475.7	941.1	1130.7	1622.7	1584.9
Ta_2O_5 .	.1	.4	.3	.7	.1	.4	.3	.9
HfO_2 ..	6.9	5.9	5.8	10.0	4.6	9.1	9.1	10.3
Sc_2O_3 .	2.0	15.7	4.4	6.8	3.0	6.9	5.8	11.0
Cr_2O_3 .	9.5	27.7	10.8	2.0	.7	1.4	1.2	4.5
CoO ...	4.0	8.9	5.0	3.9	2.2	4.0	3.3	6.5
MnO ...	147.8	718.0	359.3	225.8	176.8	211.6	197.6	422.4
CIPW norms (weight percent)								
Q	34.84	15.22	26.14	28.72	32.33	26.38	27.90	14.75
C	.73	---	---	1.67	1.07	1.54	1.22	.67
Z	.03	.03	.03	.05	.02	.05	.05	.05
Or	21.16	25.51	25.43	32.52	30.80	34.20	31.93	23.24
Ab	28.28	32.97	32.38	25.82	25.66	27.40	27.37	37.62
An	11.33	15.36	11.03	6.32	7.01	5.67	7.18	17.52
Wo	---	1.34	.06	---	---	---	---	---
En	1.21	3.84	1.77	1.32	.93	1.34	1.21	1.78
Fs	1.14	2.85	1.37	1.40	1.05	1.26	1.19	1.62
Mt	.81	1.82	1.00	1.15	.75	1.09	1.00	1.36
Cm	0	0	0	---	---	---	---	---
Hm	---	---	---	---	---	---	---	---
Il	.31	.46	.48	.70	.29	.73	.65	.91
Ap	.12	.55	.26	.29	.05	.31	.24	.43
Cc	---	---	---	---	---	---	---	---
Total	99.95	99.95	99.95	99.95	99.96	99.96	99.94	99.95
salic	96.37	89.09	95.01	95.10	96.89	95.24	95.65	93.84
femic	3.59	10.87	4.94	4.85	3.07	4.72	4.30	6.10
D index	84.28	73.69	83.95	87.06	88.79	87.99	87.19	75.61
PERAL .	1.04	.91	.98	1.10	1.08	1.09	1.07	1.01
PERALK	1.52	1.51	1.37	1.36	1.34	1.31	1.35	1.61

TABLE 3.—*Chemical data and CIPW normative mineralogy for miscellaneous samples of crystalline rocks*—Continued

[Norm calculated assuming one-third of the iron is oxidized. D index is differentiation index of Thornton and Tuttle (1960). PERAL is the molar ratio Al/(Na+K+Ca). PERALK is the molar ratio Al/(Na+K). Leaders (---) indicate no value]

Sample	BW-17	BW-20	BW-21	BW-23	BW-25	BW-33	BW-34	BW-41
Weight percent								
SiO_2 ..	75.87	75.25	76.96	74.13	71.29	63.79	67.82	68.58
Al_2O_3 .	13.33	12.64.	11.80	13.84	14.74	16.44	15.06	16.86
FeO ...	.89	1.69	1.76	1.49	2.66	6.18	4.80	2.79
MgO ...	.221	.31	.30	.42	.96	1.83	2.13	.94
CaO ...	1.24	.47	.93	1.88	2.64	4.58	3.42	3.06
Na_2O ..	2.66	2.08	2.17	3.05	3.64	4.08	3.47	4.92
K_2O ...	5.46	6.93	5.61	4.53	3.35	1.74	2.50	1.99
TiO_2 ..	.12	.19	.11	.19	.34	.88	.42	.40
P_2O_5 ..	.02	.08	.02	.12	.11	.22	.06	.16
Parts per million								
ThO_2 ..	27.5	14.7	2.4	14.8	16.1	7.7	20.1	18.6
UO_2 ...	1.6	2.8	1.7	.9	.9	.6	1.5	2.4
CuO ...	61.9	129.9	288.4	61.9	61.9	62.3	92.7	95.2
ZnO ...	35.2	63.3	46.7	40.2	86.7	120.2	135.1	87.1
Rb_2O ..	108.2	142.4	104.3	96.0	87.2	61.1	75.5	97.6
SrO ...	298.5	382.5	338.5	570.2	439.2	361.7	373.2	750.6
Y_2O_3 ..	5.1	6.5	5.2	5.1	10.3	38.7	15.5	23.2
ZrO_2 ..	117.3	236.3	122.0	170.3	174.5	248.4	205.6	269.8
Nb_2O_5 .	4.3	85.8	4.4	4.3	4.3	18.9	11.6	16.0
La_2O_3 .	15.7	29.0	9.0	65.3	38.6	37.5	42.1	57.2
Ce_2O_3 .	22.5	47.5	16.5	106.7	68.4	80.8	67.4	97.1
Nd_2O_3 .	7.9	16.3	7.2	36.1	26.6	41.7	24.9	34.8
Sm_2O_3 .	1.1	2.5	1.2	4.3	4.4	8.7	4.1	4.2
Eu_2O_3 .	1.6	1.4	1.3	1.9	1.4	1.2	1.2	1.4
Gd_2O_3 .	.9	1.5	1.0	2.7	3.5	8.2	3.5	3.4
Tb_2O_3 .	.1	.2	.1	.3	.4	1.3	.5	.6
Dy_2O_3 .	.7	1.1	.5	1.5	2.2	7.5	3.2	3.4
Tm_2O_3 .	.1	.1	.0	.1	.2	.6	.3	.3
Yb_2O_3 .	.7	.6	.3	.6	.9	3.4	1.6	1.7
Lu_2O_3 .	.0	.1	.0	.1	.1	.5	.2	.3
Cs_2O ..	.4	.7	.5	.6	.3	.2	.3	1.5
BaO ...	1002.3	2234.7	2085.2	2173.6	1156.1	407.3	1052.4	1061.8
Ta_2O_5 .	.2	.2	.1	.2	.2	1.1	.5	1.8
HfO_2 ..	4.1	9.4	4.7	5.3	5.2	6.2	6.4	6.5
Sc_2O_3 .	.8	1.5	1.0	2.3	6.7	21.2	13.4	4.6
Cr_2O_3 .	2.7	4.3	3.2	8.7	6.9	10.6	246.2	12.2
CoO ...	1.8	8.4	21.9	3.2	7.0	15.6	18.1	6.2
MnO ...	91.3	128.7	100.9	139.4	452.2	877.8	828.1	326.0
CIPW norms (weight percent)								
Q	36.06	34.28	39.28	33.78	29.30	19.33	25.71	23.70
C	.77	.91	.37	.66	.49	.02	.50	1.37
Z	.02	.04	.02	.03	.03	.04	.03	.04
Or	32.66	41.76	33.95	27.57	20.22	10.40	15.12	12.14
Ab	22.48	17.65	18.38	25.79	30.82	34.51	29.34	41.62
An	6.03	1.79	4.50	8.52	12.39	21.24	16.55	14.13
Wo	---	---	---	---	---	---	---	---
En	.55	.76	.76	1.06	2.39	4.55	5.30	2.35
Fs	.64	1.26	1.46	1.07	1.96	4.39	3.86	1.98
Mt	.48	.91	.94	.880	1.43	3.31	2.57	1.50
Cm	---	---	---	0	0	0	.04	0
Hm	---	---	---	---	---	---	---	---
Il	.23	.37	.21	.36	.65	1.68	.79	.75
Ap	.05	.19	.05	.29	.26	.53	.14	.38
Cc	---	---	---	---	---	---	---	---
Total	99.96	99.92	99.92	99.92	99.96	100.00	99.96	99.97
salic	98.01	96.42	96.50	96.34	93.26	85.54	87.25	93.00
femic	1.95	3.49	3.42	3.58	6.70	14.45	12.71	6.97
D index	91.19	93.69	91.61	87.14	80.35	64.25	70.17	77.46
PERAL .	1.06	1.06	1.03	1.03	1.02	.97	1.02	1.06
PERALK	1.29	1.14	1.21	1.38	1.52	1.91	1.78	1.64

europium anomaly (fig. 5), and the strong positive europium anomaly exhibited by LLB-14 (fig. 6*F*) could be consistent with either origin. Therefore, all samples of known Louis Lake batholith as well as those of questionable relationship were subjected to a badness-of-fit test (Stuckless, Miesch, and Wenner, 1986). This test uses the three-dimensional space defined by the 26 known samples of Louis Lake batholith. Each of the samples listed in tables 1-3 was then projected into that space to see if any other samples should be included

TABLE 3.—*Chemical data and CIPW normative mineralogy for miscellaneous samples of crystalline rocks*—Continued

[Norm calculated assuming one-third of the iron is oxidized. D index is differentiation index of Thornton and Tuttle (1960). PERAL is the molar ratio Al/(Na+K+Ca). PERALK is the molar ratio Al/(Na+K). Leaders (---) indicate no value]

Sample	GPA-7	LLB-1	LLB-6	LLB-14	PRM-12	BW-26	BW-30	BW-31
Weight percent								
SiO_2 ...	73.51	75.84	74.76	76.14	57.59	72.69	60.00	60.63
Al_2O_3 ..	13.94	13.85	13.70	13.60	12.47	14.13	16.63	16.92
FeO	3.17	.67	1.31	.85	7.73	1.08	5.67	5.16
MgO	.69	.06	.30	.20	7.78	.35	1.73	1.70
CaO	1.65	.83	.89	.96	8.25	1.05	4.7	4.46
Na_2O ...	3.51	3.89	3.38	4.26	2.84	3.00	3.66	3.63
K_2O	2.91	4.68	5.41	3.72	1.63	5.53	3.21	3.65
TiO_2 ...	.31	.03	.06	.06	.87	.14	1.06	.93
P_2O_5 ...	.05	.05	.05	.05	.41	.02	.52	.41
Parts per million								
ThO_2 ...	91.0	13.3	26.5	13.2	4.8	64.5	37.7	30.0
UO_2	7.5	5.5	8.9	2.4	2.8	3.1	1.5	1.4
CuO	62.8	114.8	72.1	62.3	113.0	42.6	77.6	61.3
ZnO	85.4	80.6	97.6	35.4	223.4	38.6	123.2	140.7
Rb_2O ...	123.1	183.1	216.1	88.8	45.5	175.0	73.3	78.7
SrO	335.4	47.1	115.1	224.5	669.0	221.1	752.1	758.1
Y_2O_3 ...	132.6	25.3	17.7	5.2	45.1	11.4	47.0	39.4
ZrO_2 ...	257.2	86.2	85.8	72.7	250.6	209.4	503.8	568.7
Nb_2O_5 ..	26.4	7.1	8.5	5.8	8.7	5.7	15.7	14.3
La_2O_3 ..	74.6	10.9	30.2	12.9	32.3	---	---	---
Ce_2O_3 ..	147.5	21.7	56.3	21.6	95.6	---	---	---
Nd_2O_3 ..	58.8	10.1	20.6	8.3	77.1	---	---	---
Sm_2O_3 ..	12.8	2.5	4.1	1.6	16.1	---	---	---
Eu_2O_3 ..	1.2	.2	.6	.4	3.4	---	---	---
Gd_2O_3 ..	12.6	3.2	3.5	1.4	11.5	---	---	---
Tb_2O_3 ..	2.3	.6	.6	.2	1.4	---	---	---
Dy_2O_3 ..	15.2	4.1	3.4	1.4	7.5	---	---	---
Tm_2O_3 ..	1.5	.4	.3	.1	.6	---	---	---
Yb_2O_3 ..	9.0	2.7	1.7	.9	3.5	---	---	---
Lu_2O_3 ..	1.4	.4	.3	.1	.5	---	---	---
Cs_2O ...	1.0	4.9	1.2	1.7	1.0	---	---	---
BaO	592.1	172.5	389.1	715.2	501.5	---	---	---
Ta_2O_5 ..	1.0	1.4	2.1	.7	.5	---	---	---
HfO_2 ...	6.2	3.1	3.0	2.2	5.6	---	---	---
Sc_2O_3 ..	8.7	2.7	3.4	2.2	27.5	---	---	---
Cr_2O_3 ..	51.5	1.1	22.3	10.4	511.2	---	---	---
CoO	4.2	.4	1.7	1.1	40.7	---	---	---
MnO	495.7	303.7	169.2	128.5	1662.6	30.3	568.1	422.6
CIPW norms (weight percent)								
Q	36.46	33.57	31.60	34.38	8.46	31.62	14.06	13.47
C	2.14	1.02	.76	.89	---	1.37	---	---
Z	.04	.01	.01	.01	.38	.04	.08	.09
Or	17.41	27.74	32.12	22.22	9.79	33.33	19.46	22.06
Ab	29.47	32.88	28.57	36.08	23.93	25.89	31.77	31.41
An	7.85	3.71	4.11	4.45	16.31	5.18	19.97	19.53
Wo	---	---	---	---	9.12	---	.19	.15
En	1.71	.15	.74	.51	19.30	.89	4.42	4.33
Fs	2.49		1.13	.74	5.90	.76	3.63	3.36
Mt	1.71	.65	.71	.46	4.13	.59	3.12	2.83
Cm	.01	---	0	0	.08	---	---	---
Hm	---	.07	---	---	---	---	---	---
Il	.58	.06	.11	.12	1.65	.27	2.07	1.81
Ap	.12	.12	.12	.12	.96	.05	1.26	.99
Cc	---	.02	---	---	---	---	---	---
Total	99.98	100.00	99.99	99.97	100.00	100.00	100.03	100.02
salic	93.36	98.93	97.17	98.03	58.87	97.44	85.33	86.55
femic	6.61	1.07	2.82	1.94	41.13	2.56	14.70	13.47
D index	83.34	94.19	92.29	92.68	42.19	90.84	65.28	66.94
PERAL ..	1.17	1.07	1.05	1.06	.58	1.10	.92	.94
PERALK .	1.56	1.21	1.20	1.23	1.93	1.29	1.75	1.71

TABLE 3.—*Chemical data and CIPW normative mineralogy for miscellaneous samples of crystalline rocks*—Continued

[Norm calculated assuming one-third of the iron is oxidized. D index is differentiation index of Thornton and Tuttle (1960). PERAL is the molar ratio Al/(Na+K+Ca). PERALK is the molar ratio Al/(Na+K). Leaders (---) indicate no value]

Sample	BW-32	BW-35	BW-36	BW-37	BW-38	BW-39	BW-40	BW-51
Weight percent								
SiO_2 ...	72.29	61.58	67.01	68.57	56.10	53.29	69.53	66.67
Al_2O_3 ..	13.87	16.30	16.06	15.88	15.23	15.65	15.13	18.69
FeO	1.65	5.43	2.70	2.27	7.59	9.23	2.38	1.16
MgO	.53	1.77	.91	.90	4.61	4.09	.54	.29
CaO	1.79	4.50	3.04	2.68	6.79	7.33	1.66	4.02
Na_2O ...	2.66	3.65	3.55	3.83	3.48	3.47	3.26	5.28
K_2O	5.19	3.39	3.78	3.43	1.99	1.84	5.13	1.92
TiO_2 ...	.37	.92	.42	.47	1.17	1.62	.29	.13
P_2O_5 ...	.09	.42	.20	.14	.61	.96	.10	.13
Parts per million								
ThO_2 ...	75.2	24.8	11.6	7.6	5.2	21.6	98.5	1.8
U02	1.5	2.0	.7	.7	.5	1.0	3.7	.2
CuO	57.6	52.6	83.9	101.4	156.5	141.5	36.3	122.7
ZnO	69.7	119.5	73.4	89.6	159.3	194.2	66.0	77.2
Rb_2O ...	100.6	95.1	75.5	82.0	83.1	66.7	194.7	21.9
SrO	409.2	654.0	818.4	648.1	774.6	775.8	290.9	935.4
Y_2O_3 ...	15.2	39.4	7.6	8.9	31.8	34.3	33.0	7.6
Zr_2O ...	240.4	424.2	291.8	306.6	275.6	407.9	429.6	94.6
Nb_2O_5 ..	11.4	14.3	2.9	5.7	20.0	22.9	14.3	4.3
La_2O_3 ..	---	---	---	---	---	---	---	---
Ce_2O_3 ..	---	---	---	---	---	---	---	---
Sm_2O_3 ..	---	---	---	---	---	---	---	---
Eu_2O_3 ..	---	---	---	---	---	---	---	---
Gd_2O_3 ..	---	---	---	---	---	---	---	---
Tb_2O_3 ..	---	---	---	---	---	---	---	---
Dy_2O_3 ..	---	---	---	---	---	---	---	---
Tm_2O_3 ..	---	---	---	---	---	---	---	---
Yb_2O_3 ..	---	---	---	---	---	---	---	---
Lu_2O_3 ..	---	---	---	---	---	---	---	---
Cs_2O ...	---	---	---	---	---	---	---	---
BaO	---	---	---	---	---	---	---	---
Ta_2O_5 ..	---	---	---	---	---	---	---	---
HfO_2 ...	---	---	---	---	---	---	---	---
Sc_2O_3 ..	---	---	---	---	---	---	---	---
CoO	---	---	---	---	---	---	---	---
MnO	161.9	506.2	286.0	267.0	841.5	1027.6	196.1	180.9
CIPW norms (weight percent)								
Q	32.62	15.20	24.22	26.22	8.37	8.13	26.53	19.77
C	.85	---	1.10	1.45	---	---	1.46	.94
Z	.04	.13	.16	.15	.15	.15	.05	.18
Or	31.12	20.38	22.82	20.59	12.00	11.09	30.88	11.52
Ab	22.84	31.42	30.68	32.91	30.04	29.95	28.10	45.37
An	8.42	18.39	14.07	12.57	20.46	22.13	7.72	19.39
Wo	---	.64	---	---	4.11	3.58	---	---
En	1.34	4.48	2.32	2.28	11.71	10.39	1.37	.73
Fs	.95	3.62	1.86	1.37	5.30	6.10	1.78	.89
Mt	.90	2.96	1.48	1.24	4.16	5.06	1.30	.63
Cm	---	---	---	---	---	---	---	---
Hm	---	---	---	---	---	---	---	---
Il	.71	1.78	.81	.91	2.27	3.14	.56	.25
Ap	.22	1.01	.48	.34	1.47	2.32	.24	.31
Cc	---	---	---	---	---	---	---	---
Total	100.00	100.02	100.01	100.01	100.03	100.05	100.01	100.01
salic	95.89	85.52	93.06	93.88	71.02	69.46	94.75	97.19
femic	4.12	14.50	6.96	6.13	29.01	30.59	5.26	2.82
D index	86.59	.67	77.72	79.72	50.41	47.18	85.51	76.67
PERAL ..	1.05	.91	1.04	1.07	.75	.74	1.09	1.03
PERALK .	1.39	1.68	1.62	1.60	1.93	2.03	1.39	1.74

in the development of a petrogenic model. The badness-of-fit values for the 26 samples are shown as average proportional differences in table 6. The values are generally less than 0.50, whereas values for BW-25 and LLB-14 are 1.03 and 0.77, respectively. A few samples in the original group of 26 with badness-of-fit values between 0.50 and 0.75 were retained because isotopic studies had shown them to be from the Louis Lake batholith and isotopically uncontaminated and undisturbed since the time of intrusion (Stuckless and others, 1985).

TABLE 3.—*Chemical data and CIPW normative mineralogy for miscellaneous samples of crystalline rocks*—Continued

[Norm calculated assuming one-third of the iron is oxidized. D index is differentiation index of Thornton and Tuttle (1960). PERAL is the molar ratio Al/(Na+K+Ca). PERALK is the molar ratio Al/(Na+K). Leaders (---) indicate no value]

Sample	BW-42	BW-43	BW-44	BW-46	BW-47	BW-48	BW-49	BW-50
Weight percent								
SiO_2 ..	75.36	67.28	74.30	75.39	74.41	59.20	67.73	56.55
Al_2O_3 .	13.81	15.75	14.58	14.01	14.38	16.85	16.82	13.68
FeO ...	1.10	5.13	.84	.43	.92	7.09	2.87	13.92
MgO ...	.37	1.43	.23	.19	.24	2.66	.76	11.89
CaO ...	1.42	3.63	1.07	1.34	2.00	5.94	2.75	.57
Na_2O ..	2.99	3.68	3.48	2.59	2.83	3.46	3.56	.62
K_2O ...	4.54	1.92	5.20	5.69	4.87	2.35	4.33	.76
TiO_2 ..	.14	.75	.11	.04	.13	1.21	.61	1.78
P_2O_5 ..	.02	.20	.02	.02	.02	.76	.16	.02
Parts per million								
ThO_2 ..	43.7	27.2	80.9	8.3	18.9	57.1	55.2	7.7
UO_2 ...	2.3	6.5	4.1	1.4	1.3	8.6	2.4	.4
CuO ...	93.0	62.6	62.3	78.8	62.0	138.4	62.5	84.4
ZnO ...	67.5	147.4	43.0	36.6	41.5	110.9	79.9	171.6
Rb_2O ..	106.5	140.6	212.1	136.5	93.9	101.9	124.7	26.1
SrO ...	248.0	172.6	122.5	346.9	163.7	956.7	434.8	29.4
Y_2O_3 ..	16.6	72.6	20.6	5.2	5.1	31.2	16.8	30.3
ZrO_2 ..	197.9	346.0	72.7	45.2	144.6	309.9	544.7	205.9
Nb_2O_5 .	4.3	29.2	14.5	4.4	4.3	16.1	10.2	14.8
La_2O_3 .	76.0	75.2	71.3	6.2	42.5	165.7	168.4	16.3
Ce_2O_3 .	131.6	136.3	134.4	7.5	67.3	321.4	270.8	32.2
Nd_2O_3 .	55.8	63.3	56.6	1.8	24.6	127.8	96.9	14.1
Sm_2O_3 .	9.2	13.3	10.6	.3	3.7	18.6	11.7	2.8
Eu_2O_3 .	1.5	2.0	1.0	1.3	1.3	4.7	2.2	.4
Gd_2O_3 .	6.6	13.5	7.9	.3	2.6	12.0	5.9	3.2
Tb_2O_3 .	.9	2.2	1.0	.0	.3	1.5	.7	.6
Dy_2O_3 .	4.5	13.0	4.3	.2	1.3	8.0	3.4	4.9
Tm_2O_3 .	.2	1.0	.2	.0	.1	.4	.2	.7
Yb_2O_3 .	11.1	5.9	.9	.1	.4	2.3	1.2	4.7
Lu_2O_3 .	.1	.8	.1	.0	.1	.3	.2	.8
Cs_2O ..	.8	3.9	1.5	.6	.3	.9	.6	.6
BaO ...	1378.1	394.2	527.3	2176.0	1172.9	1497.7	1728.2	115.8
Ta_2O_5 .	.3	3.0	1.3	.2	.1	.7	.5	1.2
HfO_2 ..	5.1	7.9	2.5	1.4	3.7	7.5	12.2	5.1
Sc_2O_3 .	3.1	16.4	3.5	1.0	2.9	19.6	6.3	48.4
Cr_2O_3 .	2.9	16.3	1.6	1.5	3.9	24.4	5.1	15.2
CoO ...	2.3	11.9	1.1	.9	1.6	19.5	6.3	45.7
MnO ...	125.2	587.8	117.9	91.5	133.0	970.6	313.0	1233.0
CIPW norms (weight percent)								
Q	36.39	27.39	31.18	34.78	34.15	13.29	22.66	26.39
C	1.36	1.46	1.30	1.05	.80	---	1.55	10.79
Z	.03	.05	.01	.01	.02	.05	.08	.03
Or	27.32	11.47	30.94	34.47	29.20	14.41	26.22	4.50
Ab	25.32	31.15	29.49	21.91	23.94	29.27	30.17	5.24
An	6.89	16.68	5.16	6.52	9.79	23.21	12.58	2.68
Wo	---	---	---	---	---	.54	---	---
En	.93	3.56	.58	.48	.60	6.63	1.90	29.48
Fs	.80	3.59	.60	.34	.66	4.69	1.69	10.03
Mt	.60	2.75	.46	.24	.50	3.80	1.54	7.44
Cm	---	0	---	---	---	0	0	0
Hm	---	---	---	---	---	---	---	---
Il	.27	1.41	.21	.08	.25	2.29	1.16	3.37
Ap	.05	.48	.05	.05	.05	1.79	.39	.05
Cc	---	---	---	---	---	---	---	---
Total	99.95	100.00	99.99	99.92	99.96	99.98	99.94	100.00
Salic	97.31	88.21	98.08	98.74	97.90	80.24	93.26	49.63
Femic	2.63	11.79	1.90	1.18	2.05	19.75	6.68	50.37
D index	89.03	70.01	91.61	91.16	87.29	56.98	79.05	36.13
PERAL .	1.11	1.07	1.09	1.08	1.05	.88	1.07	4.74
PERALK	1.39	1.93	1.28	1.33	1.44	2.02	1.58	7.39

The physical interpretation of a three-end-member model can utilize three solids, three liquids, or any combination of these that totals three. A stereographic projection of the three-dimensional cluster of sample vectors (fig. 7) shows no clear trends (such as the trace of a plane as projected on a hemisphere) that might help to choose among various possibilities. Contours for equal values of various parameters (not shown), however, do reveal patterns that can be related to possible paths of magma evolution. For example, contour lines for K/Rb values trend northwesterly in the northeastern portion of the positive space and rotate to an east-west pattern in the southernmost portion of the positive space such that the highest values (least evolved) are at the southern edge of the positive space. Europium anomalies form west-northwest trending bands such that europium anomalies change from about 1 near BW-19 (figs. 5, 7) to 0.60 and 0.59 for samples PRM-1 and BW-9, respectively. Thorium values show a similar pattern with the highest values occurring in the southwestern portion of the positive space. Other parameters, such as Rb/Sr, La/Lu, and the differentiation index of Thornton and Tuttle (1960) yield more nearly north-south trends with values increasing from east (least evolved) to west (most evolved). The lack of obvious linear trends and the dissimilarity of contour patterns suggest that magma evolution did not occur in distinct stages as proposed for the granite of the Owl Creek Mountains (Stuckless, Miesch, and Wenner, 1986).

Plots of the normative data in the systems Q-Ab-Or (quartz-albite-orthoclase) and An-Ab-Or (anorthite-albite-orthoclase) (figs. 8, 9) suggest that the magma may have developed in more than one pressure regime, and as such, at least two different solids may have crystallized from any given sample of liquid. A three-end-member model might therefore be interpreted as a starting liquid and two solids which in turn probably represent a continuum of solidus compositions between two-end-member compositions. On the basis of this hypothesis, the least evolved samples were examined as possible starting liquids from which two solids could be subtracted to account for all of the remaining samples. The projected composition (that is, the composition as represented in the three-end-member model) of sample BW-24 was found to meet this criterion.

Any of the unevolved samples from the Louis Lake batholith could have been used with two compositions whose vectors lie within the positive space shown on figure 7. However, proportions of the two end members needed for use with one of the other samples as a starting liquid are either unreasonable (such as requiring an average of 99 percent differentiation to account for the average sample) or they require that at least one of the other end members be added rather than having both subtracted.

Although addition of end members is mathematically valid and could be interpreted geologically (for example, varying amounts on assimilation of country rock

TABLE 4.—*Statistical summary of chemical data for samples for the Louis Lake batholith and Bears Ears pluton*

Oxide	Louis Lake (26 samples)		Bears Ears (18 samples)	
	Mean	Standard deviation	Mean	Standard deviation
	Weight percent			
SiO_2	67.87	4.07	72.55	2.32
Al_2O_3	15.48	.90	14.26	.86
FeO	3.64	1.45	2.37	.84
MgO	1.22	.75	.62	.35
CaO	3.20	1.29	1.60	.91
Na_2O	3.77	.53	3.14	.50
K_2O	3.65	1.28	4.79	1.31
TiO_2	.56	.29	.31	.17
P_2O_5	.25	.16	.11	.07
	Parts per million			
ThO_2	31.9	20.3	51.3	29.8
UO_2	3.8	1.9	3.9	2.3
CuO	69.1	27.5	71.7	18.2
ZnO	80.5	26.3	48.7	11.8
Rb_2O	107.4	40.6	153.2	45.9
SrO	730.6	344.0	235.4	125.3
Y_2O_3	25.8	15.5	17.0	9.9
ZrO_2	331.3	157.5	250.5	107.7
Nb_2O_5	13.1	8.8	8.4	4.0
La_2O_3	98.1	53.8	77.7	52.9
Ce_2O_3	189.5	103.1	144.1	97.2
Nd_2O_3	76.7	41.4	51.9	35.5
Sm_2O_3	12.3	6.6	8.0	4.9
Eu_2O_3	2.3	1.0	1.4	.7
Gd_2O_3	8.3	4.6	5.6	3.3
Tb_2O_3	1.1	4.6	.7	.4
Dy_2O_3	5.5	3.2	3.8	1.8
Tm_2O_3	.4	.2	.2	.1
Yb_2O_3	2.1	1.2	1.4	.7
Lu_2O_3	.3	.2	.2	.1
Cs_2O	1.5	1.2	.8	.4
BaO	1403.3	434.9	1129.6	371.5
Ta_2O_5	1.1	.7	.6	.3
HfO_2	8.2	3.8	6.8	2.8
Sc_2O_3	8.5	5.2	5.7	2.7
Cr_2O_3	26.4	25.1	20.9	20.3
CoO	9.6	5.5	5.0	2.6
MnO	482.9	261.5	247.2	107.8

TABLE 5.—*Proportions of total chemical variance in the Louis Lake batholith that could be accounted for by factor models with 2-10 end members*

Oxide	Number of end members								
	2	3	4	5	6	7	8	9	10
SiO_2	0.77	0.82	0.82	0.85	0.96	0.96	0.98	0.97	0.97
Al_2O_3	.81	.78	.79	.83	.84	.85	.88	.87	.91
FeO	.64	.75	.87	.87	.92	.95	.95	.98	.98
MgO	.70	.69	.73	.78	.90	.96	.97	.96	.96
CaO	.86	.88	.88	.88	.95	.96	.97	.98	.98
Na_2O	.53	.64	.68	.68	.78	.79	.92	.95	.97
K_2O	.56	.70	.74	.79	.90	.93	.93	.95	.95
TiO_2	.53	.80	.85	.85	.88	.93	.94	.96	.96
P_2O_5	.39	.58	.55	.56	.74	.77	.77	.87	.96
ThO_2	.37	.72	.71	.72	.74	.85	.91	.92	.92
UO_2	.03	.08	.48	.51	.58	.59	.65	.94	.95
CuO	.13	.10	.16	.76	.94	.94	.94	.95	.95
ZnO	.45	.48	.51	.50	.57	.60	.60	.67	.89
Rb_2O	.43	.59	.69	.85	.83	.84	.86	.87	.90
SrO	.36	.37	.55	.64	.80	.94	.94	.95	.95
Y_2O_3	.15	.81	.91	.91	.91	.94	.95	.95	.95
ZrO_2	.01	.73	.77	.77	.78	.84	.87	.91	.95
Nb_2O_5	.03	.61	.69	.69	.76	.81	.84	.87	.90
La_2O_3	.01	.71	.72	.72	.78	.91	.94	.96	.97
Ce_2O_3	.00	.72	.72	.72	.80	.88	.93	.96	.96
Nd_2O_3	.02	.74	.72	.72	.81	.84	.91	.94	.95
Sm_2O_3	.08	.79	.76	.76	.82	.82	.90	.95	.95
Eu_2O_3	.41	.77	.76	.75	.90	.91	.93	.95	.97
Gd_2O_3	.14	.90	.87	.87	.88	.89	.93	.94	.95
Tb_2O_3	.13	.90	.93	.93	.93	.94	.97	.98	.97
Dy_2O_3	.14	.84	.92	.92	.91	.94	.96	.97	.97
Tm_2O_3	.15	.80	.96	.96	.95	.98	.98	.97	.98
Yb_2O_3	.14	.77	.96	.96	.95	.97	.97	.96	.97
Lu_2O_3	.15	.76	.95	.95	.94	.96	.95	.95	.95
Cs_2O	.04	.13	.53	.78	.78	.79	.79	.85	.85
BaO	.03	.30	.47	.51	.72	.76	.88	.94	.94
Ta_2O_5	.03	.38	.53	.55	.62	.77	.84	.88	.89
HfO_2	.01	.79	.84	.84	.86	.92	.93	.95	.97
Sc_2O_3	.54	.71	.74	.75	.81	.84	.85	.86	.92
Cr_2O_3	.25	.24	.40	.43	.67	.88	.89	.88	.88
CoO	.69	.72	.78	.79	.91	.97	.97	.96	.96
MnO	.63	.61	.65	.70	.88	.89	.94	.95	.95

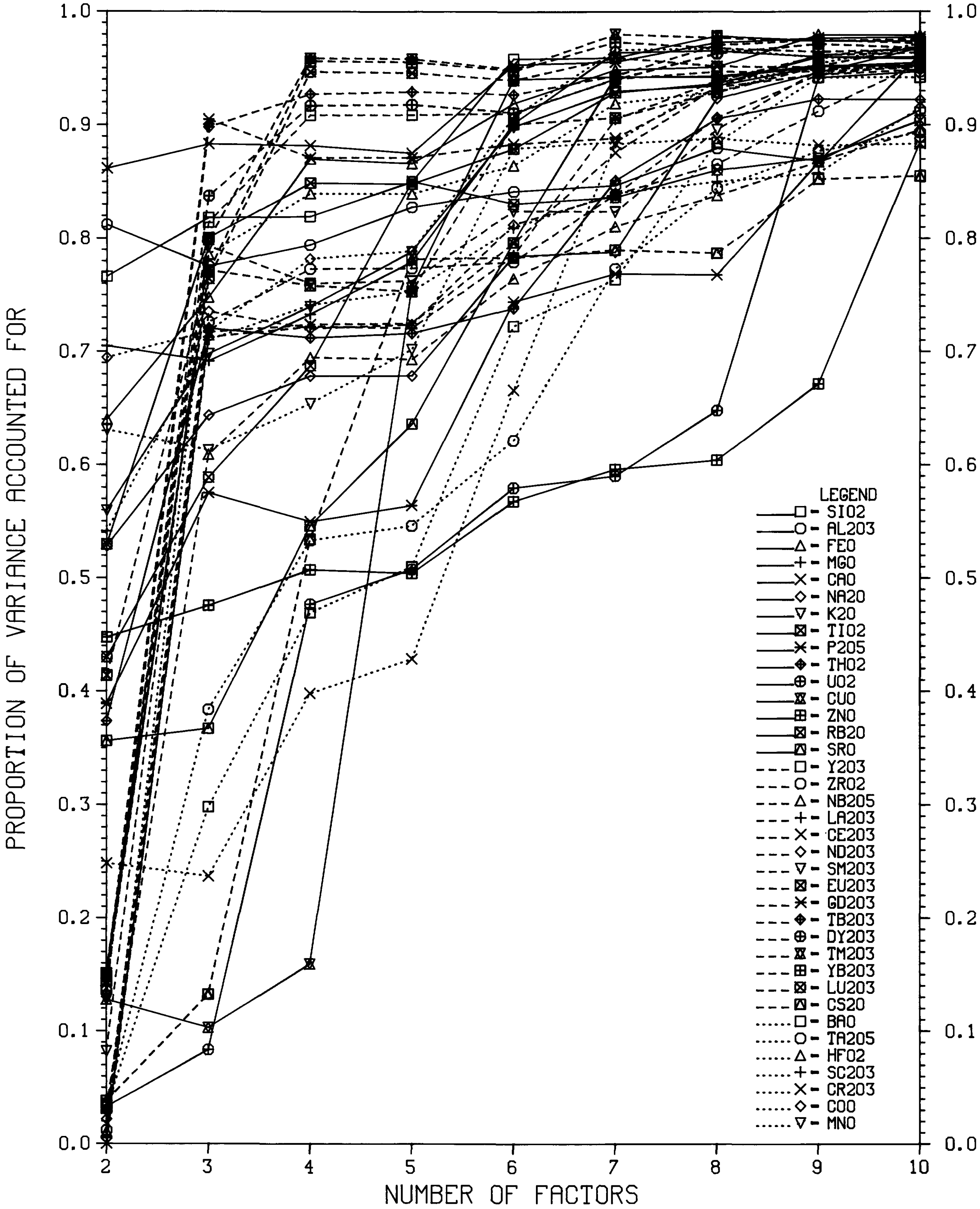

FIGURE 4.—Factor variance diagram for 26 samples of the Louis Lake batholith and 37 constituents. Data for the plot are given in table 5.

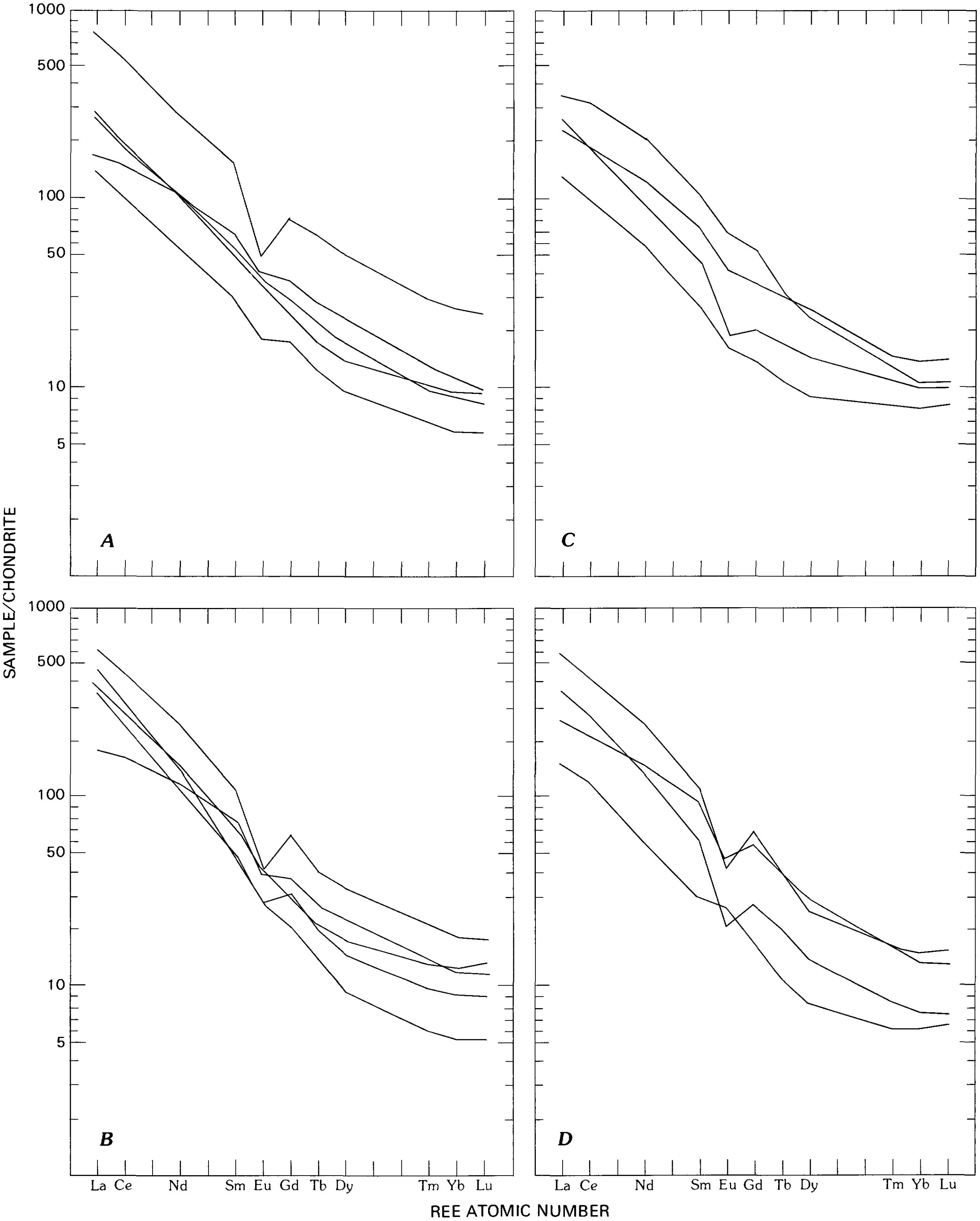

FIGURE 5 (above and facing page).—Chondrite-normalized rare-earth-element diagrams for samples of the Louis Lake batholith: *A*, Samples LLB-2, LLB-3, LLB-4, LLB-8, and GPA-6; *B*, Samples LLB-5, LLB-7, BW-3, BW-4, and BW-5; *C*, Samples LLB-9, LLB-11, LLB-12, and BW-7; *D*, Samples BW-9, BW-19, BW-22, and BW-24; *E*, Samples BW-11, PRM-3, PRM-5, and LLB-15; and *F*, Samples PRM-1, PRM-2, PRM-6, and GPA-1.

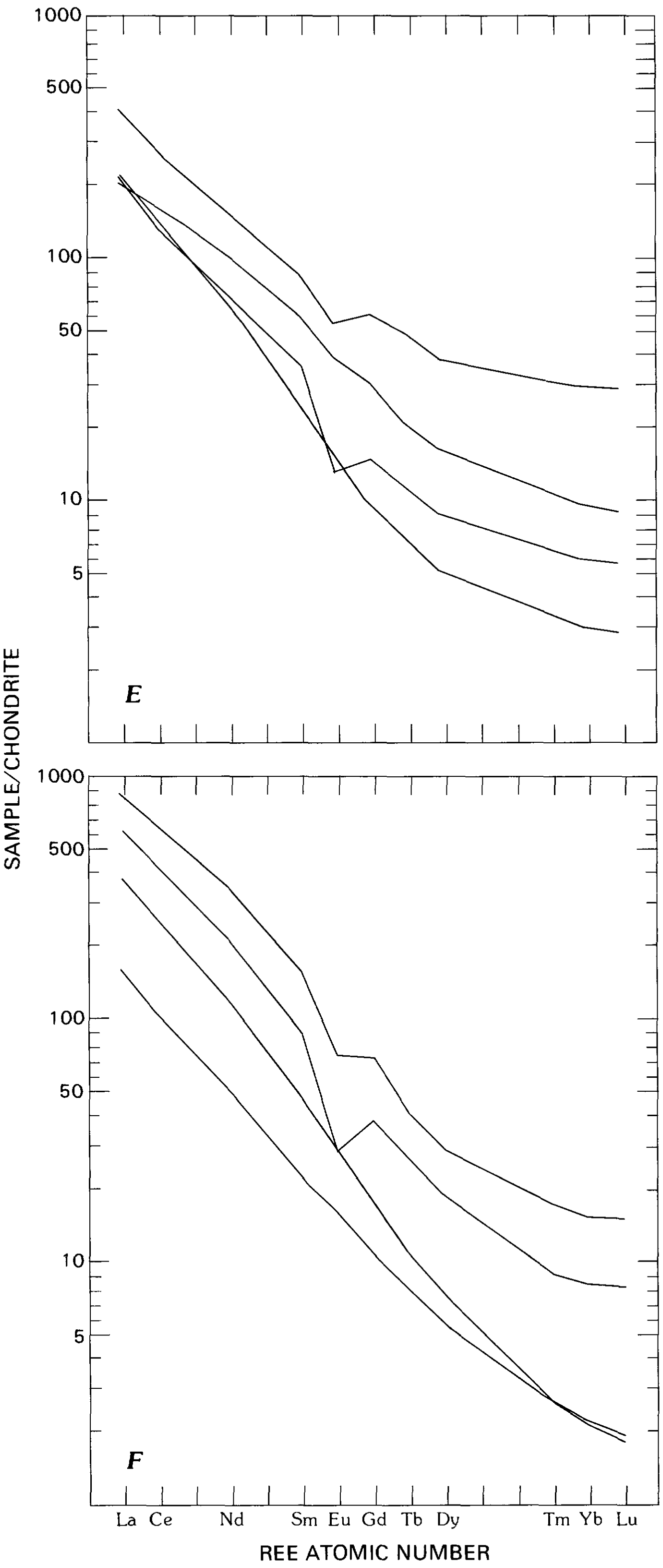

of uniform composition), this possibility was rejected in favor of a less complex and more conventional interpretation. The compositions of the solids that would have to be removed from a sample similar to BW-24 by fractional crystallization in order to account for the composition of the remaining samples are given in table 7, and the proportions of liquid and solids needed for each sample (the mixing proportions) are given in table 8. The mixing proportions show that samples range from as little as 27 percent solid removed (LLB-7) to as much as 86 percent solid removed (PRM-3). The average amount of differentiation represented by the analyzed samples and the model is 77 percent. Thus, if the analyzed samples are representative of the pluton as a whole, the exposed rocks represent 23 percent of the original liquid.

Data for REE and published partitioning coefficients can be used to test the reasonableness of the three-end-member model. First, the solid compositions need to be recast in terms of near-liquidus minerals and minerals that are actually observed in the Louis Lake batholith. Bayley and others (1973) listed an average mode of 48.4 percent plagioclase (An_{25-30}), 23.5 percent quartz, and 15.9 percent microcline for eight samples. Cheang and others (1986) listed minor constituents as 1-16 percent biotite, 4-6 percent hornblende, 3.7 percent epidote-family minerals, 2 percent sphene, 2 percent opaque oxides, and trace amounts of zircon and apatite. Table 9 presents the model solid compositions recast in terms of these minerals except for the addition of pyroxene, which was probably an early crystallizing mineral, and the omission of microcline, which was probably not part of the early solidus assemblage. If microcline had been an early crystallizing mineral, barium content and K/Rb values should both decrease with increasing differentiation (Hanson, 1978), but both actually increase (table 1). The occurrence of magmatic epidote suggests pressures of at least 6 kbar (Crawford and Hollister, 1982); at 8 kbar, clinopyroxene is an early crystalline phase in granitic magma (Naney, 1983).

Once an appropriate mineralogy has been calculated, the amounts of REE in each mineral phase can be calculated by assuming equilibrium with the proposed starting liquid and appropriate partitioning coefficients (table 10). The sums of the REE contents can then be compared to the total REE contents for each proposed solidus (fig. 10). The partitioning coefficients used were chosen from published values for igneous rocks with intermediate silica contents. Allanite was chosen to represent the epidote-family minerals because epidotes in the Louis Lake batholith are commonly cored by euhedral allanite.

The REE compositions for each solidus as calculated by the Q-mode model (shown by triangles on fig. 10) agree well with those calculated from mineralogy and partitioning coefficients (shown by squares),

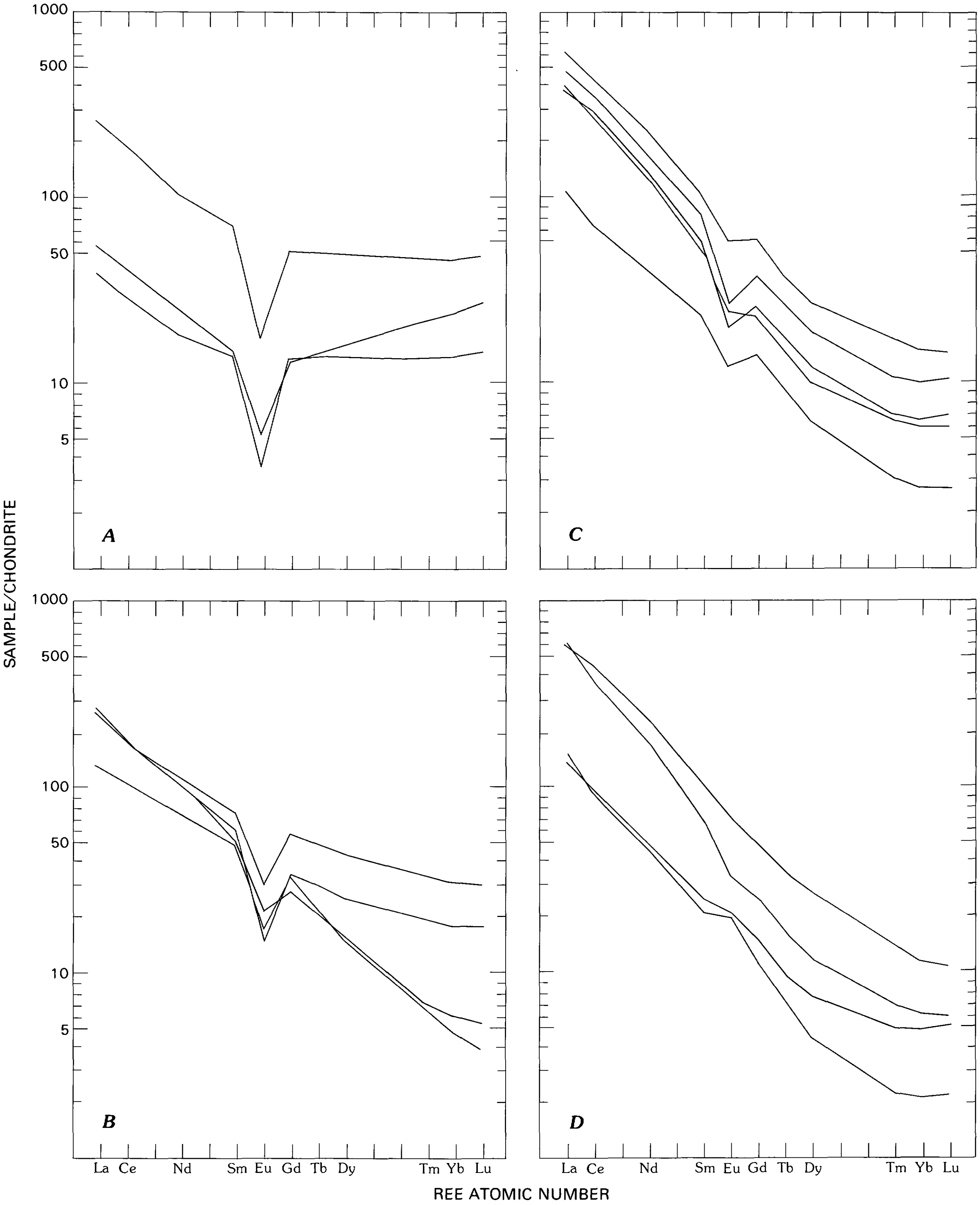

FIGURE 6 (above and facing page).—Chondrite-normalized rare-earth-element diagrams for metamorphic rocks and for igneous rocks that have been contaminated or altered: *A*, Samples LLB-1, BW-50, and GPA-7; *B*, Samples BW-33, BW-42, and BW-44; *C*, Samples BW-8, BW-10, BW-12, BW-13, and BW-14; *D*, Samples BW-25, BW-47, BW-48, and BW-49; *E*, Samples BW-6, BW-34, BW-41, and LLB-14; *F*, Samples BW-1, BW-17, BW-20, and BW-21; *G*, Samples LLB-6, PRM-12, and BW-2; and *H*, Samples BW-23 and BW-46. Note that the scale for diagram *H* is different from that of the other diagrams.

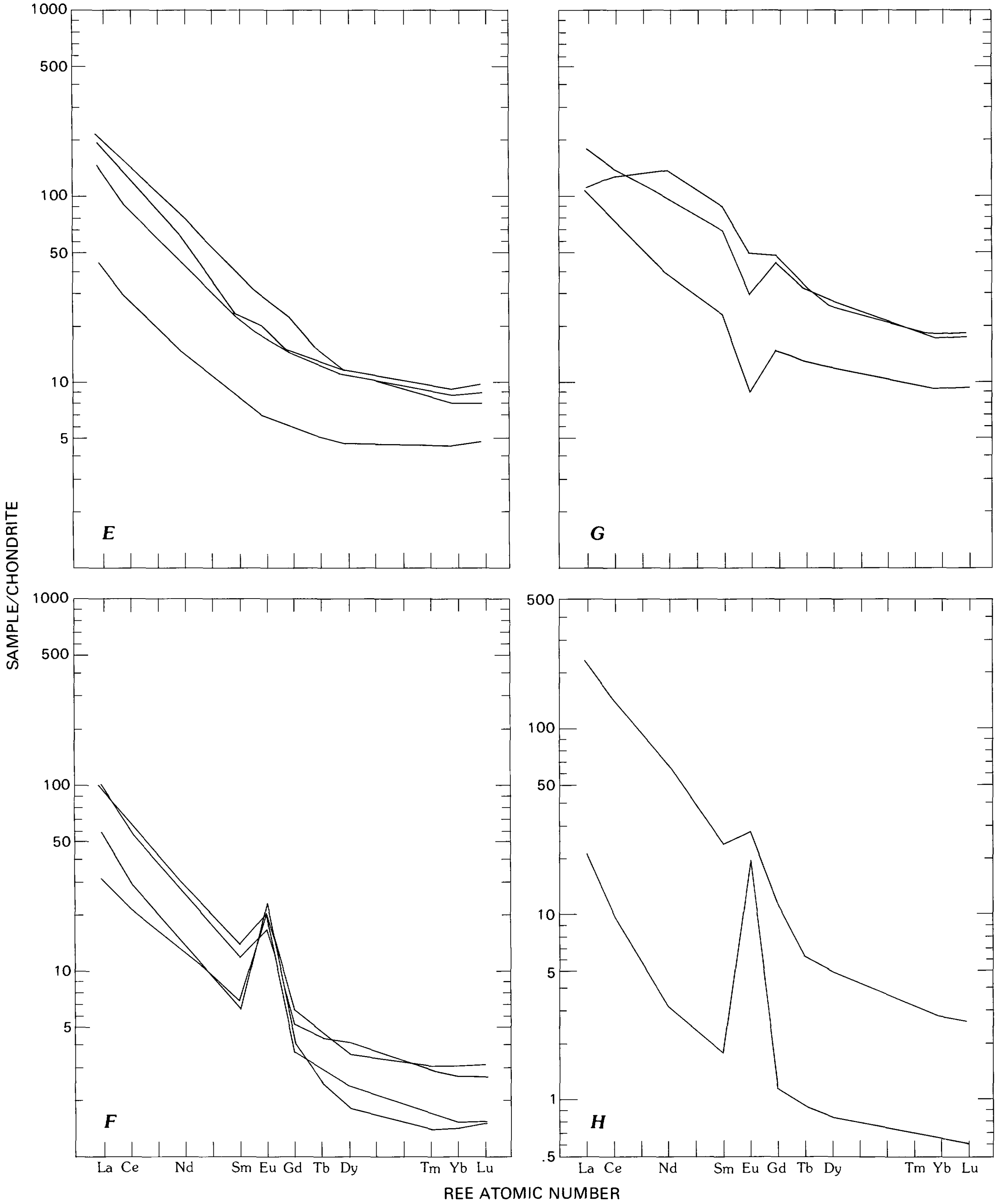

especially for the more siliceous solidus (shown by solid symbols). Minor adjustments in mineralogy and partitioning coefficients could probably produce a better agreement for the two calculations of the less siliceous solidus composition (for example, the use of more hornblende and less biotite would decrease the REE content

TABLE 6.—*Proportional differences between original chemical data and data recomputed from the 3-end-member factor model for the Louis Lake batholith*

[Average is the average of the absolute values]

Oxide	Sample No.												
	BW-3	BW-4	BW-5	BW-7	BW-9	BW-11	BW-19	BW-22	BW-24	GPA-1	GPA-6	LLB-2	LLB-3
SiO_2	0.02	0.01	0.01	-0.07	0.00	0.03	0.03	0.03	0.04	0.01	0.00	0.00	0.01
Al_2O_3	.01	.02	-.01	.05	.03	-.05	-.01	-.01	-.03	-.05	.06	.02	.00
FeO	-.08	-.34	-.13	-.32	-.15	.05	-.10	-.19	-.16	.29	-.15	-.02	-.14
MgO	-.23	-.23	-.06	-.04	.34	-.05	-.72	-.47	-.25	.16	-.32	.04	-.02
CaO	-.29	-.05	.05	.26	-.03	.03	-.08	-.18	-.02	.22	-.07	-.12	-.11
Na_2O	.11	.05	.13	.02	.00	-.29	.03	.10	-.04	-.06	.07	.05	.04
K_2O	-.11	.04	-.17	.51	.00	-.06	-.41	-.14	-.19	-.11	-.09	.03	.00
TiO_2	-.17	-1.05	-.65	-.31	.05	.05	.15	-.08	-.26	.36	-.12	.06	-.04
P_2O_5	-1.12	-.30	-.32	.03	-.05	-.23	-.43	-.26	-.05	.75	-1.65	.04	.01
ThO_2	-.35	-.46	.41	-1.14	-.03	-.58	-.25	-.20	.20	-.13	-.04	.06	-.41
UO_2	-.19	-.56	-1.14	-.15	-.34	-.14	-.50	-1.10	-3.34	.04	.09	.20	-.05
CuO	.11	-.13	-.20	.09	-6.77	.40	-.09	.16	.30	.48	-.18	-.07	.04
ZnO	.27	-.11	-.08	.00	.21	-.05	.03	-.04	.05	.10	.13	-.04	.06
Rb_2O	-.07	-.25	-.36	.15	.29	-.10	-.40	-.40	.00	-.11	.18	-.12	-.10
SrO	-.15	.11	.03	.50	-1.41	-.66	-1.45	-.39	-.06	-3.11	-.11	.10	.06
Y_2O_3	.11	-.05	-.48	.02	-.36	.12	-1.36	-.43	.03	.59	.16	.09	.06
ZrO_2	.16	-.53	-.35	-2.02	-.23	.04	.20	-.06	-.38	-.08	.12	.01	-.07
Nb_2O_5	-.01	-.53	-1.33	.43	-1.31	-.05	-.14	-.47	-.77	.29	.34	.02	-.04
La_2O_3	-.05	.11	.36	.01	-.21	-.62	-.17	.02	-.46	-.03	-.22	.11	-.61
Ce_2O_3	-.03	.04	.31	.17	-.14	-.77	-.14	.04	-.39	.03	-.17	.05	-.40
Nd_2O_3	-.01	-.12	.19	.26	-.14	-.78	-.41	.08	-.21	.19	-.13	.02	-.19
Sm_2O_3	-.05	-.21	-.07	.23	-.15	-.61	-.51	.03	-.02	.37	-.02	-.06	.00
Eu_2O_3	-.11	-.11	.02	.34	-.16	-.14	-.24	-.15	-.15	.43	-.18	-.01	-.01
Gd_2O_3	.06	.04	-.28	.21	-.18	-.26	-.41	.11	.04	.69	.19	-.17	.02
Tb_2O_3	-.01	-.05	-.35	.08	-.16	-.04	-.51	-.03	.07	.65	.19	-.14	.11
Dy_2O_3	.07	-.07	-.49	.03	-.21	.00	-.61	-.23	.01	.59	.17	-.10	.17
Tm_2O_3	.10	-.03	-.53	-.17	-.27	.23	-.49	-.19	-.15	.39	.19	.02	.04
Yb_2O_3	.07	.00	-.52	-.24	-.29	.28	-.34	-.16	-.25	.33	.17	.05	-.01
Lu_2O_3	.06	.01	-.49	-.22	-.27	.29	-.25	-.10	-.25	.24	.17	.04	-.14
Cs_2O	-.16	-6.01	-3.79	-14.78	.35	-.42	-2.13	-1.01	-5.93	-3.00	.14	-.04	-.61
BaO	-.15	.06	-.21	.28	-.26	.01	-1.03	-.19	-.40	-.24	.08	.20	.08
Ta_2O_5	-1.20	-1.18	-3.83	.50	-1.66	-.22	-.23	-.47	-.38	-.70	-.74	.05	.00
HfO_2	.03	-.42	-.25	-1.73	-.04	.04	.31	.11	-.25	-.26	.14	-.03	-.19
Sc_2O_3	-2.26	-.34	-.26	-.51	.35	.13	-1.39	.16	.02	.76	-.12	.04	-.03
Cr_2O_3	-1.71	-.64	-.45	-.28	-5.11	-.05	-1.10	.15	-1.41	.40	-.10	-.56	-.84
CoO	-.13	-.39	-.15	-.15	-.05	.08	-.42	-.40	-.23	.51	-.49	.11	-.09
MnO	-.22	-.16	.13	.35	.06	-.11	-.61	-.12	-.39	.17	-.51	-.02	-.45
Average	.24	.40	.50	.72	.59	.22	.48	.23	.46	.46	.22	.08	.14

of the model solid shown by open squares). Such fine tuning is not warranted in light of all the assumptions in the model and the fact that the liquidus composition was continually evolving such that the composition of the solidus in equilibrium with the magma was also continually changing. However, the calculations are sufficiently precise to show that the end members chosen by Q-mode modeling are consistent with petrochemical constraints.

Stuckless and others (1985) interpreted initial strontium and lead isotopic data to indicate an unevolved (low contents of incompatible elements) source for the Louis Lake batholith and proposed that the protolith was trondhjemitic to tonalitic. Oxygen isotope data (Cheang and others, 1986) for the Louis Lake batholith (average $\delta^{18}O$ = 7.3 per mil) are similar to those reported for trondhjemitic to tonalitic gneisses (Longstaffe and Schwarcz, 1977) and are therefore

TABLE 6.—*Proportional differences between original chemical data and data recomputed from the 3-end-member factor model for the Louis Lake batholith*—Continued

[Average is the average of the absolute values]

Oxide	Sample No.												
	LLB-4	LLB-5	LLB-7	LLB-8	LLB-9	LLB-11	LLB-12	LLB-15	PRM-1	PRM-2	PRM-3	PRM-5	PRM-6
SiO_2	-0.01	-0.01	-0.08	-0.02	0.00	-0.01	0.01	0.00	-0.02	0.00	-0.01	0.00	-0.04
Al_2O_3	.00	-.01	.01	.00	.00	.00	-.02	-.02	.04	.03	-.01	-.02	-.05
FeO	.12	.20	.27	.27	.05	.12	-.18	.10	.13	-.40	.09	.11	.22
MgO	.13	.04	.46	.06	-6.14	.10	.05	-.01	.36	-.05	.47	.04	.35
CaO	.03	.01	.17	.09	.16	.04	-.04	-.02	.04	-.18	-.14	-.01	.12
Na_2O	-.09	.03	-.09	.03	-.06	.00	-.02	-.03	.01	.03	-.01	-.14	-.22
K_2O	.00	-.29	.12	-.27	.01	-.12	.02	-.04	.00	.08	.09	.10	.14
TiO_2	.08	.09	.31	.19	.15	-.07	-.23	.05	.21	.20	.05	-.10	.25
P_2O_5	.03	.35	.22	-.13	-.03	.05	-.12	.00	.24	.26	.46	-.88	.54
ThO_2	.18	-.02	.81	.10	.06	.08	-.52	.35	.28	-.16	.23	-.76	.20
UO_2	.03	.46	.28	.48	.17	.54	-.41	.18	.16	-1.70	.46	-.86	.36
CuO	.02	-.06	.04	.40	.15	-.01	-.28	.01	.31	-.23	-.40	-.36	.20
ZnO	-1.22	.19	-.51	-.94	-.01	.13	-.10	.25	-.17	.18	-.28	-.15	.16
Rb_2O	-.14	.32	.55	.16	.04	-.04	.17	-.09	-.11	-.24	.07	-.26	.08
SrO	.10	.04	-.44	-.81	-.40	.06	.06	.06	.26	.16	.23	.43	.25
Y_2O_3	-.37	.36	.20	.26	.15	.25	.36	-.12	.07	-1.76	.24	-.51	.01
ZrO_2	.09	-.07	.27	.23	-.08	.02	-.20	.19	.13	.35	-.10	.10	.05
Nb_2O_5	-.56	.24	.30	.41	.47	.14	.23	.00	.11	-.10	-.54	-.64	.14
La_2O_3	.11	-.30	.47	.05	-.30	-.08	-.37	-.01	.26	.24	-.23	-.15	.29
Ce_2O_3	.00	-.10	.42	.05	-.27	-.04	-.25	.00	.25	.20	-.30	-.21	.29
Nd_2O_3	-.09	.12	.31	.01	-.22	.09	-.10	.02	.24	.09	-.15	-.27	.30
Sm_2O_3	-.17	.27	.18	.16	-.09	.14	-.08	.05	.18	-.04	.10	-.43	.25
Eu_2O_3	-.05	.11	.05	.02	-.09	.09	-.18	.00	.03	.12	-.08	-.19	.31
Gd_2O_3	-.13	.23	-.04	.13	-.14	.10	.07	.01	.07	-.36	.10	-.64	.11
Tb_2O_3	-.06	.25	-.01	.26	.05	.14	.15	-.01	.05	-.59	.13	-.64	-.06
Dy_2O_3	-.04	.30	.04	.32	.15	.18	.19	.00	.02	-.78	.17	-.70	-.12
Tm_2O_3	-.11	.28	.15	.27	.29	.22	.39	.02	-.27	-2.15	.27	-.62	-.27
Yb_2O_3	-.16	.25	.19	.27	.30	.25	.43	-.03	-.26	-2.49	.26	-.66	-.18
Lu_2O_3	-.24	.24	.25	.24	.32	.28	.46	-.08	-.27	-3.06	.25	-.72	-.17
Cs_2O	-.05	.58	.51	.85	.16	.36	.53	.09	-.13	.02	.31	-.60	.46
BaO	.15	.03	-.98	-.44	.03	.03	.01	-.02	.21	.26	-.30	.24	.33
Ta_2O_5	-.42	.35	.15	.49	.55	.35	.62	-.27	.01	-1.16	.26	-1.19	.12
HfO_2	-.03	.17	.21	.21	-.02	-.05	-.29	.15	.04	.16	-.01	.17	-.01
Sc_2O_3	.13	.14	.32	-.01	.41	.19	.05	.08	-1.09	-.02	.11	-.43	.35
Cr_2O_3	.06	.10	.71	.45	.38	.11	-.18	-.03	.24	-1.04	.18	.16	.60
CoO	.14	.04	.44	.04	.14	.07	-.18	.05	.33	-.26	.28	.01	.29
MnO	.09	.15	.44	.22	.13	.09	.25	.02	.02	-.72	.12	-.14	.17
Average	.15	.18	.30	.25	.33	.13	.21	.07	.18	.54	.20	.37	.22

consistent with the proposed protolith. The starting magma composition herein proposed for the Louis Lake batholith lends further support for an unevolved protolith.

Major- and trace-element data are consistent with a trondhjemitic to tonalitic source for the Louis Lake batholith. The unradiogenic initial ratios for strontium and lead data do not preclude an evolved source that is only slightly older than the batholith. However, such a source would be expected to yield elevated contents of LIL (large-ion lithophile) elements, a high Rb/Sr value, low contents of compatible elements, and a low K/Rb value. A starting magma, similar in composition to sample BW-24, has none of these features. Compatible elements such as strontium and calcium are strongly enriched (852 ppm and 5.25 percent, respectively, table 1). In contrast LIL elements, such as thorium, rubidium, and potassium, show no enrichment relative to typical

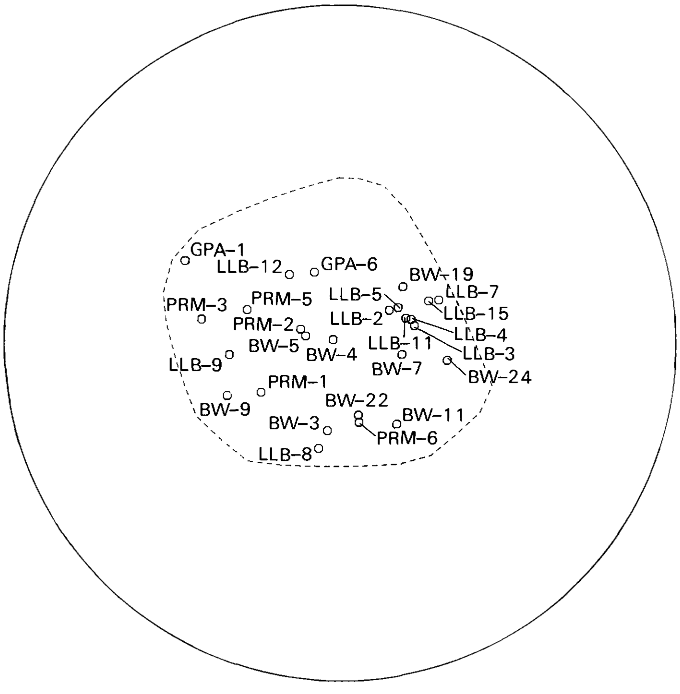

FIGURE 7.—Stereographic projection of the three-factor Q-mode vector solution derived from 37 oxides and 26 samples from the Louis Lake batholith. The dashed line outlines the area within which vectors represent compositions that are entirely positive; that is, outside this area one or more oxide values for any given vector (recomputed composition) will have a negative value.

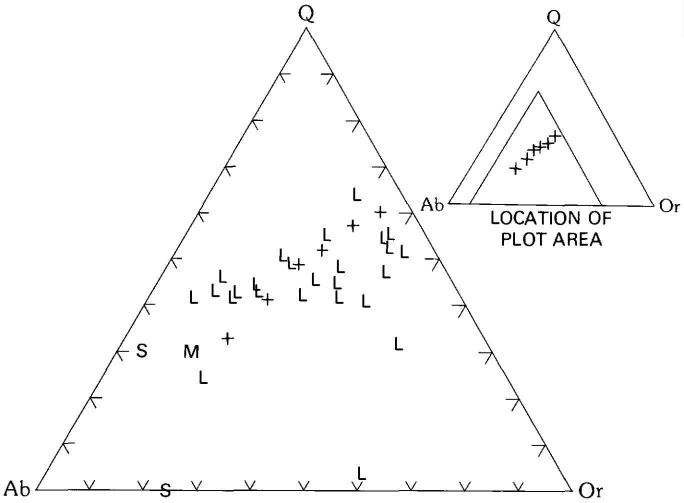

FIGURE 8.—Ternary diagram showing normative compositions of quartz (Q), albite (Ab), and orthoclase (Or) for the Louis Lake batholith (L), the composition of the starting magma (M), and the model composition of the fractionally crystallized solids (S). Also shown is the polybaric ternary minimum (shown by +, at 0.5, 1, 2, 3, 5, and 10 kbar from upper right to lower left) for the system Q-Ab-Or (Tuttle and Bowen, 1958; Luth and others, 1964). Expanded portion of the diagram is bounded by Q=O percent, Ab=25 percent, and Or=10 percent.

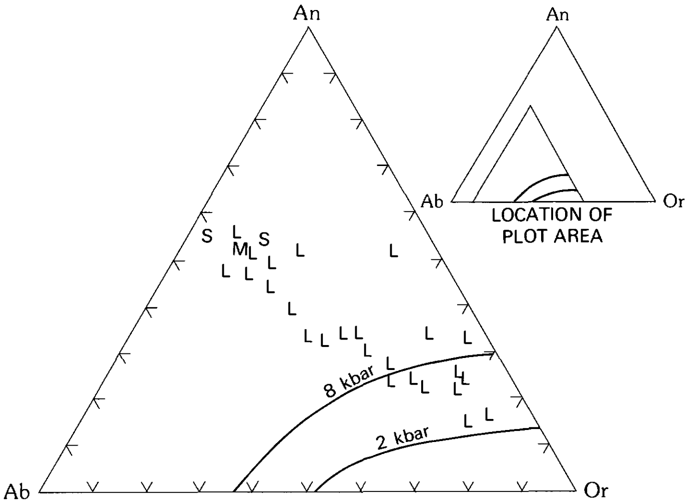

FIGURE 9.—Ternary diagram showing normative feldspar composition of samples from the Louis Lake batholith (L), the composition of the starting magma (M), and the composition of the fractionally crystallized solids (S). Also shown are the water-saturated eutectic compositions at 2 and 8 kbar (Whitney, 1975). Expanded portion of the diagram is bounded by anorthite (An) = 0 percent, albite (Ab) = 30 percent, and orthoclase (Or) = 10 percent.

granodiorites (11.4 and 52.0 ppm and 1.61 percent respectively, table 1). The Rb/Sr value is very low (0.06), and the K/Rb value is intermediate (258). High-grade metamorphism of an evolved protolith prior to magma generation could change some of the predicted features for the initial magma by depleting contents of some of the alkali metals (Rollinson and Windley, 1980), but the high alkaline-earth and low thorium contents are inconsistent with such an interpretation.

Oxygen isotope data (Cheang and others, 1986) not only support a trondhjemitic-tonalitic source, but they also argue against an evolved sedimentary source. Chemical data are also consistent with this interpretation. The whole-rock oxygen isotope data do not show the ^{18}O enrichment that is typical of Paleozoic granites derived from a sedimentary protolith (O'Neil and others, 1977); however, such an enrichment would be less pronounced for igneous rocks derived from Archean sediments (Longstaffe and Schwarcz, 1977). The whole-rock chemistry precludes a significant pelitic component for the protolith because all samples are metaluminous (table 1).

Initial lead and strontium isotope ratios for the Louis Lake batholith are not radiogenic enough to preclude totally a more primitive source than a trondhjemitic-tonalitic protolith (Stuckless and others, 1985), but the chemical data argue against any source as primitive as mantle material. The contents of potassium, rubidium, and barium in sample BW-24 (a sample with low

TABLE 7.—*Chemical compositions and CIPW normative mineralogy for the 3 end members of the factor model for the Louis Lake batholith*

[Norm calculated assuming one-third of the iron is oxidized. D index is differentiation index of Thornton and Tuttle (1960). PERAL is the molar ratio Al/(Na+K+Ca). PERALK is the molar ratio Al/(Na+K). Leaders (---) indicate no value]

Oxide	Magma	S-1	S-2
	Weight percent		
SiO_2	61.04	60.64	52.20
Al_2O_3	17.08	17.39	18.21
FeO	5.82	5.92	8.83
MgO	2.34	2.48	3.47
CaO	5.35	5.70	7.26
Na_2O	4.53	4.79	4.61
K_2O	1.94	1.25	2.16
TiO_2	.99	.96	1.73
P_2O_5	.45	.44	.80
	Parts per million		
ThO_2	12.3	.0	32.5
UO_2	3.0	2.7	3.2
CuO	43.3	45.3	.0
ZnO	116.1	120.1	152.9
Rb_2O	56.6	37.8	59.1
SrO	1118.5	1184.8	1430.3
Y_2O_3	40.1	34.6	84.8
ZrO_2	414.3	342.6	830.4
Nb_2O_5	18.0	14.8	39.0
La_2O_3	109.8	78.8	252.5
Ce_2O_3	227.8	170.5	517.3
Nd_2O_3	101.3	80.1	224.7
Sm_2O_3	17.7	14.7	38.0
Eu_2O_3	3.7	3.6	6.5
Gd_2O_3	12.9	11.0	27.9
Tb_2O_3	1.6	1.4	3.5
Dy_2O_3	8.5	7.3	18.0
Tm_2O_3	.6	.5	1.1
Yb_2O_3	3.2	2.8	6.6
Lu_2O_3	.5	.4	.9
Cs_2O	1.6	2.0	.6
BaO	1372.8	1197.6	2023.7
Ta_2O_5	1.4	1.2	2.8
HfO_2	10.2	8.3	20.7
Sc_2O_3	15.7	15.7	27.1
Cr_2O_3	42.9	48.0	50.2
CoO	17.8	18.5	27.5
MnO	840.8	893.7	1188.5
	CIPW norms (weight percent)		
Q	12.20	11.73	---
C	---	---	---
Z	.06	.50	1.23
Or	11.94	7.78	13.41
Ab	38.34	40.41	38.72
An	20.27	21.95	22.07
Wo	1.39	1.41	3.53
En	5.82	6.17	2.10
Fs	3.84	3.99	1.33
Fo	---	---	4.54
Fa	---	---	3.16
Mt	3.13	3.17	4.71
Cm	.06	.01	.01
Il	1.87	1.82	3.27
Ap	1.06	1.03	1.89
Total	99.97	99.98	99.97
salic	82.81	82.83	75.43
femic	17.16	17.60	24.53
D index	62.48	59.93	52.14
PERAL	.88	.88	.78
PERALK	1.77	1.87	1.81

TABLE 8.—*Mixing proportions for the 3-end-member factor model for the Louis Lake batholith*

Sample No.	Magma	S-1	S-2
BW-3	5.9345	-4.4385	-.4960
BW-4	4.5681	-2.8083	-.7597
BW-5	5.1372	-3.2612	-.8760
BW-7	2.7777	-1.4111	-.3666
BW-9	7.6774	-5.5960	-1.0814
BW-11	3.4280	-2.4280	.0000
BW-19	2.4535	-.8560	-.5975
BW-22	4.7268	-3.3625	-.3643
BW-24	1.0000	.0000	.0000
GPA-1	6.5957	-4.2336	-1.3621
GPA-6	4.4154	-2.4553	-.9602
LLB-2	2.9496	-1.3553	-.5943
LLB-3	2.2550	-.8441	-.4109
LLB-4	2.3430	-.8891	-.4538
LLB-5	2.6814	-1.1224	-.5590
LLB-7	1.3719	.0000	-.3719
LLB-8	6.6130	-5.1484	-.4646
LLB-9	6.9086	-4.7846	-1.1240
LLB-11	2.4961	-1.0120	-.4841
LLB-12	4.9108	-2.8754	-1.0354
LLB-15	1.7079	-.2848	-.4231
PRM-1	6.8728	-2.9262	-.9466
PRM-2	5.1757	-3.2679	-.9078
PRM-3	6.9559	-4.6990	-1.2570
PRM-5	6.0169	-3.8965	-1.1204
PRM-6	4.8068	-3.4865	-.3203
Average	4.3377	-2.6709	-.6668

concentrations of incompatible elements) are enriched by factors of 8–20 over average mantle; these enrichments require very low degrees of partial melting (5–12 percent, assuming the extreme case of a bulk distribution coefficient of 0). Production of a batholith-size intrusion by such low degrees of partial melting seems unreasonable.

An igneous or metamorphic protolith of trondhjemitic to tonalitic affinity should produce an I-type granite as defined by Chappell and White (1974), and the Louis Lake batholith has most of the diagnostic features of an I-type granite. The molar ratio of Al/(Na+K+Ca) is less than 1.1; normative corundum is generally less than 1 weight percent; silica contents exhibit a wide range (table 1); the initial $^{87}Sr/^{86}Sr$ of 0.7017 ± 0.0005 is low relative to Archean upper crustal rocks (Stuckless and others, 1985); the mafic and accessory minerals include hornblende, sphene, epidote, magnetite, and apatite; and there are abundant hornblende-bearing inclusions.

TABLE 9.—*Possible mineralogy of solids fractionally crystallized from the Louis Lake batholith*
[All values in weight percent]

Mineral	First solid	Second solid
Quartz	4.45	16.04
Zircon	.112	.046
Albite	37.69	39.05
Anorthite	23.70	23.25
Biotite	20.33	11.70
Orthopyroxene	0	0.63
Clinopyroxene	4.96	0
Hornblende	0	4.12
Magnetite	3.09	2.11
Sphene	1.41	0.53
Ilmenite	2.29	1.45
Apatite	1.89	1.02
Allanite	0.15	0.03
Total	100.07	99.98

As noted earlier, sample LLB-14 is from an area in which such inclusions are particularly abundant, and its chemistry does not fit well with other samples in a magmatic model. The inclusions are therefore most likely either restite or assimilated country rock, and in view of the evidence for the Louis Lake batholith being an I-type granite, the former interpretation is favored. If the inclusions do represent restite, they indicate residual plagioclase and hornblende in the protolith which would be consistent with a starting liquid with little or no europium anomaly (Hanson, 1978). The composition chosen as the initial magma for the Q-mode model has this feature.

Metamorphic rocks of appropriate major- and trace-element chemistry to be part of the protolith crop out in the Wind River Range (samples BW-33, 34, 41, 43, 48, and 51; table 3). Most of these examples are somewhat more siliceous than the proposed initial magma, but the large volume of material melted undoubtedly contained some more mafic material (such as sample BW-50; table 3). Furthermore, lower silica contents and other less evolved characteristics may be more typical of compositions at depths where melting occurred. All the tonalitic to trondhjemitic rocks analyzed as part of this study show steep REE patterns with little to no europium anomaly (fig. 6*B*, *D*, *E*). Partial melting of these rocks and a residuum dominated by hornblende or clinopyroxene and plagioclase could yield an initial liquid comparable to that proposed by the Q-mode model (table 7).

The normative composition of the proposed starting magma in the system Q-Ab-Or is suggestive of derivation at a pressure near 10 kbar and water-saturated conditions (fig. 8). Normative whole-rock compositions trend along the polybaric minimum and suggest somewhat lower to markedly lower pressures for crystallization, although this conclusion is reached with the caveat that a large proportion of the whole-rock chemistry is not represented by the Q-Ab-Or system. Normative compositions in the system An-Ab-Or also suggest that a few samples may have equilibrated at pressures as low as 2 kbar (fig. 9). Such pressures are difficult to reconcile with the occurrence of magmatic epidote, which indicates near-solidus temperature, high pressure, and water-saturated conditions (Naney, 1983), because such magmas should "freeze" before rising any substantial distance (Zen, 1985). Thus, if the whole-rock compositions represent equilibrium liquids, some mechanism of heat addition or dehydration with a subsequent intrusion of the batholith to a higher level is suggested by the data, an enigma similar to that noted by Coleman (in Zen, 1985).

BEARS EARS PLUTON

The choice of samples and oxide variables to be used in developing a Q-mode model for the Bears Ears pluton was less clear than in the case of the Louis Lake batholith. Various combinations of samples and oxides failed to yield particularly good agreements between the original and recomputed data, even at five factors. Successive eliminations of the most erratic sample or most erratic oxide failed to yield a readily interpretable model until so much data had been deleted as to obviate the value of a model. Therefore, the 18 samples that had been shown isotopically to be part of the Bears Ears pluton (Stuckless and others, 1985) were chosen for mathematical modeling, and the oxides chosen for use were the same as had been used for the Louis Lake batholith. The results of the factor-variance analysis are given in table 11 and shown graphically on figure 11.

Four other samples (BW-8, 10, 12, and 17; table 3) appeared on the basis of geology to be part of the Bears Ears pluton, but these yielded large (>0.75) badness-of-fit values when compared to the 18-sample data set. Seven other samples of questionable relationship to the Bears Ears pluton (BW-1, 2, 13, 14, 21, and 23, and LLB-6; table 3) were likewise found to be significantly different from the 18-sample data set. One of these samples (LLB-6) was an equigranular granite that cut the Louis Lake batholith and that was unrelated to the batholith (based on badness-of-fit value of 0.82 to the chemistry of the Louis Lake batholith). Because of the age relationship to the Louis Lake batholith, the

TABLE 10.—*Rare-earth-element contents of minerals in equilibrium with a proposed initial liquid for the Louis Lake batholith and for proposed solidus compositions*

[Partitioning coefficients used are from: Schnetzler and Philpotts (1970)—average of 5 plagioclases; Nagasawa and Schnetzler (1971)—average of 2 hornblendes, average of 5 orthopyroxenes, 1 clinopyroxene, and 1 apatite; Noyes and others (1983)—1 biotite, 1 magnetite, and 1 sphene; Gromet and Silver (1983)—1 zircon; Mahood and Hildreth (1983)—1 ilmenite]

Mineral	La	Ce	Nd	Sm	Eu	Gd	Tb	Dy	Tm	Yb	Lu
Liquid	93.62	194.5	86.84	15.23	3.237	11.24	1.425	7.406	0.482	2.819	0.405
First solid											
Plagioclase	11.98	20.99	6.68	.94	1.309	.55	.063	.297	.015	.077	.010
Biotite	5.67	12.04	5.30	.84	.158	.63	.082	.437	.034	.210	.032
Clinopyroxene ..	.91	3.49	4.05	1.15	.178	1.15	.164	.966	.058	.308	.036
Ilmenite	2.81	5.30	1.91	.24	.030	.12	.012	.063	.006	.036	.007
Magnetite	2.60	6.91	4.83	.87	.096	.59	.070	.320	.012	.057	.007
Sphene	19.05	68.29	95.26	22.98	4.272	17.91	2.288	11.59	.622	3.291	.354
Apatite	26.52	61.02	34.47	6.16	.887	4.35	.516	2.366	.099	.501	.060
Zircon	.05	.12	.06	.02	.004	.06	.021	.180	.100	.713	.121
Albite	157.7	291.0	80.89	6.44	.585	2.17	.184	.483	.015	.064	.006
Total	227.3	469.2	233.4	39.63	7.519	27.53	3.400	16.70	.960	5.256	.632
Solid	215.3	441.6	192.7	32.73	5.654	24.18	3.067	15.67	1.007	5.805	.818
Second solid											
Plagioclase	12.15	21.30	6.77	.95	1.328	.56	.064	.302	.015	.079	.010
Biotite	3.26	6.93	3.05	.48	.091	.36	.047	.251	.020	.121	.018
Orthopyroxene ..	7.02	16.93	10.81	2.36	.455	2.30	.340	1.959	.211	1.478	.245
Hornblende	3.61	11.22	14.81	4.80	.727	4.59	.619	3.967	.194	1.028	.102
Magnetite	1.78	4.72	3.30	.59	.066	.41	.048	.219	.008	.039	.005
Sphene	7.16	25.67	35.81	8.64	1.606	6.73	.860	4.357	.234	1.237	.133
Apatite	14.31	32.93	18.60	3.33	.479	2.35	.279	1.277	.053	.270	.033
Zircon	.02	.05	.02	.01	.002	.03	.009	.074	.041	.293	.050
Albite	32.64	60.21	16.74	1.33	.121	.45	.038	.100	.003	.013	.001
Ilmenite	1.78	3.36	1.21	.15	.019	.08	.007	.040	.004	.023	.004
Total	81.96	180.00	109.90	22.49	4.874	17.77	2.304	12.50	.779	4.557	.596
Solid	67.20	145.60	68.68	12.69	3.099	9.55	1.208	6.361	.420	2.468	.352

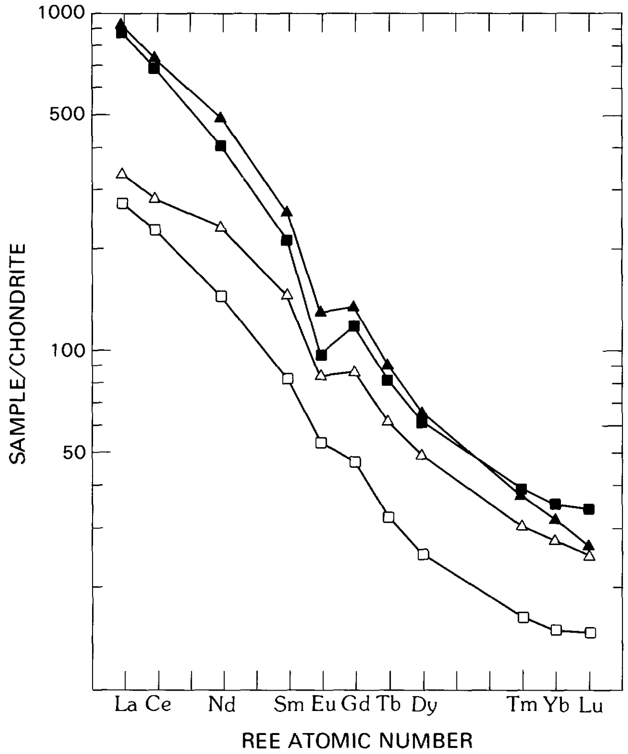

FIGURE 10.—Chondrite-normalized rare-earth-element diagrams for the fractionally crystallized solids calculated for the Louis Lake batholith. The less silicic solidus is shown by open symbols. The solid compositions derived by Q-mode analysis are shown by squares, and the compositions calculated from mineralogy, partitioning coefficients, and starting-liquid composition are shown by triangles.

sample was thought to be possibly related to the Bears Ears pluton, and the chemistry indicates a possible fit to the Bears Ears (badness-of-fit value of 0.43). However, inasmuch as no other samples were accepted on the basis of chemistry alone, the sample was not included in the Q-mode data set.

Ten of these 11 rejected samples were coarsely porphyritic, and the failure to fit with the chemistry of the Bears Ears pluton needs explanation. Samples BW-12 and -13 (badness-of-fit values 2.70 and 2.51, respectively) came from an area where xenolithic inclusions are common (fig. 3*C*) and probably fail to fit due to significant contamination. Sample BW-51 may represent another type of problem. It was collected 20 m from a metasomatized contact zone (fig. 3*B*) which grades from granite into orthogneiss in a few tens of meters.

A similar graditional contact, over a distance of several tens of meters, exists between Louis Lake batholith and apparent Bears Ears pluton for samples BW-37 through BW-39 (BW-37 being coarsely porphyritic, fig. 3*D*). Trace-element analyses were not made for sample BW-37, which is coarsely porphyritic, and therefore its chemistry could not be checked against that of the 18 isotopically analyzed samples. Nonetheless, the somewhat low silica, low rubidium, very low thorium, and very high strontium contents relative to typical Bears Ears pluton (tables 3, 4) suggest that sample BW-37 has incorporated a large component of Louis Lake batholith. By analogy to these contact-zone examples, other coarsely porphyritic samples with a poor fit to the chemistry of the Bears Ears pluton are probably contaminated, and the source of contamination may be close in a vertical direction, and as such, not visible.

The fact that contamination of the Bears Ears pluton is prevalent and not always visibly obvious may help explain the need for five factors in order to get reasonable agreement between original and recomputed data (table 12). Isotopic analyses in the rubidium-strontium and uranium-thorium-lead whole-rock systems show more scatter than can be explained by analytical error alone, and zircon analyses show a large component of inherited material (Stuckless and others, 1985). Thus, most of the samples may have some degree of contamination, and because the contaminant is most likely of variable composition, several factors must be added to the Q-mode model in order to account for all the end members that affect the chemistry of the average sample. In addition, the initial melt may have been inhomogeneous as discussed below.

The worst explained elements in the five-factor model for the Bears Ears pluton are essentially the same as those identified for the Louis Lake batholith, and they are poorly explained for largely the same reasons (high mobility or large analytical error relative to average concentration and standard deviation). Isotopic analyses show that a larger percentage of uranium was lost from the Bears Ears pluton than from the Louis Lake batholith, and the results of the factor analysis are generally in agreement with this fact.

In view of the apparently complex origin for the Bears Ears pluton and the inability to constrain the composition of possible contaminants, no attempt was made to identify specific end-member compositions. However, the data do provide some insights as to the origin of this unit. Isotopic data show that the Bears Ears pluton was derived from an evolved source that existed long enough to create fairly radiogenic initial ratios for lead and strontium (Stuckless and others, 1985). Present-day Rb/Sr and U/Pb values are low relative to those that should have been produced by partial melting of an evolved protolith given reasonable assumptions about the age of the protolith. The high barium content of the four samples with the lowest silica content (BEP-1 and -3, GPA-8, and BW-15) indicates that neither potassium feldspar nor biotite were residual phases

TABLE 11.—*Proportions of total chemical variance in the Bears Ears pluton that could be accounted for by factor models with 2-10 end members*

Oxide	Number of end members								
	2	3	4	5	6	7	8	9	10
SiO_2	0.76	0.76	0.77	0.83	0.88	0.89	0.91	0.91	0.91
Al_2O_3	.50	.50	.50	.73	.76	.78	.89	.90	.90
FeO	.75	.75	.78	.85	.86	.88	.88	.89	.88
MgO	.78	.80	.82	.81	.94	.97	.97	.97	.98
CaO	.82	.90	.90	.91	.94	.96	.97	.97	.98
Na_2O	.57	.65	.67	.79	.81	.81	.82	.82	.94
K_2O	.70	.87	.87	.89	.94	.94	.94	.94	.96
TiO_2	.89	.92	.93	.92	.94	.95	.96	.97	.97
P_2O_5	.71	.73	.74	.77	.86	.89	.90	.90	.90
ThO_2	.03	.61	.63	.83	.85	.89	.89	.92	.91
UO_2	.02	.05	.18	.45	.54	.55	.66	.90	.93
CuO	.06	.14	.17	.23	.46	.46	.63	.76	.76
ZnO	.20	.38	.46	.44	.43	.60	.68	.73	.88
Rb_2O	.60	.66	.66	.69	.77	.77	.90	.90	.91
SrO	.52	.54	.55	.70	.71	.73	.83	.84	.88
Y_2O_3	.26	.43	.68	.69	.70	.70	.93	.94	.95
ZrO_2	.43	.63	.66	.71	.72	.71	.87	.87	.87
Nb_2O_5	.26	.26	.26	.43	.48	.77	.78	.78	.86
La_2O_3	.32	.86	.85	.85	.92	.92	.92	.92	.92
Ce_2O_3	.35	.86	.85	.85	.91	.91	.91	.91	.92
Nd_2O_3	.37	.88	.87	.88	.93	.93	.93	.94	.94
Sm_2O_3	.39	.90	.91	.92	.94	.94	.94	.95	.95
Eu_2O_3	.51	.72	.74	.78	.78	.82	.89	.90	.90
Gd_2O_3	.43	.84	.89	.92	.93	.92	.94	.94	.94
Tb_2O_3	.44	.81	.93	.93	.94	.94	.95	.95	.95
Dy_2O_3	.42	.75	.92	.91	.93	.93	.94	.94	.94
Tm_2O_3	.18	.46	.64	.62	.71	.74	.84	.85	.90
Yb_2O_3	.36	.48	.75	.74	.86	.88	.97	.98	.98
Lu_2O_3	.34	.45	.70	.69	.83	.87	.97	.98	.98
Cs_2O	.06	.09	.48	.50	.61	.72	.73	.82	.83
BaO	.07	.12	.48	.60	.70	.78	.86	.86	.88
Ta_2O_5	.22	.21	.28	.35	.55	.61	.63	.63	.80
HfO_2	.47	.75	.77	.84	.84	.84	.91	.91	.91
Sc_2O_3	.77	.75	.85	.84	.85	.91	.92	.92	.97
Cr_2O_3	.00	.02	.02	.27	.37	.37	.49	.73	.74
CoO	.87	.91	.91	.90	.92	.95	.97	.97	.97
MnO	.73	.77	.78	.78	.78	.78	.80	.84	.86

(Hanson, 1978). The small to moderate negative europium anomaly for these same samples (fig. 12) indicates that plagioclase (possibly with much lesser amounts of hornblende) was a residual phase. Assuming that the ratio of plagioclase to hornblende in the residuum was only as large as 3:1, the partitioning

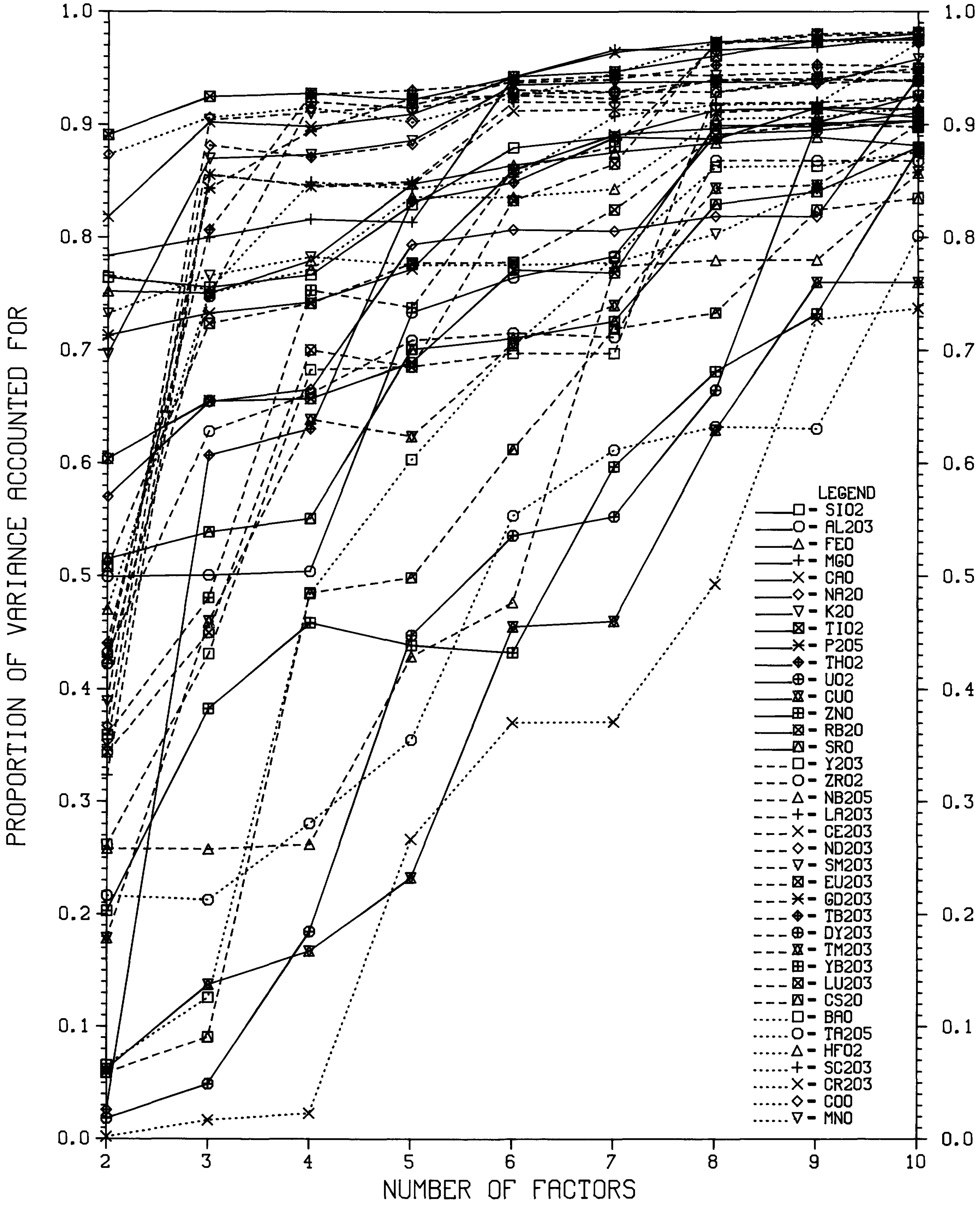

FIGURE 11.—Factor variance diagram for 18 samples of the Bears Ears pluton and 37 constituents. Data for the plot are given in table 11.

TABLE 12.—*Proportional differences between original chemical data and data recomputed from the 5-end-member factor model for the Bears Ears pluton*

[Average is the average of the absolute values]

Oxide	Sample No.								
	BEP-1	BEP-2	BEP-3	BEP-4	BW-15	BW-16	BW-18	GPA-2	GPA-3
SiO_2	-0.03	0.00	-0.01	-0.01	-0.01	0.01	0.01	0.00	0.00
Al_2O_3	.02	.00	-.02	.03	.03	-.06	-.02	-.02	.00
FeO	.22	-.09	.05	-.19	-.03	.00	-.20	.23	.10
MgO	.28	-.64	.05	-.32	-.02	-.02	-.17	-.39	-.26
CaO	-.12	.03	-.05	.24	.11	-.02	.11	.21	.14
Na_2O	.04	.09	-.03	.12	-.01	-.10	.00	-.14	-.03
K_2O	.10	-.09	.24	.00	.03	.05	-.10	.05	-.03
TiO_2	.11	-.25	.05	-.01	.16	.11	.02	.17	-.22
P_2O_5	.24	-.01	.11	.17	.14	.05	-.06	.00	-.40
ThO_2	.14	-.45	.32	.27	-.09	.12	-.29	-.10	.14
UO_2	.81	-1.34	-.01	.06	.44	.32	-.22	.25	-.55
CuO	.00	-.04	-.30	-.05	.06	.08	.19	.01	.47
ZnO	-.21	-.21	.17	-.01	.20	.15	-.18	-.10	.12
Rb_2O	.09	-.26	.21	.15	.01	-.18	-.24	.00	-.04
SrO	.27	-.07	-.37	.15	.23	-.03	.12	.27	.15
Y_2O_3	.28	.27	-.14	-.46	.25	.23	-.25	.22	.25
ZrO_2	-.03	-.18	-.12	-.08	.33	.12	-.02	.02	.34
Nb_2O_5	.35	-.97	-.01	.25	.01	-.02	-.52	-.37	.25
La_2O_3	-.11	-.25	.15	.30	.03	-.14	.18	-1.27	.42
Ce_2O_3	-.02	-.32	.12	.34	.05	-.20	.15	-1.16	.40
Nd_2O_3	-.03	-.30	.13	.31	.14	-.13	.11	-.53	.41
Sm_2O_3	.08	-.11	.14	.23	.13	-.12	-.05	-.34	.38
Eu_2O_3	.03	-.14	-.14	-.04	.33	.07	.07	.37	.20
Gd_2O_3	.08	-.14	.06	-.06	.21	-.05	.01	.06	.36
Tb_2O_3	.14	.06	.09	-.15	.14	.00	-.16	-.01	.26
Dy_2O_3	.12	.07	.11	-.21	.16	-.02	-.19	-.03	.18
Tm_2O_3	.29	.11	.19	-.38	.29	.20	-.24	.19	-.17
Yb_2O_3	.22	-.08	-.12	-.45	.24	.16	-.20	.20	-.47
Lu_2O_3	.26	-.12	-.20	-.53	.24	.19	-.20	.26	-.59
Cs_2O	-.41	.21	.02	.64	.45	-2.49	.44	.29	-.05
BaO	.13	-.01	-.02	-.20	.33	.10	-.25	.17	.04
Ta_2O_5	.48	-.70	-.21	-.02	.12	-.50	-.59	-.09	-.23
HfO_2	-.12	-.23	-.11	-.16	.26	.11	.01	.22	.04
Sc_2O_3	.04	-2.32	.19	-.15	-.07	.18	-.06	.01	-.19
Cr_2O_3	.55	.45	.32	10.08	-.24	-.65	-.16	-.21	-.19
CoO	.21	-.34	.08	-.09	.03	.10	-.19	.13	.03
MnO	.06	-.19	.18	.29	.11	.09	-.09	.28	-.09
Average	.18	.30	.13	.46	.16	.19	.16	.23	.21

TABLE 12.—*Proportional differences between original chemical data and data recomputed from the 5-end-member factor model for the Bears Ears pluton*—Continued

[Average is the average of the absolute values]

Oxide	Sample No.								
	GPA-4	GPA-5	GPA-8	GPA-9	GPA-10	GPA-11	GPA-12	GPA-13	PRM-7
SiO_2	0.00	-0.02	-0.02	0.01	0.01	0.01	0.00	0.02	0.01
Al_2O_3	-.02	.03	.08	.00	-.02	-.01	.00	-.03	-.01
FeO	-.02	.12	-.10	.00	-.15	.05	.12	-.10	-.36
MgO	.21	.62	.06	-.16	.29	.34	-.49	-.14	-.88
CaO	-.51	.00	.03	.13	-.77	-2.74	.28	-.02	.14
Na_2O	.05	-.18	.00	-.05	-.03	.09	-.05	-.01	.12
K_2O	.09	.12	.16	-.07	.01	-.10	- .05	-.37	-.05
TiO_2	.03	.40	.01	-.06	.23	-.20	-.53	-.28	.56
P_2O_5	.30	.36	.24	-.88	.12	-.33	-.75	-1.72	.37
ThO_2	-.09	-.19	-.95	.08	.04	-.06	-.12	.55	.12
UO_2	-.10	-.13	-.85	.41	.33	.09	-.89	-.78	.32
CuO	.03	-.11	-.33	-.09	-.24	-.05	-.10	.03	-.03
ZnO	-.18	.06	-.51	.12	.22	.05	-.06	.05	-.11
Rb_2O	-.12	.21	.38	-.08	-.03	.04	-.07	-.38	-.09
SrO	.26	-.26	-.85	-.39	.06	-1.42	-.26	.07	.46
Y_2O_3	.23	-1.06	-1.01	-.07	.42	-.10	-.62	-.31	.08
ZrO_2	.13	-.15	-.36	-.22	.05	.01	-.36	.00	-.17
Nb_2O_5	-.27	.19	-.42	-.33	.07	.49	-.67	.12	-.26
La_2O_3	.03	-.86	-.79	.11	-.62	-.12	-.31	.42	.92
Ce_2O_3	-.04	-1.14	-.70	.07	-.61	-.09	-.26	.37	.91
Nd_2O_3	-.10	-1.17	-.63	-.03	-.44	-.05	-.22	.24	.68
Sm_2O_3	-.15	-.56	-.45	.03	-.29	.03	-.10	.13	.05
Eu_2O_3	.09	-.04	-.12	-.23	-.03	-.36	-.46	-.31	.37
Gd_2O_3	-.03	-.26	-.22	-.03	.08	.05	-.21	-.20	-.03
Tb_2O_3	-.02	-.11	-.13	.03	.05	.10	-.11	-.23	-.11
Dy_2O_3	.00	-.03	-.06	.05	.08	.12	-.14	-.25	-.11
Tm_2O_3	.18	.09	.15	-.17	.25	-.12	-.53	.10	.03
Yb_2O_3	.24	.22	.02	-.12	.29	-.18	-.47	-.26	.00
Lu_2O_3	.27	.26	.03	-.15	.30	-.38	-.52	-.30	.00
Cs_2O	-.19	-.49	-.23	.08	-.42	-.98	-.48	-.15	.13
BaO	.22	.08	.11	.13	.03	-.26	-.43	-.51	-.45
Ta_2O_5	.26	.25	-.17	.28	.29	.28	-1.94	.06	-.22
HfO_2	.05	.20	-.05	.08	.02	-.06	-.38	.02	-.49
Sc_2O_3	.03	.54	-.16	-.04	.18	.13	-.10	-.05	-.43
Cr_2O_3	.60	.71	-.43	.36	-.77	-.13	-2.30	-.04	-1.40
CoO	.07	.35	-.20	.04	.12	.11	-.22	-.11	-.68
MnO	.07	.08	-.47	.09	-.19	-.59	-.19	-.12	.05
Average	.14	.31	.31	.14	.22	.28	.40	.24	.30

coefficients for rubidium and strontium given by Noyes and others (1983), and a change in Rb/Sr from 0.125 (given by Stuckless and others, 1985) to 0.33 (the average of the seven lowest Rb/Sr values) allows a partial melting of nearly 70 percent. Similar arguments suggest that melting of an evolved source should yield lower K/Rb and higher U/Pb values for the low-silica samples than are observed.

The low Rb/Sr and U/Pb values and high K/Rb values relative to those expected from the partial melting of an evolved source can be explained by granulite-facies metamorphism of the source region prior to generation of the granite. There are abundant examples of depletion of certain LIL elements (especially the alkaline metals and uranium) in response to granulite-facies metamorphism (Lambert and Heier, 1968; Lewis and Spooner, 1973; Dostal and Capedri, 1978). Some studies have also shown depletion of uranium relative to thorium (Moorbath and others, 1969; Gray, 1977) and depletion of rubidium relative to potassium (Rollinson and Windley, 1980). Thus, high-grade metamorphism could create a protolith that would yield a radiogenic granite, but with enrichment of only relative immobile LIL elements such as thorium and not other LIL elements such as uranium, cesium, potassium, and rubidium. This same source could also produce a magma with an intermediate K/Rb value without evidence for potassium feldspar in the residuum.

Much of the observed chemistry of the Bears Ears pluton could be explained by a model of contamination and open-system evolution of a magma derived from a primitive to intermediate protolith. Such a model would be consistent with the abundant evidence for contamination, and the wide-spread occurrence of young pegmatites could be consistent with loss of volatiles and labile LIL elements during late differentiation. However, isotopic evidence would require the contaminant to be the same age as that proposed for the source region (about 3,100 Ma, Stuckless and others, 1985) or to have a very minor observable effect on the isotopic compositions. The known areas of gradational contact with the country rock, and hence, areas of most notable

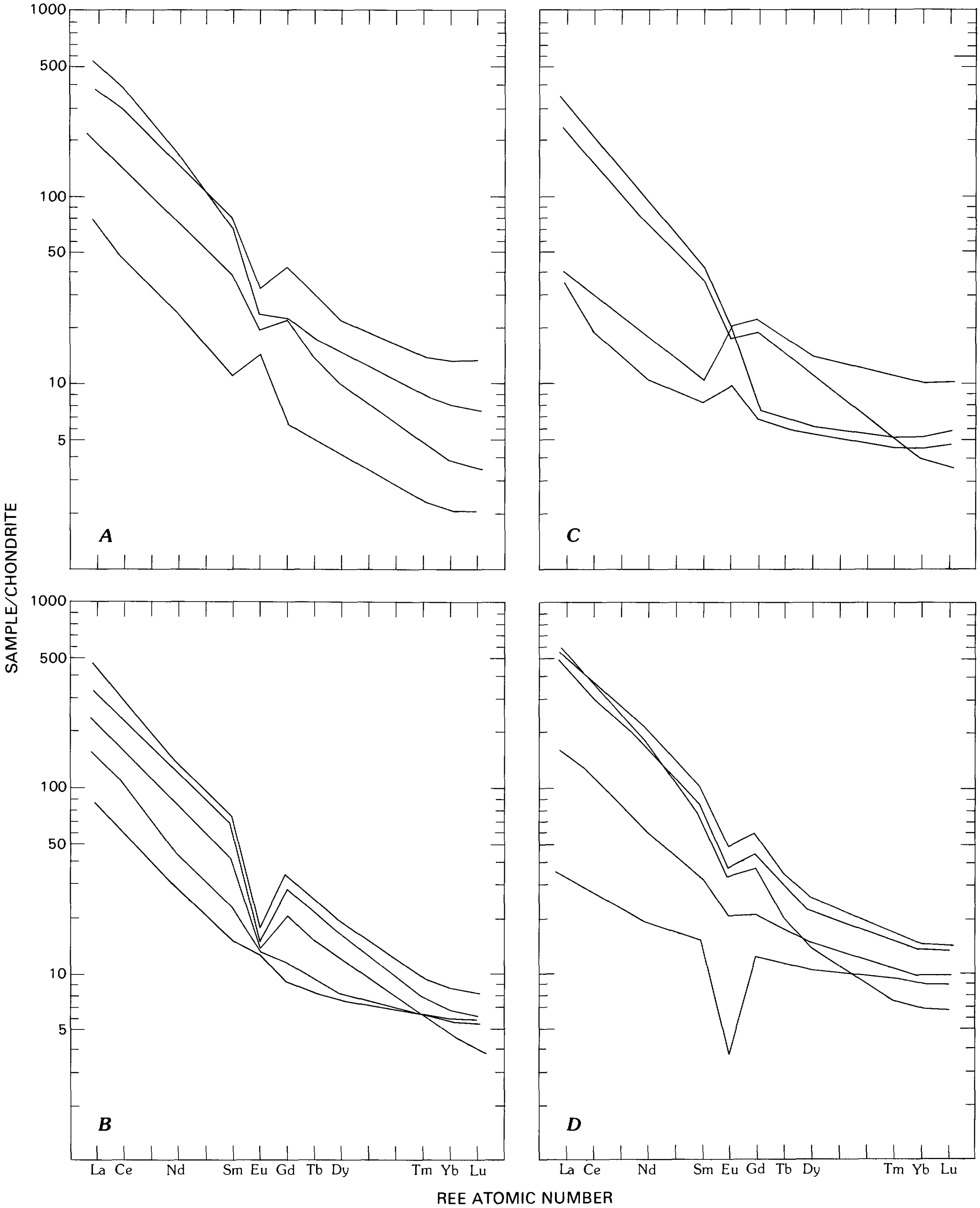

FIGURE 12.—Chondrite-normalized rare-earth-element diagrams for samples of the Bears Ears pluton: *A*, Samples BEP-1, BEP-2, BEP-3, and BEP-4; *B*, Samples GPA-9, GPA-10, GPA-11, GPA-12, and GPA-13; *C*, Samples GPA-2, GPA-3, GPA-4, and GPA-5; and *D*, Samples BW-15, BW-16, BW-18, GPA-8, and PRM-7.

contamination, are not old enough or otherwise radiogenic enough to be similar to the initial isotopic composition of the Bears Ears pluton, and strontium contents are very high such that even small amounts of assimilation would be observable. Thus, if these rocks represent the contaminant, the effect of assimilation would be to cause scatter by addition of an unradiogenic component to a radiogenic magma. The effect on whole-rock chemistry caused by assimilation of relatively unevolved rocks would be consistent with the generally low to moderate LIL-element contents observed for the Bears Ears pluton.

In contrast to the Louis Lake batholith, most features of the Bears Ears pluton indicate that it is an S-type granite (Chappell and White, 1974). The granite is peraluminous as indicated by normative corundum greater than 1 percent and a molar ratio of Al/(Na+K+Ca) greater than 1 (table 2). Thus, the source region most likely had a pelitic component. Other S-type features include: (1) a generally low sodium content (Na_2O <3.2 percent) in potassium rich (K_2O >5.0 percent) samples, (2) a narrow silica range, and (3) an elevated initial strontium ratio. The $\delta^{18}O$ values for the Bears Ears pluton (Stuckless and others, 1985) are low relative to those observed for S-type granites of Paleozoic age (O'Neil and others, 1977). However, Archean sediments may have been much less enriched in ^{18}O than those of younger age (Longstaffe and Schwarcz, 1977). Alternatively, the relatively low $\delta^{18}O$ values for the Bears Ears pluton may have developed in response to the proposed high-grade metamorphism of the protolith.

The classification of S-type granite suggests an alternate interpretation to explain the complex chemistry of the Bears Ears pluton and the nonideal behavior of the isotopic systems. Partial melting of a metasedimentary protolith that was isotopically and chemically (especially with respect to trace elements) inhomogeneous and subsequently intruded without homogenization of the melt could explain most of the features observed in the granite without appealing to contamination. This hypothesis would be consistent with the disconnected appearance of intrusions in map view, and varying degrees of partial melting from area to area could create a complex chemistry. A similar explanation has been proposed for granites from the Granite Mountains and the Owl Creek Mountains, Wyo. (Stuckless and Miesch, 1981; Stuckless, Miesch, and Wenner, 1986). Data for these granites also require five-end-member models, but a larger proportion of the variance is accounted for in these granites than is accounted for in the Bears Ears pluton, and the isotopic systems display better linearity and slopes correspond more closely with independently determined ages for these other granites.

If all the complex chemistry for the Bears Ears pluton is attributed to source region inhomogeneities, inherited zircons could be interpreted as entrained restite material. None of analytical data show any zircons as old as the proposed protolith, but old zircons could exist as small cores of the analyzed samples. There are no other data that strongly indicate the acquisition of an inhomogeneous character directly from the source region, but this mechanism can not be ruled out. In contrast, contamination from the country rocks is observed and is probably responsible for much of the isotopic and chemical variability present at the time of crystallization.

Even though most samples of the Bears Ears pluton seem to have incorporated some xenolithic material, the whole-rock normative data do provide some constraints on the physical conditions of crystallization, if the amount of contamination is assumed to be small. This assumption is reasonable because the 18 samples that were chosen yield near-linear relationships in the rubidium-strontium and thorium-lead isotopic systems (Stuckless and others, 1985). Figure 13 shows that data for all the samples of the Bears Ears pluton plot in the low-pressure portion of the system Q-Ab-Or. Several samples are displaced to the right of the polybaric minimum which could be interpreted as indicating crystallization at water-undersaturated conditions (Luth, 1969), the effect of a moderate anorthite content (Winkler and others, 1975), or a metasomatic introduction of potassium. Several lines of evidence suggest that water was abundant during crystallization: (1) the presence of hydrous minerals such as biotite, (2) the presence of abundant pegmatites, and (3) the growth of large potassium feldspars in the country rock. The latter feature indicates that potassium metasomatism was common during crystallization of the pluton, and therefore, this mechanism plus the effects of moderate anorthite in some samples (table 2) are probably responsible for the observed displacement of data points from the polybaric minimum. The higher anorthite samples also stand out in the An-Ab-Or system in that they plot away from equilibrium feldspar compositions and in the field where plagioclase is expected to crystallize first (fig. 14).

None of the samples of the Bears Ears pluton have retained any evidence of a high-pressure equilibration in the Q-Ab-Or system. Thus, both partial melting and differentiation may have occurred at pressures less than 3 kbar. Evidence is more equivocal in the feldspar system, but data for the low calcium samples plot on or below the 2-kbar water-saturated boundary curves

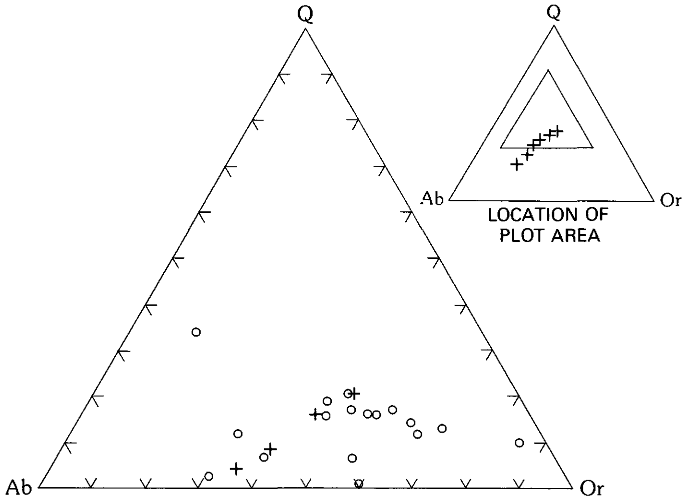

FIGURE 13.—Ternary diagram showing normative compositions for samples from the Bears Ears pluton and the polybaric ternary minimum (shown by +) for the system quartz-albite-orthoclase (Q-Ab-Or) (Tuttle and Bowen, 1958; Luth and others, 1964). Expanded portion of the diagram is bounded by Q=30 percent, Ab=15 percent, and Or=10 percent.

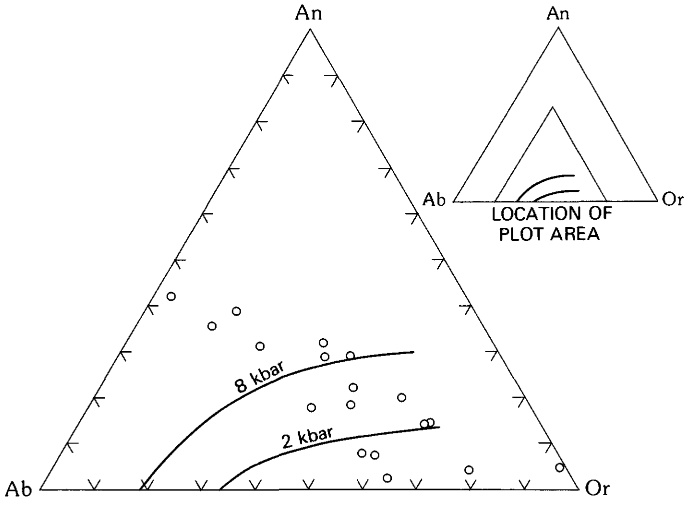

FIGURE 14.—Ternary diagram showing normative feldspar composition of samples from the Bears Ears pluton and the water-saturated eutectic compositions at 2 and 8 kbar (Whitney, 1975). Expanded portion of the diagram is bounded by anorthite (An) = 0 percent, albite (Ab) = 25 percent, and orthoclase (Or) = 20 percent.

(fig. 14) and, as such, suggest low pressure for at least the end stage of crystallization.

COMPARISON OF THE LOUIS LAKE BATHOLITH AND BEARS EARS PLUTON

The two granitoids from the Wind River Range are similar enough chemically that standard petrologic and variation diagrams do not delineate distinct fields for the two data sets. The similarity in major-element compositions is predictable in that relative proportions of these elements are controlled largely by physical conditions of melting or crystallization (Tuttle and Bowen, 1958). Because both granitoids equilibrated at moderate to low partial pressures of water, both data sets occupy similar fields in the Q-Ab-Or system (figs. 8, 13). Likewise, normative feldspar compositions are fairly similar, although there are more data points in the region of the two-feldspar field for the Louis Lake batholith (figs. 9, 14).

In these and other major-element systems, samples from the Bears Ears pluton could be interpreted as late-stage differentiates of the Louis Lake batholith. For example, the variation of CaO with SiO_2 shows a broad-band trend for samples of the Louis Lake batholith. Data for the Bears Ears pluton overlap with this trend at intermediate silica values and extend the trend to higher silica values (fig. 15*A*). White and Chappell (1983) have shown that data for S- and I-type granites are generally separated on a plot of Na_2O versus K_2O. There is some overlap, especially in the range of 2.5–4.5 percent K_2O and 2–3 percent Na_2O. Most of the data for the two granitoids from the Wind River Range plot within this overlapping range and do not form distinct fields (fig. 15*B*).

Trace-element contents of granitic rocks are less dependent upon the physical conditions of crystallization and are generally controlled by the trace-element chemistry and mineralogy of the protolith, the degree of partial melting, and the mineralogy of the solidus separated during differentiation (Hanson, 1978). A plot of K/Rb versus Rb/Sr (fig. 15*C*) shows that samples of the Bears Ears pluton are generally more evolved than those of the Louis Lake batholith (slightly lower K/Rb values and generally much higher Rb/Sr values). However, data fields overlap, and the two sets of data could be related by varying degrees of differentiation or partial melting.

Other trace elements, such as the rare earths, show similar concentrations and distributions for the two granitoids (figs. 5, 12), although samples from the Bears Ears pluton show more variability. Elsewhere in Wyoming, chrondrite-normalized REE patterns do not distinguish between granites from the Granite Mountains and those from the Owl Creek Mountains (Stuckless and Miesch, 1981; Stuckless, Miesch, and Wenner, 1986), and in fact, REE patterns for both of these Archean granites are similar to those for the two Wind River granitoids.

Even discrimination diagrams, such as those proposed by Pearce and others (1984), show considerable overlap between the two sets of data. The best separation is shown by the plot of Rb versus Y+Nb (fig. 15*D*). Within

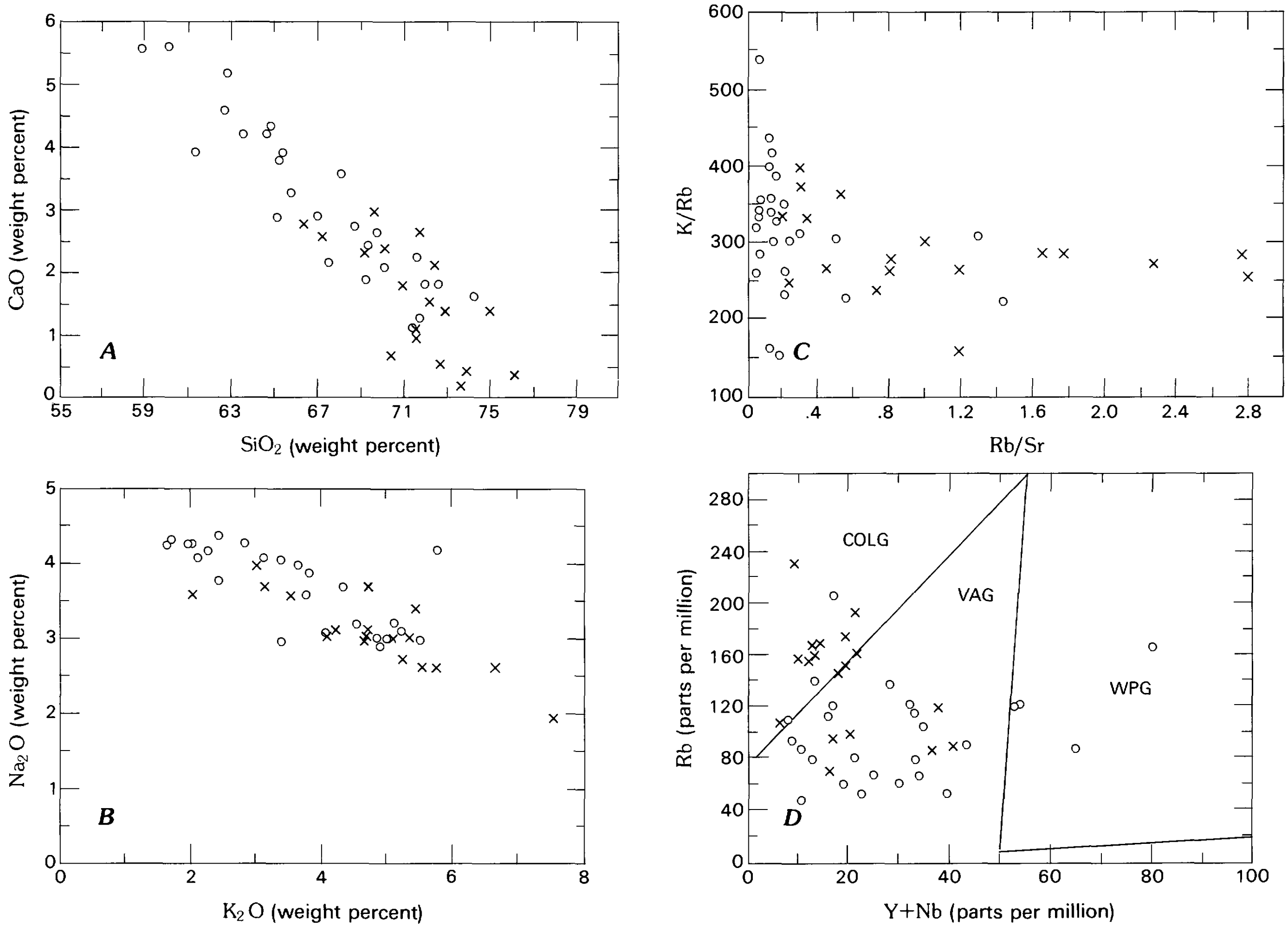

FIGURE 15.—X-Y plots for data from the Louis Lake Batholith (X's) and the Bears Ears pluton (squares). Fields shown in *D* are from Pearce and others (1984) and represent the tectonic settings of syncollisional granites (CLOG), volcanic arc granites (VAG), and within plate granites (WPG).

this system, most of the samples of the Louis Lake batholith plot within the field for volcanic-arc granites (VAG, fig. 15*D*). Most of the data for the Bears Ears pluton plot within or on the boundary of the field for syncollisional granites (COLG). Neither set of data plots within a single field.

The two granitoids are most distinct in terms of their isotopic and Q-mode characteristics. Stuckless and others (1985) have shown that the rubidium-strontium and uranium-thorium-lead systems are distinct for the two granites, but that the petrogenetic lineage for individual samples may not be obvious from one isotopic system alone. For example, data for a given sample may plot close to both rubidium-strontium isochrons, whereas lead data for either the thorium-lead or lead-lead system may plot distinctly on one isochron or the other. Initial isotopic ratios for the two granitoids show that the Bears Ears pluton was much more radiogenic than the Louis Lake batholith at their respective times of intrusion and that the Bears Ears was slightly enriched in ^{18}O.

In spite of the fact that simple X-Y and ternary plots do not show major differences between the two granitoids, Q-mode factor analysis shows that sample vectors for the two data sets lie in distinctly different groupings. One of the most diagnostic differences between the two data sets is their compositonal structures. Variables are better correlated for the Louis Lake batholith, and therefore, the unit has a relatively simple compositional structure. Variables are poorly correlated for the Bears Ears pluton, and therefore, it has a complex compositional structure.

COMPARISON TO OTHER LATE ARCHEAN GRANITOIDS OF WYOMING

The Louis Lake batholith differs markedly from the two Wyoming granitoids that are associated with uranium deposits. The granites of the Granite Mountains (Stuckless and Miesch, 1981) and the granites of the Owl Creek Mountains (Stuckless, Miesch, and Wenner, 1986) are of S-type affinity, whereas the Louis Lake batholith is an I-type granitoid. This broad difference in granite type is based on several specific differences as noted in previous sections. A significant consequence of these differences is that the protolith for the Louis Lake batholith lacks a cycle in development during which enrichment in incompatible elements, such as uranium, can occur. Therefore, the Louis Lake batholith as well as other I-type granitoids are unlikely candidates for uranium source rocks.

In addition to never being enriched in uranium, labile elements seem to be more firmly bound in the Louis Lake batholith than in the S-type Archean granites of Wyoming. Uranium distributions and to a lesser extent cesium distributions are much more poorly explained than distributions for other elements in the S-type granites. This is due to redistribution (including loss) of labile elements during exposure to the near-surface environment. Although uranium and cesium distributions are not well explained for the Louis Lake batholith, they are explained with many fewer factors than are needed for the S-type granites.

The Louis Lake batholith differs from other Late Archean granitoids, which have been studied in detail, in two major ways. Like other I-type granitoids (for example, Miesch, 1976b; Miesch and Reed, 1979), the Louis Lake batholith has a relatively simple compositional structure as is demonstrated by its fit to a model that has a small number of end members. The Louis Lake batholith also seems to have had a history of higher pressure than the S-type granites.

The Bears Ears pluton is more similar to the uraniferous Archean granites of Wyoming as would be expected from its S-type affinities. Nonetheless, it is not currently uraniferous, isotopic studies do not indicate a large loss of uranium during Tertiary exposure to the near-surface environment, and it is not associated with sedimentary-type uranium deposits. Stuckless and others (1985) suggested that the granite may have lost uranium towards the end stages of crystallization and that uranium may exist in young pegmatites of the Wind River Range. Some uranium may have been lost by this mechanism, but there is a general depletion of labile LIL elements relative to concentrations expected in a radiogenic granite and relative to immobile LIL elements such as thorium. Therefore, the lack of uranium enrichment in the Bears Ears pluton relative to the other S-type granites of Wyoming is best attributed to a granulite-facies metamorphism of the protolith in the vicinity of the Wind River Range that did not affect protoliths to the east beneath the Owl Creek or Granite Mountains.

SUMMARY

The two Late Archean intrusives exposed in the Wind River Range, Wyo., demonstrate a marked contrast in petrologic histories. The older unit, the Louis Lake batholith, was derived from a trondhjemitic to tonalitic protolith that formed more than 3,500 Ma. The initial magma had little or no europium anomaly, and therefore both hornblende and plagioclase were likely constituents of the residuum. Abundant inclusions within the Louis Lake batholith have this same mineralogy and are therefore interpreted to be restite. Partial melting produced a quartz-diorite to granodiorite magma of I-type affinity at a pressure of at least 8 kbar. Differentiation proceeded at water-saturated condition, initially at a pressure of at least 6 kbar as indicated by the presence of primary epidote, but pressure may have decreased later in the crystallization history.

The magmatic evolution of the Louis Lake batholith is well represented by a three-end-member model which in turn can be interpreted as a starting magma and subtraction of two different solidus compositions. The model is internally consistent in that the solidus compositions can be cast in terms of minerals known to exist in the Louis Lake batholith, and REE contents can be calculated for those minerals by assuming equilibrium with the initial magma. The sum of the REE contents in the minerals in the solids yields a good match to the total REE contents of the mathematically derived solidus compositions.

The Bears Ears pluton was derived from a younger and much more highly evolved protolith than that of the Louis Lake batholith. This younger protolith must have had a pelitic component because the Bears Ears pluton is peraluminous. Q-mode factor analysis shows that five end members are needed in a mixing model to match the chemistry of the Bears Ears pluton and that, even with five end members, the statistical distribution of several elements is poorly explained. The greater chemical variability of this unit is attributed to a high degree of contamination from the country rocks along with some effects of potassium metasomatism and the possible generation of an inhomogeneous magma during initial melting. Several lines of evidence suggest that the younger protolith was depleted in LIL elements prior to generation of the Bears Ears pluton. That depletion was probably in response to granulite-facies metamorphism. The Bears Ears pluton probably crystallized at lower pressures than the Louis Lake batholith, and it may have been derived at lower pressure as well. The more pronounced negative europium anomaly for samples of the Bears Ears pluton suggests a more dominant feldspar effect for this unit (either during partial melting or differentiation) than for the Louis Lake batholith.

Previous field and isotopic studies have shown that neither granitoid acted as a source rock for uranium deposits, and thus these granitoids differ from similar-aged granites to the east. The Louis Lake batholith is markedly different from the uranium source-rock granites in that it is an I-type granitoid, and this class of granite may generally lack uranium enrichment. The S-type affinities of the Bears Ears pluton together with its thorium enrichment suggest that it could have been a uranium source rock, but uranium was apparently lost from the protolith prior to generation of the granite and a further loss of uranium may have occurred during the end stage of crystallization such that the outcrops exposed during the Tertiary had little labile uranium that could be leached and redeposited in adjacent sediments.

REFERENCES CITED

Barker, Fred, Millard, H.T., Jr., and Lipman, P.W., 1979, Four low-K siliceous rocks of the western U.S.A., *in* Barker, F., ed., Trondhjemites, dacites, and related rocks: Elsevier, Amsterdam, p. 415–433.

Bassett, W.A., and Giletti, B.J., 1963, Precambrian ages in the Wind River Mountains, Wyoming: Geologic Society of America Bulletin, v. 74, p. 209–212.

Bayley, R.W., 1965a, Geologic map of the Miners Delight quadrangle, Fremont County, Wyoming: U.S. Geological Survey Geologic Quadrangle Map GQ–460, scale 1:24,000.

______1965b, Geologic map of the Louis Lake quadrangle, Fremont County, Wyoming: U.S. Geological Survey Geologic Quadrangle Map GQ–461, scale 1:24,000.

______1965c, Geologic map of the South Pass City quadrangle, Fremont County, Wyoming: U.S. Geological Survey Geologic Quadrangle Map GQ–458, 1:24,000.

Bayley, R.W., Proctor, P.D., and Condie, K.C., 1973, Geology of the South Pass area, Fremont County, Wyoming: U.S. Geological Survey Professional Paper 793, 39 p.

Bunker, C.M., and Bush, C.A., 1966, Uranium, thorium, and radium analyses by gamma-ray spectrometry (0.184–0.352 million electron volts), *in* Geological Survey research 1967: U.S. Geological Survey Professional Paper 550–B, p. B176–B181.

Butler, A.P., Jr., 1972, Uranium, *in* Mallory, W.W., ed., Geologic atlas of the Rocky Mountain region: Rocky Mountain Association of Geologists, p. 315–317.

Chappell, B.W., and White, A.J.R., 1974, Two contrasting granite types: Pacific Geology, v. 8, p. 173–174.

Cheang, K.K., Wenner, D.B., and Stuckless, J.S., 1986, Oxygen isotope constraints on the origin of Precambrian granites from the southern Wind River Range and the Granite Mountains, central Wyoming, *in* Peterman, Z.E., and Schnabel, D.C., eds., Shorter contributions to isotope geology: U.S. Geological Survey Bulletin 1622, p. 109–130.

Condie, K.C., Leech, A.P., and Baadsgaard, H., 1969, Potassium-argon ages of Precambrian mafic dikes in Wyoming: Geological Society of America Bulletin, v. 80, p. 899–906.

Crawford, M.L., and Hollister, L.S., 1982, Contrast of structural and metamorphic histories across the Work Channel lineament, Coast plutonic complex, British Columbia: Journal of Geophysical Research, v. 87, p. 3849–3860.

Dostal, J., and Capedri, E., 1978, Uranium in metamorphic rocks: Contributions to Mineralogy and Petrology, v. 66, p. 409–414.

Evensen, N.M., Hamilton, P.J., and O'Nions, R.K., 1978, Rare-earth abundances in chondritic meteorites: Geochimica et Cosmochimica Acta, v. 42, p. 1199–1212.

Giletti, B.J., and Gast, P.W., 1961, Absolute age of Precambrian rocks in Wyoming and Montana: Annals of the New York Academy of Science, v. 91, p. 454–458.

Gordon, G.E., Randle, K., Goles, G., Corliss, J., Beeson, M., and Oxley, S., 1968, Instrumental activation analysis of standard rocks with high resolution gamma-ray detectors: Geochimica et Cosmochimica Acta, v. 32, p. 369–396.

Granger, H.C., McKay, E.J., Mattick, R.E., Patten, L.L., and MacIlroy, Paul, 1971, Mineral resources of the Glacier Primitive Area, Wyoming: U.S. Geological Survey Bulletin 1319–F, 113 p.

Gray, C.M., 1977, The geochemistry of central Australian granulites in relation to the chemical and isotopic effects of granulite facies metamorphism: Contributions to Mineralogy and Petrology, v. 65, p. 79–89.

Gromet, L.P., and Silver, L.T., 1983, Rare earth element distributions among minerals in a granodiorite and their implications: Geochimica et Cosmochimica Acta, v. 47, p. 935–939.

Hanson, G.N., 1978, The application of trace elements to the petrogenesis of igneous rocks of granitic composition, *in* Allegre, C.J., ed., Trace elements in igneous petrology: Earth and Planetary Science Letters, v. 38, p. 26–43.

Hedge, C.E., Simmons, K.R., and Stuckless, J.S., 1986, Geochronology of an Archean granite, Owl Creek Mountains, Wyoming: U.S. Geological Survey Professional Paper 1388–B, p. 22–33.

Hills, F.A., and Armstrong, R.L., 1974, Geochronology of Precambrian rocks in the Laramie Range and implications for the tectonic framework of Precambrian southern Wyoming: Precambrian Research, v. 1, p. 213–225.

Lambert, I.B., and Heier, K.S., 1968, Geochemical investigations of high grade regional metamorphics and associated rocks in the Australian Shield: Lithos, v. 1, p. 30–53.

Lewis, J.D., and Spooner, C.M., 1973, K/Rb ratios in Precambrian granulite terranes: Geochimica et Cosmochimica Acta, v. 37, p. 1111–1118.

Longstaffe, F.J., and Schwarcz, H.P., 1977, $^{18}O/^{16}O$ of Archean clastic metasedimentary rocks—a petrogenetic indicator for Archean gneisses: Geochimica et Cosmochimica Acta, v. 41, p. 1303–1312.

Love, J.D., Wietz, J.L., and Hose, R.K., 1955, Geologic map of Wyoming: U.S. Geological Survey, scale 1:500,000.

Luth, W.C., 1969, The systems $NaAlSi_3O_8$–SiO_2 and $KAlSi_3O_8$–SiO_2 to 20 kb and the relationship between H_2O content, total pressure and P_{H_2O} in granitic magmas: American Journal of Science, Schairer volume 267A, p. 325–341.

Luth, W.C., Jahns, R.H., and Tuttle, O.F., 1964, The granite system at pressures of 4 to 10 kilobars: Journal of Geophysical Research, v. 69, p. 759–773.

Mahood, Gail, and Hildreth, Wes, 1983, Large partition coefficients for trace elements in high-silica rhyolites: Geochimica et Cosmochimica Acta, v. 47, p. 11–30.

Miesch, A.T., 1976a, Interactive computer programs for petrologic modeling with extended Q-mode factor analysis: Computers and Geoscience, v. 2, p. 439–492.

______1976b, Q-mode factor analysis of geochemical and petrologic data matrices with constant row-sums: U.S. Geological Survey Professional Paper 574–G, 47 p.

______1981, Computer methods for geochemical and petrologic mixing problems, *in* Merriam, D.F, ed., Computer applications in earth sciences: New York, Plenum Publishing, p. 243–265.

Miesch, A.T., and Reed, B.L., 1979, Compositional structures in two batholiths of circumpacific North America: U.S. Geological Survey Professional Paper 574–H, 31 p.

Millard, H.T., Jr., 1976, Determination of uranium and thorium in U.S. Geological Survey standard rocks by the delayed neutron technique, *in* Flanigan, F.J., ed., Descriptions and analyses of eight new USGS rock standards: U.S. Geological Survey Professional Paper 840, p. 61-65.

Moorbath, S., Welke, H., and Gale, N.H., 1969, The significance of lead isotope studies in ancient high-grade metamorphic basement complexes, as exemplified by the Lewsian rocks of northwest Scotland: Earth and Planetary Science Letters, v. 6, p. 245-256.

Nagasawa, H., and Schnetzler, C.C., 1971, Partitioning of rare-earth and alkali earth elements between phenocryst and acidic igneous magma: Geochimica et Cosmochimica Acta, v. 35, p. 953-968.

Naney, M.T., 1983, Phase equilibria of rock-forming ferromagnesian silicates in granitic systems: American Journal of Science, v. 283, p. 993-1033.

Naylor, R.S., Stieger, R.H., and Wasserburg, G.J., 1970, U-Th-Pb and Rb-Sr systematics in 2700×10^9-year old plutons from the southern Wind River Range, Wyoming: Geochimica et Cosmochimica Acta, v. 4, p. 1133-1159.

Noyes, H.J., Frey, F.A., and Wones, D.R., 1983, A tale of two plutons—geochemical evidence bearing on the origin and differentiation of the Red Lake and Eagle Peak plutons, central Sierra Nevada, California: Journal of Geology, v. 91, p. 487-509.

O'Neil, J.R., Shaw, S.E., and Flood, R.H., 1977, Oxygen and hydrogen isotope compositions as indicators of granite genesis in the New England batholith, Australia: Contributions to Mineralogy and Petrology, v. 62, p. 313- 328.

Pearce, J.A., Harris, N.B.W., and Tindle, A.G., 1984, Trace element discrimination diagrams for the tectonic interpretations of granitic rocks: Journal of Petrology, v. 25, p. 956-983.

Pearson, R.C., Kiilsgaard, T.H., Patten, L.L., and Mattich, R.E., 1971, Mineral resources of the Popo Agie Primitive Area, Fremont and Sublette Counties, Wyoming: U.S. Geological Survey Bulletin 1353-B, 55 p.

Peterman, Z.E., 1979, Geochronology and the Archean of the United States: Economic Geology, v. 74, p. 1544-1562.

Rollinson, H.R., and Windley, B.F., 1980, Selective element depletion during metamorphism of Archean granulites, Scourie, NW Scotland: Contributions to Mineralogy and Petrology, v. 72, p. 257-263.

Rosholt, J.N., Zartman, R.E., and Nkomo, I.T., 1973, Lead isotope systematics and uranium depletion in the Granite Mountains, Wyoming: Geological Society of America Bulletin, v. 84, p. 989-1002.

Schnetzler, C.C., and Philpotts, J.A., 1970, Partition coefficients of rare-earth elements between igneous matrix material and rock-forming phenocrysts II: Geochimica et Cosmochimica Acta, v. 34, p. 331-340.

Seeland, D.A., 1976, Relationship between early Tertiary sedimentation pattern and uranium mineralization in the Powder River Basin, Wyoming: Twenty-eighth Annual Field Conference—1976, Wyoming Geological Association Guidebook, p. 53-64.

______1978, Eocene fluvial drainage patterns and their implications for uranium and hydrocarbon exploration in the Wind River Basin, Wyoming: U.S. Geological Survey Bulletin 1446, 21 p.

Spall, H., 1971, Paleomagnetism and K-Ar ages of mafic dikes from the Wind River Range, Wyoming: Geological Society of America Bulletin, v. 82, p. 2457-2472.

Steiger, R.H., and Jager, E., 1977, Subcommission on geochronology—convention on the use of decay constants in geo- and cosmochronology: Earth and Planetary Science Letters, v. 36, p. 359-367.

Stuckless, J.S., 1983, A program in Hewlett-Packard BASIC for calculation of mesonormative minerals using HP-series 80 computers and VISICALC electronic worksheet: U.S. Geological Survey Open-File Report 83-923, 24 p.

Stuckless, J.S., Hedge, C.E., Worl, R.G., Simmons, K.R., Nkomo, I.T., and Wenner, D.B., 1985, Isotopic studies of the Late Archean plutonic rocks of the Wind River Range, Wyoming: Geological Society of America Bulletin, v. 96, p. 850-860.

Stuckless, J.S., and Miesch, A.T., 1981, Petrogenetic modeling of a potential uranium source rock, Granite Mountains, Wyoming: U.S. Geological Survey Professional Paper 1225, 39 p.

Stuckless, J.S., Miesch, A.T., and Wenner, D.B., 1986, Geochemistry and petrogenesis of an Archean granite from the Owl Creek Mountains, Wyoming: U.S. Geological Survey Professional Paper 1388-A, p. 1-21.

Stuckless, J.S., and Nkomo, I.T., 1978, Uranium-lead isotope systematics in uraniferous alkali-rich granites from the Granite Mountains, Wyoming—implications for uranium source rocks: Economic Geology, v. 73, p. 427-441.

Stuckless, J.S., Nkomo, I.T., and Butt, K.A., 1986, Uranium-thorium-lead systematics of an Archean granite from the Owl Creek Mountains, Wyoming: U.S. Geological Survey Professional Paper 1388-C, p. 34-48.

Stuckless, J.S., Nkomo, I.T., and Doe, B.R., 1982, U-Th-Pb systematics in hydrothermally altered granite from the Granite Mountains, Wyoming: Geochimica et Cosmochimica Acta, v. 45, p. 635-645.

Stuckless, J.S., and VanTrump, George, Jr., 1979, A revised version of Graphic Normative Analysis Program (GNAP) with examples of petrologic problem solving: U.S. Geological Survey Open-File Report 79-1237, 115 p.

Taggart, J.E., Jr., Lichte, F.E., and Wahlberg, J.S., 1982, Methods of analysis for samples using X-ray fluorescence and induction-coupled plasma spectrometry, *in* Lipman, P.W., and Mullineaux, D.R., eds., The 1980 eruption of Mount St. Helens, Washington: U.S. Geological Survey Professional Paper 1250, p. 683-687.

Thornton, C.P., and Tuttle, O.F., 1960, Chemistry of igneous rocks, I, Differentiation index: American Journal of Science, v. 258, p. 664-684.

Tuttle, O.F., and Bowen, N.L., 1958, Origin of granite in the light of experimental studies in the system $NaAlSi_3O_8$-$KAlSi_3O_8$-SiO_2-H_2O: Geological Society of America Memoir 74, 153 p.

White, A.J.R., and Chappell, B.W., 1983, Granitoid types and their distribution in the Lachlan Fold Belt, southeastern Australia: Geological Society of America Memoir 159, p. 21- 34.

Whitney, J.A., 1975, The effects of pressure, temperature, and X_{H_2O} on phase assemblage in four synthetic rock compositions: Journal of Geology, v. 83, p. 1-31.

Winkler, H.G.F., Boese, M., and Marcopulos, T., 1975, Low temperature granitic melts: Neues Jahrbuch fuer Mineralogie, Monatshefte, v. 6, p. 245-268.

Worl, R.G., Koesterer, M.E., and Hulsebosch, T.P., 1986, Geologic map of the Bridger Wilderness and the Green-Sweetwater Roadless Area, Sublette and Freemont Counties, Wyoming: U.S. Geological Survey Miscellaneous Field Studies Map MF-1636-B, scale 1:250,000.

Worl, R.G., Lee, G.K., Long, C.L., and Ryan, G.S., 1984, Mineral resource potential map of the Bridger Wilderness and Sweetwater Roadless Area, Sublette and Freemont Counties, Wyoming: U.S. Geological Survey Miscellaneous Field Studies Map MF-1636-A, scale 1:250,000.

Zen, E-an, 1985, Implications of magmatic epidote-bearing plutons on crustal evolution in accreted terranes of northwestern North America: Geology, v. 13, p. 266-269.

Zielinski, R.A., Lipman, P.W., and Millard, H.T., Jr., 1977, Minor-element abundances in obsidian, perlite, and felsite of calc-alkalic rhyolites: American Mineralogist, v. 62, p. 426-437.

☆ U.S. GOVERNMENT PRINTING OFFICE: 1989—673-047/86,064 REGION NO. 8

SELECTED SERIES OF U.S. GEOLOGICAL SURVEY PUBLICATIONS

Periodicals

Earthquakes & Volcanoes (issued bimonthly).
Preliminary Determination of Epicenters (issued monthly).

Technical Books and Reports

Professional Papers are mainly comprehensive scientific reports of wide and lasting interest and importance to professional scientists and engineers. Included are reports on the results of resource studies and of topographic, hydrologic, and geologic investigations. They also include collections of related papers addressing different aspects of a single scientific topic.

Bulletins contain significant data and interpretations that are of lasting scientific interest but are generally more limited in scope or geographic coverage than Professional Papers. They include the results of resource studies and of geologic and topographic investigations; as well as collections of short papers related to a specific topic.

Water-Supply Papers are comprehensive reports that present significant interpretive results of hydrologic investigations of wide interest to professional geologists, hydrologists, and engineers. The series covers investigations in all phases of hydrology, including hydrogeology, availability of water, quality of water, and use of water.

Circulars present administrative information or important scientific information of wide popular interest in a format designed for distribution at no cost to the public. Information is usually of short-term interest.

Water-Resources Investigations Reports are papers of an interpretive nature made available to the public outside the formal USGS publications series. Copies are reproduced on request unlike formal USGS publications, and they are also available for public inspection at depositories indicated in USGS catalogs.

Open-File Reports include unpublished manuscript reports, maps, and other material that are made available for public consultation at depositories. They are a nonpermanent form of publication that may be cited in other publications as sources of information.

Maps

Geologic Quadrangle Maps are multicolor geologic maps on topographic bases in 7 1/2- or 15-minute quadrangle formats (scales mainly 1:24,000 or 1:62,500) showing bedrock, surficial, or engineering geology. Maps generally include brief texts; some maps include structure and columnar sections only.

Geophysical Investigations Maps are on topographic or planimetric bases at various scales; they show results of surveys using geophysical techniques, such as gravity, magnetic, seismic, or radioactivity, which reflect subsurface structures that are of economic or geologic significance. Many maps include correlations with the geology.

Miscellaneous Investigations Series Maps are on planimetric or topographic bases of regular and irregular areas at various scales; they present a wide variety of format and subject matter. The series also includes 7 1/2-minute quadrangle photogeologic maps on planimetric bases which show geology as interpreted from aerial photographs. Series also includes maps of Mars and the Moon.

Coal Investigations Maps are geologic maps on topographic or planimetric bases at various scales showing bedrock or surficial geology, stratigraphy, and structural relations in certain coal-resource areas.

Oil and Gas Investigations Charts show stratigraphic information for certain oil and gas fields and other areas having petroleum potential.

Miscellaneous Field Studies Maps are multicolor or black-and-white maps on topographic or planimetric bases on quadrangle or irregular areas at various scales. Pre-1971 maps show bedrock geology in relation to specific mining or mineral-deposit problems; post-1971 maps are primarily black-and-white maps on various subjects such as environmental studies or wilderness mineral investigations.

Hydrologic Investigations Atlases are multicolored or black-and-white maps on topographic or planimetric bases presenting a wide range of geohydrologic data of both regular and irregular areas; principal scale is 1:24,000 and regional studies are at 1:250,000 scale or smaller.

Catalogs

Permanent catalogs, as well as some others, giving comprehensive listings of U.S. Geological Survey publications are available under the conditions indicated below from the U.S. Geological Survey, Books and Open-File Reports Section, Federal Center, Box 25425, Denver, CO 80225. (See latest Price and Availability List.)

"Publications of the Geological Survey, 1879- 1961" may be purchased by mail and over the counter in paperback book form and as a set of microfiche.

"Publications of the Geological Survey, 1962- 1970" may be purchased by mail and over the counter in paperback book form and as a set of microfiche.

"Publications of the U.S. Geological Survey, 1971- 1981" may be purchased by mail and over the counter in paperback book form (two volumes, publications listing and index) and as a set of microfiche.

Supplements for 1982, 1983, 1984, 1985, 1986, and for subsequent years since the last permanent catalog may be purchased by mail and over the counter in paperback book form.

State catalogs, "List of U.S. Geological Survey Geologic and Water-Supply Reports and Maps For (State)," may be purchased by mail and over the counter in paperback booklet form only

"Price and Availability List of U.S. Geological Survey Publications," issued annually, is available free of charge in paperback booklet form only.

Selected copies of a monthly catalog "New Publications of the U.S. Geological Survey" available free of charge by mail or may be obtained over the counter in paperback booklet form only. Those wishing a free subscription to the monthly catalog "New Publications of the U.S. Geological Survey" should write to the U.S. Geological Survey, 582 National Center, Reston, VA 22092.

Note.--Prices of Government publications listed in older catalogs, announcements, and publications may be incorrect. Therefore, the prices charged may differ from the prices in catalogs, announcements, and publications.